

Phase transitions

Doruk Efe Gökmen

June 20, 2019

Contents

I	Tools from functional calculus	4
1	Functional derivatives	5
2	Functional integrals	9
2.0.1	N -dimensional gaussian integrals	9
2.0.2	Functional gaussian integrals	11
II	Critical phenomena	12
3	Entropic interactions and computational phase transitions	13
3.1	Entropic interactions with hard spheres	13
3.1.1	Asakura-Oosawa depletion interaction	13
3.2	Hard spheres in 2-d	13
4	Mean-field theory	14
4.1	Magnetic phase transitions and Weiss mean-field theory	14
4.1.1	$O(n = 1)$ (Ising) model	14
4.1.2	$O(n \geq 2)$ model	19
4.2	Liquid-gas transition and the van der Waals mean-field theory	24
4.2.1	van der Waals equation of state	24
4.2.2	Universal form	24
4.2.3	The Maxwell construction	24
4.2.4	The critical region of van der Waals model	25
5	Spin models and analytical methods	27
5.1	Ising model	27
5.1.1	1-d Ising model transfer matrix solution	27
5.2	Transverse field Ising model and quantum dynamics	35
5.2.1	2-d Ising model	37
5.2.2	4-d Ising model and the mean-field result	38
5.3	XY model in d -dimensions	38
5.3.1	Kosterlitz-Thouless-Berezinskii transition in 2-d XY model	44
5.3.2	Order parameter, energy, susceptibility and the specific heat	49

5.4	Heisenberg model in d -dimensions	49
5.4.1	Quantum Heisenberg model	50
5.5	Monte-Carlo methods for spin models	50
5.5.1	Metropolis algorithm	52
5.5.2	Cluster algorithms	53
5.6	Mermin-Wagner-Hohenberg theory	53
5.6.1	Equipartition theorem and susceptibility sum rule	53
6	Landau mean-field theory	55
6.1	Saddle point approximation	56
6.1.1	Second order phase transitions	57
6.1.2	First order phase transitions	60
6.1.3	Multicritical points	62
6.2	Beyond Landau theory	63
6.3	Gauss model	64
6.4	Gaussian approximation to free energy functionals	67
6.4.1	Φ^4 theory and the Hartree approximation	67
6.5	Ginzburg criterion	67
7	Critical properties of Bose-Einstein condensation	69
7.1	Introduction to Bose-Einstein condensation (BEC)	69
7.2	Gross-Pitaevskii equation (GPE)	69
7.3	Bogoliubov approximation	69
7.3.1	Superfluidity	69
7.4	Reduced one-body density matrix	69
7.4.1	Order parameter of the condensate	69
8	Scaling hypothesis	70
8.1	Geometric (length) scaling	70
8.2	Widom scaling	73
8.3	Homogeneous function scaling	73
8.4	Untypical examples	73
8.4.1	Scaling form near multicritical point	73
8.4.2	Vortex-glass scaling in a superconductor near T_c	74
8.5	Scaling in finite sized systems	74
8.5.1	Binder cumulant	75
9	Renormalisation-group theory	77
9.1	Renormalisation-group (RG) equations	78
9.1.1	Fixed points K^*	78
9.1.2	Linearised RG equations	79
9.1.3	Kadanoff's block spin transformation	79
9.2	Position space RG in lattice systems	79
9.2.1	Decimation RG and the transfer matrix method	80
9.2.2	The Niemeijer-van Leeuwen cumulant approximation	80
9.2.3	The Migdal-Kadanoff bond moving approximation	81

<i>CONTENTS</i>	3
9.2.4 Monte Carlo simulations	81
9.2.5 BKT-transition	81
9.3 k -space RG	81
9.4 Renormalisation-group Monte Carlo (MCRG)	81
10 Real space RG using neural networks	82
10.1 Machine learning	82
10.2 Neural networks	82
10.2.1 Restricted Boltzmann machines	82
11 RG in catastrophe optics and caustics	83
12 Critical exponents	84
III Non-equilibrium statistical mechanics	86
12.0.1 Temporal correlations	88
12.1 Time dependent Ginzburg-Landau (TDGL) model	89
12.2 Non-equilibrium phase transitions	90
12.2.1 Directed percolation	90
12.2.2 Dicke model phase transition	90
12.2.3 Exciton-polariton condensation	90
12.2.4 Mott transition	90

Part I

**Tools from functional
calculus**

Chapter 1

Functional derivatives

Consider a function $f(\vec{y})$, with $\vec{y} = (y_1, \dots, y_n) = \sum_i y_i \hat{e}_i \in \mathbb{R}^n$, $y_i \in \mathbb{R}$. Partial derivative of f with respect to i th component of y is defined by

$$\begin{aligned} \frac{\partial f(y_1, \dots, y_i, \dots, y_n)}{\partial y_i} &:= \lim_{\epsilon \rightarrow 0} \frac{f(\vec{y} + \epsilon \hat{e}_i) - f(\vec{y})}{\epsilon} \\ &= \lim_{\epsilon \rightarrow 0} \frac{f(\sum_k (y_k - \epsilon \delta_k^i) \hat{e}_k) - f(\sum_k y_k \hat{e}_k)}{\epsilon}. \end{aligned} \quad (1.1)$$

Note that the k th component of i th unit vector is δ_i^k , i.e. $\hat{e}_i = \sum_k \delta_i^k \hat{e}_k$. The chain rule for the partial derivative of $f(\vec{y}(\vec{x}))$ is as follows

$$\frac{\partial f(\vec{y}(\vec{x}))}{\partial x_i} = \sum_j \frac{\partial f}{\partial y_j} \frac{\partial y_j}{\partial x_i}. \quad (1.2)$$

In the continuum limit of vector components (from discrete to uncountably many vector components) we pass from $y_i \in \mathbb{R}$ to $y(\vec{r}) \in C^\infty(\mathbb{R})$, with $\vec{r} \in \mathbb{R}^d$. Then the components of the unit vectors become the Dirac delta distribution $\delta(\vec{r} - \vec{r}')$. By virtue of this correspondance, we get a direct generalisation of the partial derivative to the functional case, namely the functional derivative of $F[M(\vec{r})]$ with respect to function $M(\vec{r}')$:

$$\frac{\delta F[M(\vec{r})]}{\delta M(\vec{r}')} := \lim_{\epsilon \rightarrow 0} \frac{F[M(\vec{r}) + \epsilon \delta(\vec{r} - \vec{r}')] - F[M(\vec{r})]}{\epsilon}. \quad (1.3)$$

Similarly, the chain rule for functional derivatives is as follows

$$\frac{\delta G[F[M(\vec{r})]]}{\delta M(\vec{r})} = \int d^d r' \frac{\delta G[F]}{\delta F[M(\vec{r}')] } \frac{\delta F[M(\vec{r}')] }{\delta M(\vec{r})}. \quad (1.4)$$

If the functional is of the form

$$F[M(\vec{r})] = \int d^d r f[M(\vec{r}), \nabla M(\vec{r})], \quad (1.5)$$

one can express the functional derivative in terms of the gradient and the partial derivatives. Using 1.3 we get

$$\begin{aligned} \epsilon \frac{\delta F}{\delta M(\vec{r}')} &= \int d^d r \{f[M(\vec{r}) + \epsilon \delta(\vec{r} - \vec{r}'), \nabla[M(\vec{r}) + \epsilon \delta(\vec{r} - \vec{r}')]]\} \\ &\quad - \int d^d r f[M(\vec{r}), \nabla[M(\vec{r})]]. \end{aligned}$$

Taylor expanding to the lowest order in ϵ , one gets

$$\begin{aligned} \epsilon \frac{\delta F}{\delta M(\vec{r}')} &= \int d^d r \epsilon \left[\frac{\partial f}{\partial M(\vec{r})} \delta(\vec{r} - \vec{r}') + \frac{\partial f}{\partial \nabla M(\vec{r})} \nabla \delta(\vec{r} - \vec{r}') \right] \\ &= \int d^d r \epsilon \left[\frac{\partial f}{\partial M(\vec{r})} \delta(\vec{r} - \vec{r}') - \nabla \cdot \left(\frac{\partial f}{\partial \nabla M(\vec{r})} \right) \delta(\vec{r} - \vec{r}') \right] \\ &\quad + \epsilon \frac{\partial f}{\partial \nabla M(\vec{r})} \delta(\vec{r} - \vec{r}') \Big|_{r=0}^{\infty} \\ &= \epsilon \left[\frac{\partial f}{\partial M(\vec{r}')} - \nabla \cdot \left(\frac{\partial f}{\partial \nabla M(\vec{r}')} \right) \right], \end{aligned}$$

where the last line follows using the divergence theorem and because the boundary term vanishes. Thus we have

$$\frac{\delta}{\delta M(\vec{r}')} \int d^d r f[M(\vec{r}), \nabla M(\vec{r})] = \frac{\partial f}{\partial M(\vec{r}')} - \nabla \cdot \left(\frac{\partial f}{\partial \nabla M(\vec{r}')} \right). \quad (1.6)$$

If LHS is 0, we impose the condition that the functional F is extremal. Indeed identifying F with the Hamiltonian action, one recovers the Euler-Lagrange equation for the lagrangian $f[M(\vec{r}), \nabla M(\vec{r})]$ from 1.6.

The Heisenberg ferromagnetic hamiltonian on a lattice is

$$\mathcal{H} = -J \sum_{\langle i,j \rangle} \vec{S}_i \cdot \vec{S}_j - \mu \vec{h} \cdot \sum_i \vec{S}_i. \quad (1.7)$$

Note the average magnetisation is $\vec{M} = \sum_i \vec{S}_i$. Coarse graining $\{\vec{h}_i, \vec{S}_i\} \rightarrow \{\vec{h}(\vec{r}), \vec{S}(\vec{r})\}$ yields

$$\mathcal{H}[h(\vec{r}), M(\vec{r})] = - \int_{\text{nn}} d^d r d^d r' J(\vec{r}, \vec{r}') S(\vec{r}) S(\vec{r}') - \int d^d r h(\vec{r}) M(\vec{r}). \quad (1.8)$$

The partition function is

$$\int \mathcal{D}^n[\sigma(r)] \mathcal{D}^n[\pi(r)] \exp[-\beta \mathcal{H}[h(\vec{r}), M(\vec{r})]], \quad (1.9)$$

where the functional integral covers all possible sets of orientations of spins with n -degrees of freedom. The Gibbs free energy functional is $G[T, h(\vec{r})] =$

$-k_{\text{B}}T \log Z(T, h(\vec{r}))$. Let us calculate

$$\begin{aligned} -\frac{\delta G[T, h(\vec{r})]}{\delta h(\vec{r}')} &= \frac{\delta \log Z(h(\vec{r}), M(\vec{r}))}{\delta \beta h(\vec{r}')} \\ &= \frac{1}{Z} \int \mathcal{D}^n[\sigma(r)] \mathcal{D}^n[\pi(r)] \frac{\delta}{\delta \beta h(\vec{r}')} \exp[-\beta \mathcal{H}[h(\vec{r}), M(\vec{r})]]. \end{aligned} \quad (1.10)$$

By chain rule we get

$$\begin{aligned} \frac{\delta \log Z}{\delta \beta h(\vec{r}')} &= \frac{1}{Z} \int \mathcal{D}^n[\sigma(r)] \mathcal{D}^n[\pi(r)] \frac{\delta \beta \int d^d r h(\vec{r}) M(\vec{r})}{\delta \beta h(\vec{r}')} \exp[-\beta \mathcal{H}] \\ &= \lim_{\epsilon \rightarrow 0} \frac{1}{Z} \int \mathcal{D}^n[\sigma(r), \pi(r)] \frac{\int d^d r M(\vec{r}) [h(\vec{r}) + \epsilon \delta^d(\vec{r} - \vec{r}') - h(\vec{r})]}{\epsilon} e^{-\beta \mathcal{H}} \\ &= \frac{1}{Z} \int \mathcal{D}^n[\sigma(r), \pi(r)] \int d^d r M(\vec{r}) \delta^d(\vec{r} - \vec{r}') e^{-\beta \mathcal{H}} \\ &= \frac{\int \mathcal{D}^n[\sigma(r), \pi(r)] M(\vec{r}') e^{-\beta \mathcal{H}}}{Z} = \langle M(\vec{r}') \rangle. \end{aligned} \quad (1.11)$$

In other words

$$\boxed{\langle M(\vec{r}') \rangle = -\frac{\delta G[T, h(\vec{r})]}{\delta h(\vec{r}')}}. \quad (1.12)$$

Similarly, the second derivative gives the cumulant

$$\begin{aligned} \frac{\delta^2 \log Z}{\delta \beta h(\vec{r}) \delta \beta h(\vec{r}')} &= \frac{\int \mathcal{D}^n[\sigma(r), \pi(r)] M(\vec{r}') M(\vec{r}) e^{-\beta \mathcal{H}}}{Z} \\ &\quad - \frac{\int \mathcal{D}^n[\sigma(r), \pi(r)] M(\vec{r}') e^{-\beta \mathcal{H}}}{Z^2} \int \mathcal{D}^n[\sigma(r), \pi(r)] M(\vec{r}) e^{-\beta \mathcal{H}}, \end{aligned}$$

or

$$\frac{\delta^2 \log Z}{\delta \beta h(\vec{r}) \delta \beta h(\vec{r}')} = \langle M(\vec{r}) M(\vec{r}') \rangle - \langle M(\vec{r}) \rangle \langle M(\vec{r}') \rangle \equiv \langle \langle M(\vec{r}) M(\vec{r}') \rangle \rangle. \quad (1.13)$$

Therefore the magnetic susceptibility $\chi_{ij}(\vec{r}, \vec{r}')$ is given by

$$\boxed{\chi_{ij}(\vec{r}, \vec{r}') = \frac{\delta \langle M_i(\vec{r}) \rangle}{\delta h_j(\vec{r}')} = -\frac{1}{\beta} \frac{\delta^2 G[h(\vec{r})]}{\delta h_j(\vec{r}) \delta h_i(\vec{r}')} = \langle \langle M(\vec{r}) M(\vec{r}') \rangle \rangle}. \quad (1.14)$$

One can also get the entropy by the usual expression $S = -\frac{\partial F[T, h(\vec{r})]}{\partial T}$.

Alternative approach One can define the functional differential as $\lim_{\Delta \rightarrow 0} dF(M_i) = \epsilon \delta F[M(\vec{r})]$, with $0 < \epsilon \ll 1$, where $M_i \equiv M(\vec{r}_i)$, Δ is the lattice spacing between each i th site and such that

$$\epsilon \delta F[M, \eta] = F[M + \epsilon \eta] - F[M] \quad (1.15)$$

On the other hand, given $dM_i = \epsilon\eta(\vec{r}_i)$ and $\eta(\vec{r})$ vanishes in the domain boundary ∂D , we would have

$$\begin{aligned}\epsilon\delta F[M, \eta] &= \lim_{\Delta \rightarrow 0} dF(M_i) = \lim_{\Delta \rightarrow 0} \sum_i \Delta^3 \frac{\partial F(M_i)}{\partial M_i \Delta^3} dM_i \\ &= \int d^3r \frac{\delta F[M[\vec{r}]]}{\delta M(\vec{r})} \epsilon\eta(\vec{r}) \\ \implies \delta F[h, \eta] &= \int d^3r \frac{\delta F}{\delta M} \eta.\end{aligned}\quad (1.16)$$

Note that in contrast to the ordinary derivative, the functional derivative has the unit of inverse quantity per volume. Using 1.15, we get

$$\lim_{\epsilon \rightarrow 0} \frac{F[M + \epsilon\eta] - F[M]}{\epsilon} \triangleq \frac{d}{d\epsilon} F[M + \epsilon\eta] \Big|_{\epsilon=0} = \int d^3r \frac{\delta F}{\delta M} \eta. \quad (1.17)$$

For the functional 1.5, we now have

$$\begin{aligned}\int d^3r \frac{\delta F}{\delta M} \eta &= \frac{d}{d\epsilon} F[M + \epsilon\eta] \Big|_{\epsilon=0} \\ &= \int d^3r \frac{d}{d\epsilon} \left\{ f + \frac{\partial f}{\partial M} \epsilon\eta + \frac{\partial f}{\partial \nabla M} \cdot \epsilon \nabla \eta \right. \\ &\quad \left. + \frac{\epsilon^2}{2} \left[\frac{\partial^2 f}{\partial M^2} \eta^2 + \frac{\partial^2 f}{\partial (\nabla M)^2} (\nabla \eta)^2 + \frac{\partial f}{\partial M} \frac{\partial f}{\partial \nabla M} \cdot \eta \nabla \eta \right] + \dots \right\} \Big|_{\epsilon=0} \\ &= \int d^3r \left[\frac{\partial f}{\partial M} \eta + \frac{\partial f}{\partial (\nabla M)} \cdot \nabla \eta \right] \\ &= \int d^3r \left[\frac{\partial f}{\partial M} \eta + \nabla \cdot \left(\frac{\partial f}{\partial (\nabla M)} \eta \right) - \eta \nabla \cdot \frac{\partial f}{\partial (\nabla M)} \right] \\ &= \frac{\partial f}{\partial (\nabla M) \eta} \Big|_{\partial D} + \int d^3r \left[\frac{\partial f}{\partial M} - \nabla \cdot \frac{\partial f}{\partial (\nabla M)} \right] \eta\end{aligned}\quad (1.18)$$

$$= \int d^3r \left[\frac{\partial f}{\partial M} - \nabla \cdot \frac{\partial f}{\partial (\nabla M)} \right] \eta \quad (1.19)$$

Thus the integrand of LHS and RHS must match at each point hence we get the same identity as before

$$\frac{\delta F}{\delta M} = \frac{\partial f}{\partial M} - \nabla \cdot \frac{\partial f}{\partial (\nabla M)}. \quad (1.6)$$

Chapter 2

Functional integrals

2.0.1 N -dimensional gaussian integrals

It can be proven by diagonalisation that the following general N -dimensional gaussian integral is

$$\mathcal{Z}_N = \int_{-\infty}^{\infty} \prod_{i=0}^N d\phi_i \exp \left[-\frac{1}{2} \phi^T \mathbf{G}^{-1} \phi + \mathbf{h} \cdot \phi \right] = \det(2\pi \mathbf{G})^{1/2} \exp \left(\frac{1}{2} \mathbf{h}^T \mathbf{G} \mathbf{h} \right). \quad (2.1)$$

It can easily be seen that

$$\left\langle \prod_{i=1}^N \phi_i^{r_i} \right\rangle_c = \left[\left(\prod_{i=1}^N \frac{\partial^{r_i}}{\partial k_i^{r_i}} \right) \log \langle e^{\mathbf{k} \cdot \phi} \rangle \right]_{\mathbf{k}=0}, \quad (2.2)$$

where *the joint characteristic function is*

$$\begin{aligned} \langle e^{\mathbf{k} \cdot \phi} \rangle &= \frac{\int_{-\infty}^{\infty} \prod_{i=0}^N d\phi_i \exp \left[-\frac{1}{2} \phi^T \mathbf{G}^{-1} \phi + (\mathbf{k} + \mathbf{h}) \cdot \phi \right]}{\int_{-\infty}^{\infty} \prod_{i=0}^N d\phi_i \exp \left[-\frac{1}{2} \phi^T \mathbf{G}^{-1} \phi + \mathbf{h} \cdot \phi \right]} \\ &= \frac{\det(2\pi \mathbf{G})^{1/2} \exp \left(\frac{1}{2} (\mathbf{k}^T + \mathbf{h}^T) \mathbf{G} (\mathbf{k} + \mathbf{h}) \right)}{\det(2\pi \mathbf{G})^{1/2} \exp \left(\frac{1}{2} \mathbf{h}^T \mathbf{G} \mathbf{h} \right)} \\ &= \exp \left(\sum_{i,j} k_i G_{ij} h_j + \frac{1}{2} \sum_{m,n} k_m G_{mn} k_n \right), \end{aligned} \quad (2.3)$$

because \mathbf{G} is symmetric. Hence we calculate the first and second cumulants, which are the only non-zero cumulants since this expression is quadratic in k_i

$$\langle \phi_j \rangle_c = \frac{\partial}{\partial k_j} \log \langle e^{\mathbf{k} \cdot \phi} \rangle = \sum_i G_{ij} h_i \quad (2.4)$$

$$\langle \phi_i \phi_j \rangle_c = \frac{\partial}{\partial k_i} \frac{\partial}{\partial k_j} \log \langle e^{\mathbf{k} \cdot \phi} \rangle = G_{ij}. \quad (2.5)$$

Consider an arbitrary linear combination $\mathbf{a} \cdot \langle \phi \rangle_c$ and $\mathbf{a}^T \langle \phi \phi \rangle_c \mathbf{a}$ of these cumulants:

$$\begin{aligned}\mathbf{a} \cdot \langle \phi \rangle_c &= \langle \mathbf{a} \cdot \phi \rangle_c = \sum_{i,j} a_i G_{ij} h_j \\ \mathbf{a}^T \langle \phi \phi \rangle_c \mathbf{a} &= \langle \mathbf{a}^T \phi \phi \mathbf{a} \rangle_c = \sum_{i,j} a_i G_{ij} a_j.\end{aligned}$$

Hence comparing this to the right hand side of 2.3, we obtain a useful result for the joint characteristic function:

$$\boxed{\langle e^{\mathbf{a} \cdot \phi} \rangle = e^{\langle \mathbf{a} \cdot \phi \rangle_c + \langle (\mathbf{a} \cdot \phi)^2 \rangle_c / 2}}. \quad (2.6)$$

Expectation values of any product of ϕ 's can be obtained starting from this identity.

Cumulant expansion. It is interesting to note the resemblance of the formula 2.6 to the *cumulant expansion*, where one approximates the quantity $\langle \exp(-S') \rangle_0 := \int \prod_i d\phi_i \exp(-S) \exp(-S')$, with the perturbative action S' being a small compared to the action $S := \frac{1}{2} \phi^T \mathbf{G}^{-1} \phi - \mathbf{h} \cdot \phi$. We can expand the former as

$$\langle e^{-S'} \rangle_0 \approx 1 - \langle S' \rangle_0 + \langle S'^2 \rangle_0 / 2 - \dots.$$

Using $\log(1+x) = x - x^2/2 + \mathcal{O}(x^3)$,

$$\begin{aligned}\log \langle e^{-S'} \rangle_0 &\approx \log(1 - \langle S' \rangle_0 + \langle S'^2 \rangle_0 / 2 - \dots) \\ &\approx -\langle S' \rangle_0 + [\langle S'^2 \rangle_0 - \langle S' \rangle_0^2] / 2 + \dots, \\ \implies \langle e^{-S'} \rangle_0 &= e^{-\langle S' \rangle_0 + [\langle S'^2 \rangle_0 - \langle S' \rangle_0^2] / 2 + \dots} = e^{-\langle S' \rangle_{c,0} + \langle S'^2 \rangle_{c,0} / 2 - \dots}.\end{aligned} \quad (2.7)$$

We thus recognise that the cumulant expansion up to quadratic order becomes exact for perturbations on the Gaussian action given by linear maps on fields.

Wick's theorem.

Consider now $\mathbf{h} = 0$. Obviously, the means involving odd powers of ϕ vanish, thus we are left with

$$\langle e^{\mathbf{a} \cdot \phi} \rangle = e^{\langle (\mathbf{a} \cdot \phi)^2 \rangle / 2}. \quad (2.8)$$

Expanding both sides of this equation in powers of $\{a_i\}$ leads to

$$\begin{aligned}1 + a_i \langle \phi_i \rangle_0 + \frac{a_i a_j}{2} \langle \phi_i \phi_j \rangle_0 + \frac{a_i a_j a_k}{6} \langle \phi_i \phi_j \phi_k \rangle_0 + \frac{a_i a_j a_k a_l}{24} \langle \phi_i \phi_j \phi_k \phi_l \rangle_0 + \dots \\ = 1 + \frac{a_i a_j}{2} \langle \phi_i \phi_j \rangle_0 + \langle \phi_i \phi_j \phi_k \rangle_0 \\ + \frac{a_i a_j a_k a_l}{24} [\langle \phi_i \phi_j \rangle_0 \langle \phi_k \phi_l \rangle_0 + \langle \phi_j \phi_k \rangle_0 \langle \phi_l \phi_i \rangle_0 + \langle \phi_i \phi_k \rangle_0 \langle \phi_j \phi_l \rangle_0] + \dots.\end{aligned} \quad (2.9)$$

Matching powers of $\{a_i\}$ on LHS and RHS, one arrives at the so-called *Wick's theorem*

$$\left\langle \prod_{i=1}^{\ell} \phi_i \right\rangle = \begin{cases} 0, & \text{for } \ell \text{ odd,} \\ \text{sum over all pairwise contractions,} & \text{for } \ell \text{ even.} \end{cases} \quad (2.10)$$

It allows us to simplify the expectation values of products of Gaussian distributed variables $\{\phi_i\}$ into quadratic terms, for example,

$$\langle \phi_i \phi_j \phi_k \phi_l \rangle_0 = \langle \phi_i \phi_j \rangle_0 \langle \phi_k \phi_l \rangle_0 + \langle \phi_j \phi_k \rangle_0 \langle \phi_l \phi_i \rangle_0 + \langle \phi_i \phi_k \rangle_0 \langle \phi_j \phi_l \rangle_0.$$

2.0.2 Functional gaussian integrals

A natural generalisation of 2.1 is given by

$$\begin{aligned} \mathcal{Z} &= \int \mathcal{D}[\phi(\vec{r})] \exp \left[-\frac{1}{2} \int d^d r d^d r' \phi(\vec{r}) G^{-1}(\vec{r}, \vec{r}') \phi(\vec{r}') + \int d^d r h(\vec{r}) \phi(\vec{r}) \right] \\ &= (\det G)^{1/2} \exp \left[\frac{1}{2} \int d^d r d^d r' h(\vec{r}) G(\vec{r}, \vec{r}') h(\vec{r}') \right]. \end{aligned} \quad (2.11)$$

Also analogously we have the joint characteristic function

$$\begin{aligned} &\left\langle \exp \left[\int d^d r k(\vec{r}) \phi(\vec{r}) \right] \right\rangle \\ &= \exp \left[\left\langle \int d^d r a(\vec{r}) \phi(\vec{r}) \right\rangle + \frac{1}{2} \left\langle \int d^d r d^d r' a(\vec{r}) \phi(\vec{r}) a(\vec{r}') \phi(\vec{r}') \right\rangle - \frac{1}{2} \left\langle \int d^d r a(\vec{r}) \phi(\vec{r}) \right\rangle^2 \right], \end{aligned} \quad (2.12)$$

which generates cumulants through functional derivatives

$$\left. \frac{\delta^\gamma \log \mathcal{Z}}{\delta (k(\vec{r}))^\gamma} \right|_{k(\vec{r})=0} = \langle (\phi(\vec{r}))^\gamma \rangle. \quad (2.13)$$

Note that such arguments for the functional integrals are restricted to the gaussian case. In general, there is no systematics for the symbolic manipulation of functional integrals, and one has to define the measure in each case by taking the continuum limit on an underlying *discrete lattice*. Functional integrals are sometimes called path integrals.

Part II

Critical phenomena

Chapter 3

Entropic interactions and computational phase transitions

Include the simulation results from week 3 (also 2?) of Monte Carlo studies.

3.1 Entropic interactions with hard spheres

3.1.1 Asakura-Oosawa depletion interaction

3.2 Hard spheres in 2-d

Chapter 4

Mean-field theory

4.1 Magnetic phase transitions and Weiss mean-field theory

4.1.1 $O(n = 1)$ (Ising) model

The spins have only one degree of freedom, which is chosen to be along the z axis: $\vec{S}_i \rightarrow S_i^z$. The corresponding symmetry is the so called Ising symmetry given by the discrete group $Z_2 = \{\mathbb{1}, R, \text{ with } R^2 = \mathbb{1}\}$. This is the simplest case.

The Weiss mean-field theory [24] regards each spin to be influenced only by the external magnetic field h and the mean value of the spin per particle $\langle S \rangle$. The effective (Weiss) field on a spin with z nearest neighbours is given by $\mu h' = \mu h + zJ\langle S \rangle$. Note that the dimensionality of the problem manifests itself in the number of nearest neighbours $z(d)$. Equivalently, by neglecting the quadratic and further fluctuations on the spins, one gets the mean field hamiltonian:

$$\mathcal{H}_{\text{mf}} = \frac{J}{2} z N \langle S \rangle^2 - \mu h' \sum_i S_i^z = \sum_i \mathcal{H}_1(S_i^z), \quad (4.1)$$

where the single particle hamiltonians are

$$\mathcal{H}_1(S_i^z) = \frac{J}{2} z \langle S \rangle^2 - \mu h' S_i^z. \quad (4.2)$$

Number of possible ways to assign spins ± 1 to N particles on a lattice is

$$g_{\pm} = \frac{N!}{N_-! N_+!} = \binom{N}{N_+}. \quad (4.3)$$

The mean-field partition function for hamiltonian 4.1 is obtained using g_{\pm} in

4.3

$$\begin{aligned}
Z_N(T, h) &= \exp(-\beta N J z \langle S \rangle^2 / 2) \sum_{\{S_i\}} \prod_i e^{\beta \mu h' S_i} \\
&= \exp(-\beta N J z \langle S \rangle^2 / 2) \sum_{\{N_\sigma\}_N} \prod_{\sigma=\pm} \binom{N}{N_+} e^{\beta \mu h' N_\sigma \sigma}. \quad (4.4)
\end{aligned}$$

By the binomial theorem this simplifies as

$$Z_N(T, h) = \exp(-\beta N J z \langle S \rangle^2 / 2) [\exp(\beta \mu h' N_+) + \exp(\beta \mu h' N_-)]^N = Z_1^N, \quad (4.5)$$

where Z_1 is the partition function for the single particle hamiltonian in 4.2

$$\begin{aligned}
Z_1(T, h) &= \exp(-\beta J z \langle S \rangle^2 / 2) \sum_{\sigma=\pm} \exp(\beta \mu h \sigma) \\
&= 2 \exp(\beta J z \langle S \rangle^2 / 2) \cosh \beta \mu h'. \quad (4.6)
\end{aligned}$$

An important point is that the logarithm of this partition function is related to the Gibbs free energy $g(T, h)$ instead of the Helmholtz free energy $f(T, m)$. The reason is that, unlike the non-magnetic gas¹, the magnetic Hamiltonian already contains an external drive due to the external field h , and this corresponds to the Legendre transformation from the variable m to h , hence the free energy is *pre-transformed* from f to g .

For $h = 0$, the internal energy is given by

$$U(T, h = 0) \equiv U_0 = -N \frac{\partial}{\partial \beta} \log Z_1(T, h = 0) = -\frac{zJ}{2} \langle S \rangle^2. \quad (4.7)$$

The mean spin is thus given by

$$\langle S \rangle = \frac{1}{N} \frac{\partial \log Z_N}{\partial \beta \mu h'} = \frac{\partial \log Z_1}{\partial \beta \mu h'} = \tanh \left(\frac{\mu h + z h \langle S \rangle}{k_B T} \right). \quad (4.8)$$

Notice this means that averaging the spin for a single particle is the same as magnetisation per particle, i.e. averaging the spin through all particles in the lattice, or $M = N \langle S \rangle$.

The entropy \mathcal{S} , i.e. the number of possible microstates of this system is given by

$$\mathcal{S} = k_B \log g_{\pm}. \quad (4.9)$$

Recognising that $N = N_+ + N_-$ and $N \langle S \rangle = N_+ - N_- \implies N_{\pm} = N(1 \pm \langle S \rangle)$, and using Stirling's formula, one gets

$$\mathcal{S} \simeq k_B \frac{N}{2} [2 \log 2 - (1 + \langle S \rangle) \log(1 + \langle S \rangle) - (1 - \langle S \rangle) \log(1 - \langle S \rangle)], \quad (4.10)$$

¹Here, the analog of p is h and the analog of V is m .

which is simply the *entropy of mixing*. For small $\langle S \rangle$, we can do a Taylor expansion around $\langle S \rangle = 0$. Using

$$(1 \pm x) \log(1 \pm x) = \pm x + \sum_{n=2}^{\infty} \frac{(\pm x)^n (n-2)!}{n!}$$

$$(1+x) \log(1+x) + (1-x) \log(1-x) = 2 \sum_{n=1}^{\infty} \frac{x^{2n} (2n-2)!}{(2n)!}, \quad (4.11)$$

we get up to quartic order

$$\mathcal{S}/N = k_B \log 2 - k_B \left(\frac{\langle S \rangle^2}{2} + \frac{\langle S \rangle^4}{12} \right) + \mathcal{O}(6). \quad (4.12)$$

The **Bragg Williams approach** considers the simplified mean field hamiltonian $U_0/N = -\frac{1}{2}zJ\langle S \rangle^2$ in the absence of the external field and uses Bogoliubov variational principle $f \leq f_0 + k_B T \langle \mathcal{H} - \mathcal{H}_0 \rangle_0$ to construct the free energy from f_0

$$f_0(T, \langle S \rangle) \equiv \frac{U_0 - T\mathcal{S}}{N}$$

$$= \frac{1}{2}(k_B T - Jz)\langle S \rangle^2 + \frac{k_B T}{12}\langle S \rangle^4 - k_B T \log 2 + \mathcal{O}(6). \quad (4.13)$$

In Figure 4.1, one sees that at the critical isotherm, curvature of the free

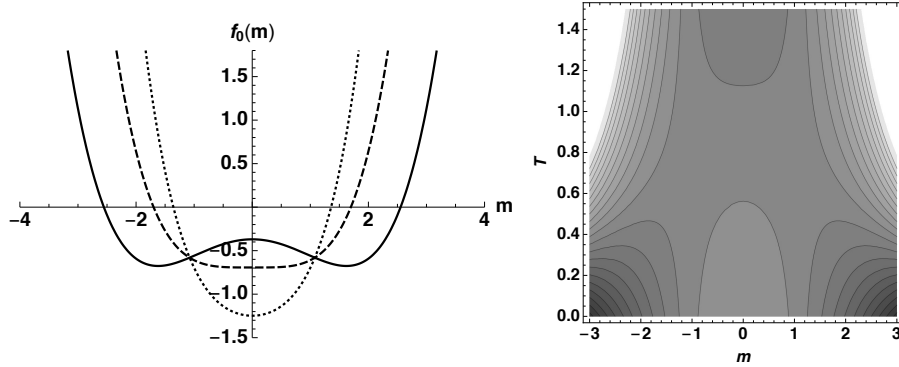


Figure 4.1: Bragg-Williams as free energy a function of average spin $m = \langle S \rangle$ in the absence of an external field. The dashed line is for $T = T_c \equiv Jz/k_B$, the solid line is for $T < T_c$, and the dotted line is for $T > T_c$.

energy changes sign at $\langle S \rangle = 0$. For $T > T_c$ there is a single minima at $\langle S \rangle = 0$, i.e. no magnetisation, but for $T < T_c$ system admits two minima with finite magnetisations. By $\partial_{\langle S \rangle}^2 f_0|_{\langle S \rangle=0} = 0$ one can see that this transition happens at $k_B T = k_B T_c \equiv Jz$. Notice that these minima are always symmetric since the external field is 0. Below T_c , to collectively produce this finite overall magnetisation, the spins undergo a phase transition from a *disordered* phase

with randomly pointing directions that average out the magnetisation, into an *ordered* phase where they choose either + or – direction. Thus we see that the Ising symmetry of the spins is spontaneously broken at $T < T_c$. Inverting 4.8 we get the self consistency equation for $\langle S \rangle$

$$\mu h = k_B T \tanh^{-1} \langle S \rangle - zJ \langle S \rangle. \quad (4.14)$$

We solve the transcendental equation 4.14 to determine the dependence of $\langle S \rangle$ on h and T . Taylor expanding up to the cubic order around $\langle S \rangle$ we get

$$\mu h = k_B T \left(\langle S \rangle + \frac{\langle S \rangle^3}{3} \right) - zJ \langle S \rangle. \quad (4.15)$$

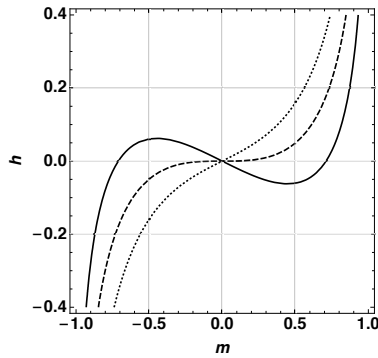


Figure 4.2: Magnetisation m versus the field h . The dashed line is the critical isotherm. Solid line is at $T > T_c$, and dotted line $T < T_c$.

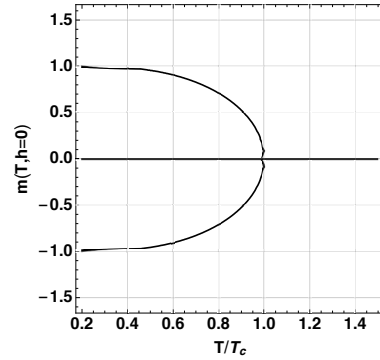


Figure 4.3: The order parameter $m(T)$ in the absence of the external field. 1 denotes the critical temperature T_c .

The sign of the slope of this curve² at $h = 0$, i.e. the inverse magnetic susceptibility χ^{-1} , changes at the critical temperature T_c , below which the system admits two roots at $h = 0$ for $\langle S \rangle$, or the magnetisation. Note that in addition to these, the system also has a solution at $\langle S \rangle = 0$. However, since the free energy f_0 in 4.13 (see Figure 4.1) has a local maxima there, this phase is unstable. This is another indication of *spontaneous symmetry breaking*. This spontaneous magnetisation $m = \mu \langle S \rangle$ is to be regarded as the order parameter for the system. Below T_c , m indicates system's choice of ordered phase, and above T_c it is 0. In fact we see that mean-field theory predicts the existence of a phase transition independent of the dimensionality.

By $\partial_{\langle S \rangle}(h) = 0$, to the first order in $\langle S \rangle$, the critical temperature is found to be

$$T_c = Jz, \quad (4.16)$$

²See Figure 4.2 for a plot of the numerical solution.

in agreement with the Bragg-Williams result. We see that the T_c increases with increasing number of nearest neighbours. z is roughly proportional to $2d$, the dimensionality of crystal. This suggests that the system gets in the ordered phase more easily in higher dimensions.

This enables us to obtain physical details about the magnetic phase transition by investigating the properties of the order parameter m near T_c . First, we look at the dependence on temperature in the absence of the external field. From 4.15, one obtains

$$\langle S \rangle^2(T, h = 0) = 3 \frac{T_c}{T} \left(1 - \frac{T}{T_c} \right),$$

$$m(T, h = 0) = \mu \langle S \rangle(T \approx T_c, h = 0) \approx \pm \sqrt{3} \sqrt{1 - \frac{T}{T_c}}.$$

If we define $\tau \equiv \sqrt{1 - \frac{T}{T_c}}$, we get

$$m(\tau, h = 0) \propto \pm |\tau|^\beta, \quad (4.17)$$

where $\beta = 1/2$ is the mean-field critical exponent at $h = 0$. Note that same result can be obtained by minimising the free energy f_0 in 4.13 below T_c . This is plotted in Figure 4.3. Note again that the $\langle S \rangle$ solution is unstable as seen from the free energy 4.13.

Secondly, we seek the dependence of m on h on the critical isotherm. From 4.15, in $T = T_c$, one obtains

$$\langle S \rangle(T = T_c, h) = (3\mu)^{1/3} h^{1/3}$$

$$\rightarrow m(T = T_c, h) \propto h^{1/\delta}, \quad (4.18)$$

with $1/\delta = 1/3$ being the critical exponent on the critical isotherm.

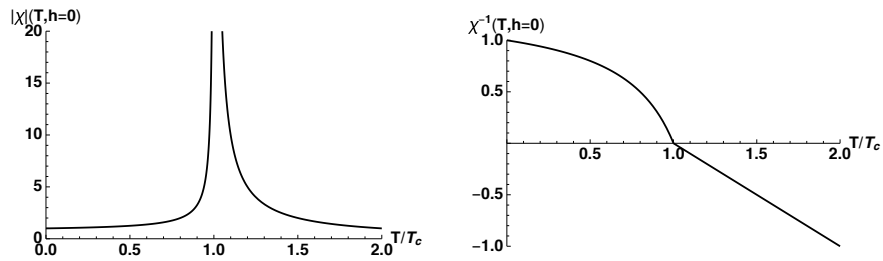


Figure 4.4: Dependence of magnetic susceptibility in temperature in the absence of an external field.

The scaling of the magnetic susceptibility can be obtained from 4.15, via $\chi^{-1} = -V \partial_{\langle S \rangle} (h/\mu)$.

$$\chi^{-1}(T, h) = \frac{V k_B T_c}{\mu^2} \left(1 - \frac{T}{T_c} \right) - \frac{V k_B T}{\mu^2} \langle S \rangle^2. \quad (4.19)$$

At $T > T_c$, $m = \langle S \rangle = 0$, thus we have

$$\begin{aligned}\chi^{-1}(T > T_c, h) &= \frac{Vk_B T_c}{\mu^2} \tau = \kappa \tau \\ \chi(T > T_c, h) &\propto \frac{1}{\tau^{\gamma_+}}, \quad \text{with } \gamma_+ = 1.\end{aligned}\tag{4.20}$$

At $T < T_c$, $m \neq 0$, but from 4.17, we have $\langle S \rangle^2 = 3\tau$

$$\begin{aligned}\chi^{-1}(T < T_c) &= \frac{Vk_B}{\mu^2} (T_c - 3T) \left(1 - \frac{T}{T_c}\right) \\ \rightarrow \chi^{-1}(T \lesssim T_c) &= -2 \frac{Vk_B T_c}{\mu^2} \left(1 - \frac{T}{T_c}\right) = -2\kappa \tau \\ \rightarrow \chi(T \lesssim T_c) &\propto \frac{1}{\tau^{\gamma_-}}, \quad \text{with } \gamma_- = 1.\end{aligned}\tag{4.21}$$

Hence we see that in both left and right proximity of T_c , one gets the same critical exponent $\delta_{\pm} = \delta = 1$ for magnetic susceptibility. Note that the divergence of susceptibility near phase transition is a universal behaviour.

Finally, from the free energy f_0 in 4.13, we can calculate the specific heat $c_v \equiv \frac{\partial_T Q|_V}{N}$ at $h = 0$. Since $dS = \frac{\delta Q}{T}$, we have that $\partial_T S|_V = \frac{N c_v}{T}$. $-\partial_T F = S$, thus

$$c_v(T, h = 0) = -T \frac{\partial^2 f_0}{\partial T^2}.\tag{4.22}$$

For $T > T_c$, $\langle S \rangle = 0$, thus

$$\begin{aligned}f_0(T > T_c) &= -k_B T \log 2 \\ \rightarrow c_v(T > T_c, h = 0) &= 0\end{aligned}\tag{4.23}$$

For $T < T_c$, $\langle S \rangle^2 = 3\tau$, then

$$\begin{aligned}f_0(T < T_c) &= -\frac{3k_B T_c}{2} \tau^2 + \frac{3k_B T}{4} \tau^2 - k_B T \log 2 \\ &= -\frac{3k_B T_c}{4} (\tau^3 + \tau^2) - k_B T \log 2 \\ c_v(T < T_c, h = 0) &= -\frac{T}{T_c^2} \frac{\partial^2 f_0(T < T_c)}{\partial \tau^2} \\ \rightarrow c_v(T < T_c, h = 0) &= \frac{3k_B}{2} \frac{T}{T_c} (3\tau + 1)\end{aligned}\tag{4.24}$$

Hence we conclude that $c_v \propto |\tau|^{\alpha_{\pm}}$, with $\alpha_+ = 0$, and $\alpha_- = 1$. Note that, as a convention, we choose the $\alpha = 0$ exponent which denotes a *jump discontinuity*.

4.1.2 $O(n \geq 2)$ model

The mean-field ansatz for spins with $n \geq 2$ degrees of freedom is

$$\mu \vec{h}' = \mu \vec{h} + zJ \langle \vec{S} \rangle,\tag{4.25}$$

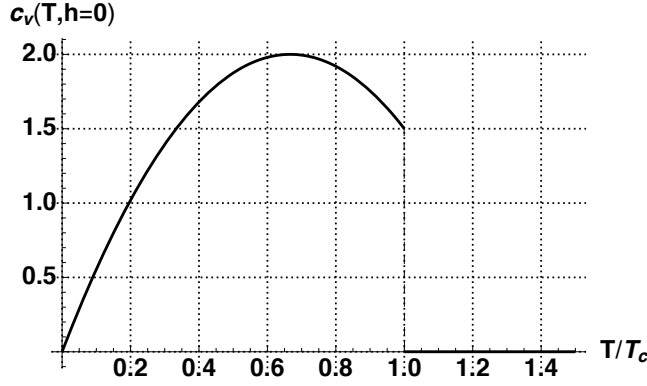


Figure 4.5: Heat capacity exhibits a jump discontinuity at $T = T_c$ in the absence of an external field.

where $\vec{h}, \vec{S} \in \mathbb{R}^n$. Since the hamiltonian is a sum of single particle hamiltonians, $Z_N = Z_1^{N^3}$, and the corresponding statistical mechanics can again be calculated from the single particle partition function

$$Z_1 \propto \int d\Omega e^{\beta\mu\vec{h}' \cdot \vec{S}}. \quad (4.26)$$

Using the solid angle differential $d\Omega$ in n -dimensions, one gets the self consistency equation for $\langle \vec{S} \rangle$ by

$$\langle \vec{S} \rangle = \frac{\partial Z_1}{\partial \beta\mu\vec{h}} = \frac{\int d\Omega e^{\beta\mu\vec{h}' \cdot \vec{S}} \vec{S}}{\int d\Omega e^{\beta\mu\vec{h}' \cdot \vec{S}}} \quad (4.27)$$

From now on we assume $\vec{h} = h\hat{e}_x$.

XY model, $O(2)$

$S^x = \cos \phi$. The mean given by 4.27 is

$$\langle S^x \rangle = \frac{\int d\phi e^{\beta\mu\vec{h}'_x \cos \phi} \cos \phi}{\int d\phi e^{\beta\mu\vec{h}'_x \cos \phi}}. \quad (4.28)$$

Since the modified Bessel functions I_α are defined by

$$I_\alpha = \frac{1}{\pi} \int d\phi e^{x \cos \phi} \cos \alpha \phi - \frac{\sin \alpha \pi}{\pi} \int dt e^{-x \cosh t - \alpha t}, \quad (4.29)$$

we simply have

$$\langle S^x \rangle = \frac{I_1[\beta(\mu h_x + zJ\langle S^x \rangle)]}{I_0[\beta(\mu h_x + zJ\langle S^x \rangle)]}. \quad (4.30)$$

³In this case, this is proven by the multinomial theorem.

Heisenberg model, $O(3)$

$$S^x = \cos \Theta,$$

$$\langle S^x \rangle = \frac{\int \int d\phi d \cos \Theta e^{\beta \mu \tilde{h}'_x \cos \Theta} \cos \Theta}{\int \int d\phi d \cos \Theta e^{\beta \mu \tilde{h}'_x \cos \Theta}}. \quad (4.31)$$

Defining $\alpha = \mu h'_x \cos \Theta = kx$, with $\cos \Theta = x$,

$$\begin{aligned} \langle S^x \rangle &= \frac{\frac{1}{k^2} \int_{-k}^k d\alpha \alpha e^{\beta \alpha}}{\frac{1}{k} \int_{-k}^k d\alpha e^{\beta \alpha}} = \frac{1}{k} \frac{\partial}{\partial \beta} (k \sinh \beta k / \beta) \\ &= \coth [\beta(\mu h_x + zJ \langle S^x \rangle)] - \frac{1}{\beta(\mu h_x + zJ \langle S^x \rangle)}. \end{aligned} \quad (4.32)$$

The numerical solution for equations 4.30 and 4.32 are given in Figure 4.6.

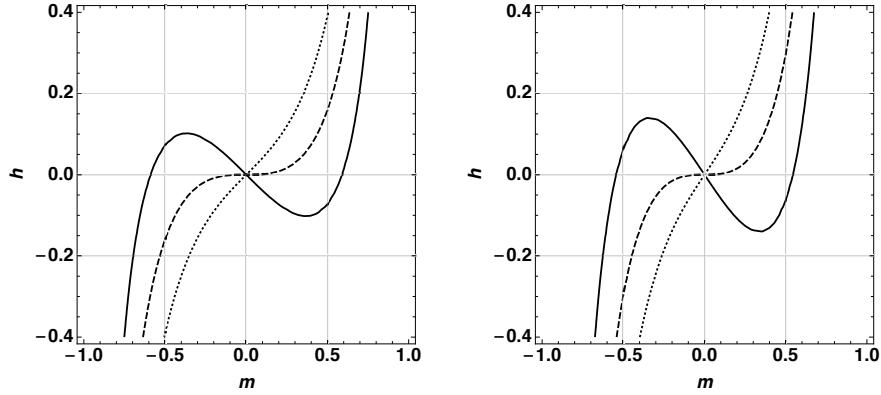


Figure 4.6: The order parameter m as a function of the external field h for the XY model (left) and for the Heisenberg model (right). We see that the qualitative behaviour of $O(n = 1, 2, 3)$ are equivalent in mean-field theory.

It is found that⁴

$$k_B T_c = J \frac{2d}{n}. \quad (4.33)$$

The critical temperature increases with increasing dimensionality d , and it decreases with increasing number of degrees of freedom n for the spins. The latter is due to the fact that the system has more possibilities to become disordered for higher n .

On the other hand, the qualitative behaviour of the mean-field theory results are *superuniversal*, i.e., the critical exponents are the same regardless of both d and n . Furthermore, it predicts a phase transition at a finite critical temperature in all 9 cases, which is inaccurate. Nevertheless, it is also worthwhile to note that mean-field theory is exact when the number of nearest neighbours is sufficiently large to support the mean-field, e.g. in fractal geometries and in $d \geq 4$.

⁴Note that if one considers an arbitrary spin amplitude S , the mean-field critical temperature is given by $k_B T_c = S^2 J \frac{2d}{n}$.

Quantum Heisenberg model

If the spins are quantised, then the spin S along the quantisation axis chosen as the magnetisation axis \vec{m} can only take the values

$$m_S = -S, -S + 1, \dots, S - 1, S.$$

We define the mean-field hamiltonian in the same way as done in the previous subsections

$$\mathcal{H}_{\text{mf}} = \sum_i \left(J \frac{z}{2} \langle S \rangle^2 - Jz \langle \vec{S} \rangle \cdot \vec{S}_i \right),$$

where to account for all interactions, we have replaced the sum over nearest neighbours with a half sum over all spins times the number of nearest neighbours z for each of them. We shall denote $\langle \vec{S} \rangle$ by \vec{m} from now on. We again have the partition function for the single particle hamiltonians

$$\begin{aligned} Z_1 &= \sum_{\{\vec{S}_i\}} \exp \left[-\beta J \frac{z}{2} \left(m^2 - 2\vec{m} \cdot \vec{S}_i \right) \right] \\ &= \exp(-\beta J \frac{z}{2} m^2) \sum_{x=-S}^S \exp(\beta J z m x), \quad S \in \mathbb{Z} \\ &= \exp \left(-\beta J \frac{z}{2} m^2 \right) \frac{\sinh \left[\frac{\beta J z}{2} m (2S + 1) \right]}{\sinh \left(\frac{\beta J m z}{2} \right)}. \end{aligned} \quad (4.34)$$

Note that if $S = \frac{1}{2}$, this is the same as the classical mean-field partition function for the Ising model 4.6.

The free energy is given by

$$\begin{aligned} f(T, m) &= -k_B T \log Z_1 \\ &= \frac{1}{2} J z m^2 - k_B T \log \left[\sinh \left(\frac{\beta z J m}{2} (2S + 1) \right) \right] + k_B T \log \left[\sinh \left(\frac{\beta z J m}{2} \right) \right]. \end{aligned} \quad (4.35)$$

By minimising f with respect to m , we get the self consistency relation for m , i.e. we get the possible states that relate the temperature and the magnetisation of the system:

$$0 = \frac{\partial f}{\partial m} = J z m - \frac{1}{2} (2S + 1) \coth \left[\frac{\beta J z m}{2} (2S + 1) \right] + \frac{1}{2} \coth \left[\frac{\beta J z m}{2} \right] \quad (4.36)$$

$$= J z m - J z S B_S(\beta J z m S). \quad (4.37)$$

Note that the RHS is the Brillouin function $B_S(x)$. It is clear from the plot 4.1.2 that we get another occurrence of a spontaneous symmetry breaking at a critical temperature T_c where system suddenly starts to admit two degenerate

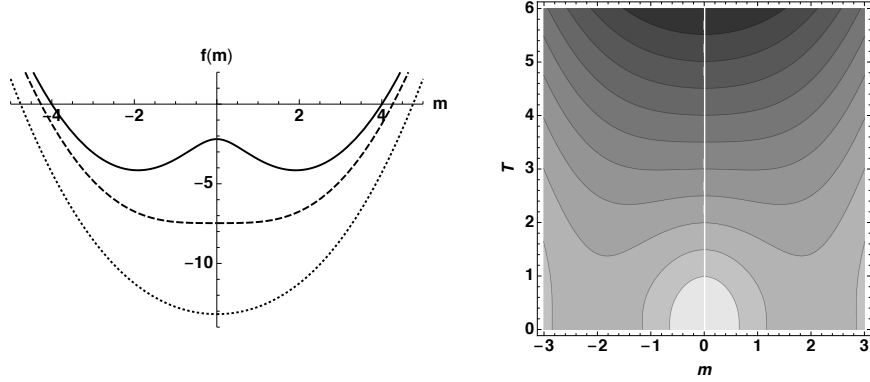


Figure 4.7: The plot of quantum Heisenberg mean-field free energy for $S = 4$. In the left figure, the dashed line is for $T = T_c \equiv Jz/k_B$, the solid line is for $T < T_c$, and the dotted line is for $T > T_c$.

states with finite magnetisations of opposite sign. Thus, as before, T_c is the temperature where the curvature $\partial_m^2 f$ of the curve changes sign at point $m = 0$.

$$0 = \frac{\partial^2 f}{\partial m^2} = zJ - zJS \frac{\partial B_S(\beta_c JzmS)}{\partial m} \quad (4.38)$$

We expand the Brillouin function up to third order in m :

$$B_S(x) \simeq \frac{x}{3} \left(\frac{S+1}{S} \right) - \frac{x^3}{90} \frac{2S^2 + 2S + 1}{S^2}. \quad (4.39)$$

Therefore, inserting this expression in 4.38, we obtain the critical temperature

$$k_B T_c = \frac{JzS(S+1)}{3}. \quad (4.40)$$

Observe that $S = \frac{1}{2}$ we get $\frac{k_B T_c}{Jz} = \frac{1}{4}$, whereas in the classical Heisenberg mean-field model one gets $\frac{k_B T_c}{Jz} = \frac{1}{12}$. The reason for the higher T_c in the quantum case is the reduced degree of freedom of the spins due to the discrete symmetry along the quantisation axis, as opposed to the continuous symmetry in the classical case.

Using the self consistency equation and the expansion of $B_S(\beta JzmS)$ around $m = 0$, we get the behaviour of the magnetisation around $T = T_c$ with the same mean-field critical exponent $\beta = \frac{1}{2}$:

$$m \propto \left(1 - \frac{T}{T_c} \right)^\beta. \quad (4.41)$$

4.2 Liquid-gas transition and the van der Waals mean-field theory

Focus on $p - V$ diagram. Hysteresis: characteristic of 1st order transitions. Supercooling and superheating due to metastable phases which are terminated by spinodals (draw $g - p$ diagram!!), compare with magnetic hysteresis! **What happens for a gas in the *multivalued region* and let the system equilibrate?...**

4.2.1 van der Waals equation of state

Derivation from microscopic analysis? Use Lennard-Jones potential for the interparticle interaction, and modify the ideal (non-interacting) gas Gibbs free energy in the microcanonical ensemble using this potential and also by considering the finite volume of each particle! Then use V as a constrained parameter for G (G has natural variable p) and minimize wrt. V to get the equation of state. See exercise 4.2 !!

The heuristics for the van der Waals equation of state is built upon the equation of state for the ideal gas $pv = RT$, where v is the volume per particle. The idea is that we account for the finite size of the atoms resulting in a total reduction b in the volume per particle. Secondly, we take into account the short ranged attractive interaction between the atoms which reduce the pressure on the boundary of the gas which constitutes its volume, since it has no particle which it is attracted to on the other side of the boundary. We consider a mean field theory, where all particles mutually interact, and hence the interaction scales with the number of pairings between particles per unit volume $U_{\text{mf}} = -a\frac{N^2}{V}$. Hence the reduction in pressure is given by this interaction per volume, $\Delta p \sim \frac{\partial U_{\text{mf}}}{\partial V} = a\frac{N^2}{V^2} = \frac{a}{v^2}$. The resulting equation is

$$(v - b) \left(p + \frac{a}{v^2} \right) = RT. \quad (4.42)$$

Microscopic derivation A precise derivation of the van der Waals equation of state from a microscopical analysis can be achieved starting from a modified Gibbs potential, where we consider the volume reduction and an additional mutual interaction as the Lennard-Jones potential

$$V_{\text{LJ}}(r) = 4\epsilon \left[\left(\frac{\sigma}{r} \right)^{12} - \left(\frac{\sigma}{r} \right)^6 \right]. \quad (4.43)$$

finish the derivation using the solution of 4th exercise sheet.

4.2.2 Universal form

4.2.3 The Maxwell construction

The presentation script in the exercise class is already handwritten. Includes the explanation of the necessity of Maxwell's construction (or correction): to

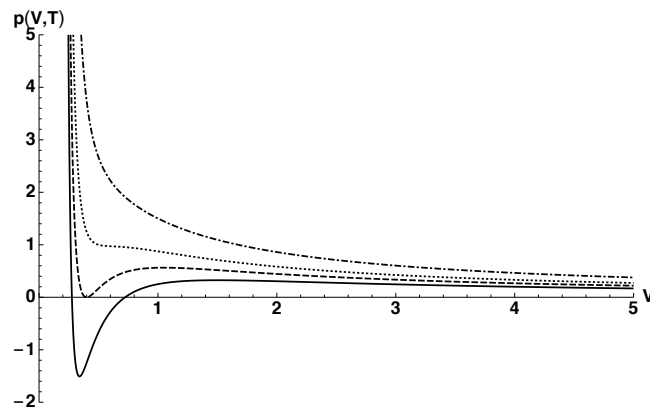


Figure 4.8: Lennard-Jones potential

avoid the negative compressibility region. Explain using (constraint) Gibbs free energy diagram (which only shows the equilibrium points as the minima, the non-minimal points are non-equilibrium). Show that the convex continuation of the free energy directly corresponds to the Maxwell construction $\mu_1 = \mu_2$.

4.2.4 The critical region of van der Waals model

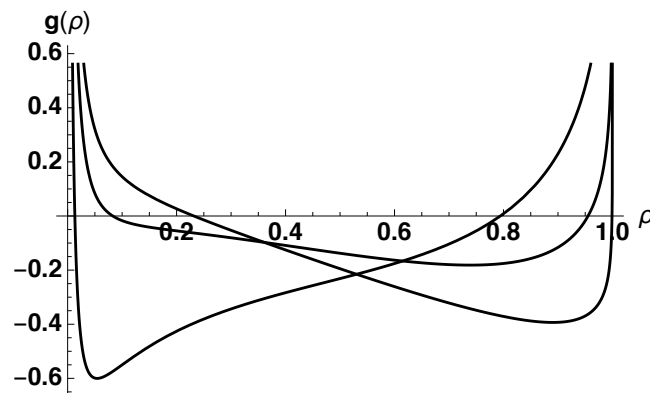


Figure 4.9:

Lorem ipsum dolor sit amet, consectetur adipiscing elit. Etiam lobortis facilisis sem. Nullam nec mi et neque pharetra sollicitudin. Praesent imperdiet mi nec ante. Donec ullamcorper, felis non sodales commodo, lectus velit ultrices augue, a dignissim nibh lectus placerat pede. Vivamus nunc nunc, molestie ut, ultricies vel, semper in, velit. Ut porttitor. Praesent in sapien. Lorem ipsum dolor sit amet, consectetur adipiscing elit. Duis fringilla tristique neque. Sed interdum libero ut metus. Pellentesque placerat. Nam rutrum augue a

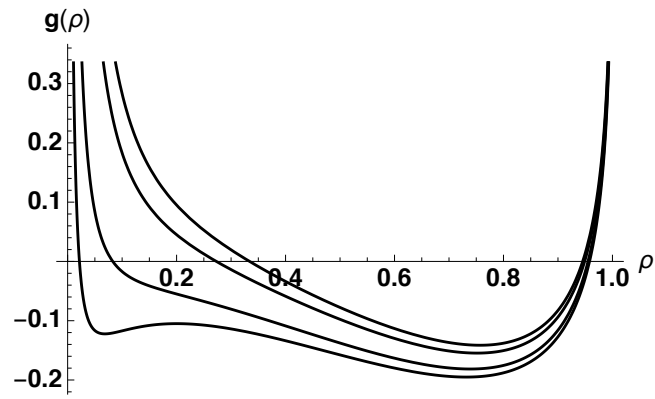


Figure 4.10:

leo. Morbi sed elit sit amet ante lobortis sollicitudin. Praesent blandit blandit mauris. Praesent lectus tellus, aliquet aliquam, luctus a, egestas a, turpis. Mauris lacinia lorem sit amet ipsum. Nunc quis urna dictum turpis accumsan semper.

Chapter 5

Spin models and analytical methods

5.1 Ising model

5.1.1 1-d Ising model transfer matrix solution

Emphasise that the transfer matrix method used here resembles the RG solution of the problem.

We use periodic boundary conditions, $S_N = S_1$. $d = 1$ Ising hamiltonian is

$$\begin{aligned}\mathcal{H}(J, h) &= - \sum_{k=1}^N (JS_k S_{k+1} + \mu h S_k) \\ &= - \sum_{k=1}^N [JS_k S_{k+1} + \frac{\mu h}{2} (S_k + S_{k+1})].\end{aligned}\quad (5.1)$$

The partition function is a sum over all possible spin configurations $\{S_i\}$

$$Z_N(\beta, h) = \sum_{\{S_k\}} \prod_{k=1}^N \exp \left\{ \beta \left[JS_k S_{k+1} + \frac{\mu h}{2} (S_k + S_{k+1}) \right] \right\}$$

We introduce the transfer matrix,

$$T \equiv \begin{pmatrix} e^{\beta(J+\mu h)} & e^{-\beta J} \\ e^{-\beta J} & e^{\beta(J-\mu h)} \end{pmatrix}, \quad \langle S|T|S' \rangle = \exp \left(\beta [JS S' + \frac{\mu h}{2} (S + S')] \right). \quad (5.2)$$

T gives the Boltzmann factor for interaction of the neighbouring spins and their

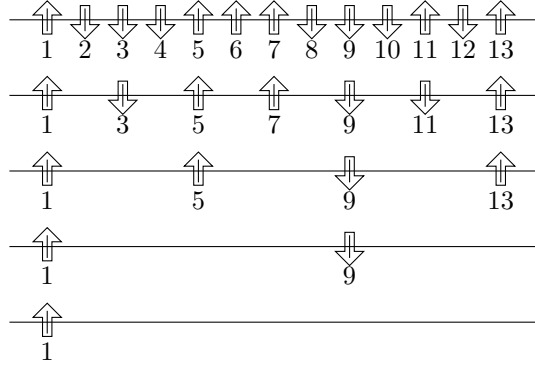


Figure 5.1: Informal picture for the decimation procedure applied in the transfer matrix method for the 1-d Ising model. The fact that the consecutive steps of combining spins into *blocks* preserve the partition function implies the form invariance of $T[\{K\}] \rightarrow T^b[\{K\}] = T[\{K'\}]$ over coarse graining and rescaling (renormalisation), where $\{K\}$ and $\{K'\}$ are the set of coupling coefficients in the original and the coarse grained scale, respectively.

coupling to the external field. Using T , we can simplify Z_N

$$\begin{aligned}
 Z_N &= \sum_{\{S_k\}} \prod_{k=1}^N \langle S_k | T | S_{k+1} \rangle \\
 &= \sum_{S_1=\pm 1} \cdots \sum_{S_{N-1}=\pm 1} \langle S_1 | T | S_2 \rangle \cdots \langle S_{N-2} | T | S_{N-1} \rangle \langle S_{N-1} | T | S_1 \rangle \\
 &= \sum_{S_1=\pm 1} \langle S_1 | T^N | S_1 \rangle = \text{Tr } T^N,
 \end{aligned} \tag{5.3}$$

where we used the resolution of identity. [What is the physical meaning of this transfer matrix? See Figure 5.1](#) The physical picture here is that we start with a 1-dimensional lattice with nearest neighbour couplings, and successively sparse the lattice by only taking each next spin and dropping the ones in between, modifying the interaction accordingly until we eventually end up with only one spin i.e. $T \rightarrow T^2 \rightarrow T^3 \rightarrow \cdots T^N$. This is analogous to the coarse-graining procedure which is used in the renormalisation group theory treatment.

Assuming that T is diagonalisable, we have $T = U^{-1} \Lambda U$, where Λ is a diagonal matrix with the eigenvalues λ_i of T . Then we have

$$\begin{aligned}
 \text{Tr}(T^N) &= \text{Tr}(U^{-1} \Lambda U U^{-1} \Lambda U \cdots U^{-1} \Lambda U) \\
 &= \text{Tr}(U^{-1} \Lambda^N U) \\
 &= \text{Tr}(U U^{-1} \Lambda^N) = \text{Tr}(\Lambda^N) = \sum_i \langle i | \Lambda^N | i \rangle,
 \end{aligned}$$

where in the last line we used the cyclic property of trace. $\Lambda = \sum_i |i\rangle \langle i| \lambda_i$,

$\Lambda^N = \sum_i |i\rangle\langle i| \lambda_i^N$. Thus

$$Z_N = \text{Tr}(T^N) = \sum_i \lambda_i^N = \lambda_+^N + \lambda_-^N. \quad (5.4)$$

Assuming $\lambda_+ > \lambda_-$, in the thermodynamic limit $N \rightarrow \infty$ $\lambda_+^N \gg \lambda_-^N$, thus we have

$$Z_N \simeq \lambda_+^N,$$

and the eigenvalues of the transfer matrix are obtained by a standard calculation

$$\lambda_{\pm} = e^{\beta J} \left[\cosh \beta \mu h \pm \sqrt{\sinh^2 \beta \mu h + e^{-4\beta J}} \right].$$

Thereby we finally arrive at the intended result

$$Z_N(\beta, h) \simeq e^{\beta J N} \left[\cosh \beta \mu h + \sqrt{\sinh^2 \beta \mu h + e^{-4\beta J}} \right]^N. \quad (5.5)$$

Note that in the absence of an external field the exact expression reduces to

$$Z_N(\beta, h = 0) = (2 \cosh \beta J)^N + (2 \sinh \beta J)^N. \quad (5.6)$$

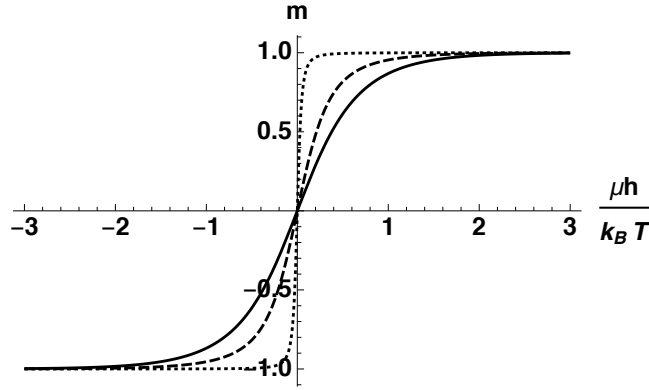


Figure 5.2: The magnetisation $m\left(\frac{\mu h}{k_B T}\right)$ at $\frac{J}{k_B T} = 0.2$ (solid), $\frac{J}{k_B T} = 0.5$ (dashed), $\frac{J}{k_B T} = 1.5$ (dotted). We see that when the thermal energy scale is smaller than the one of external field (left and right sides of the figure), there is driven magnetisation. There is no magnetisation in the absence of an external field. If the spin-spin interaction energy is comparable to the thermal energy scale, we see that the magnetisation occurs more steeply, which exhibits the competition between randomness and the external drive in the presence of an external field.

The Gibbs free energy per particle g in the thermodynamic limit is

$$\begin{aligned}
 g(T, h) &= -k_B T \lim_{N \rightarrow \infty} \frac{\log Z_N}{N} \\
 &= -k_B T \lim_{N \rightarrow \infty} \frac{\log(\lambda_+^N + \lambda_-^N)}{N} \\
 &= -k_B T \lim_{N \rightarrow \infty} \frac{\log \left[1 + \left(\frac{\lambda_+}{\lambda_-} \right)^N \right]}{N} - k_B T \log \lambda_+ = -k_B T \log \lambda_+ \\
 &= -J - k_B T \log \left[\cosh \beta \mu h + \sqrt{\sinh^2 \beta \mu h + e^{-4\beta J}} \right]. \quad (5.7)
 \end{aligned}$$

The magnetisation is

$$m(T, h) = -\frac{1}{V} \frac{\partial g(T, h)}{\partial h} = \frac{\mu}{V} \frac{\sinh \left(\frac{\mu h}{k_B T} \right)}{\sqrt{\sinh^2 \left(\frac{\mu h}{k_B T} \right) + e^{-4 \frac{J}{k_B T}}}}. \quad (5.8)$$

We see that on contrary to the mean field prediction, $m \rightarrow 0$ as $h \rightarrow 0$, i.e. no spontaneous magnetisation.

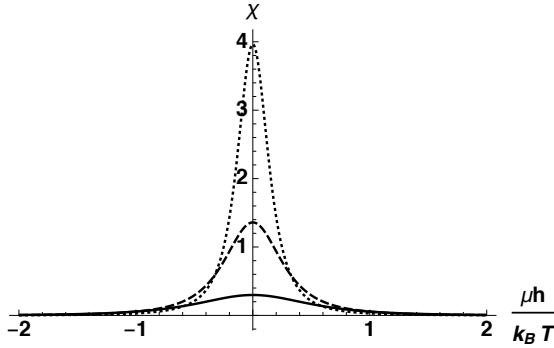


Figure 5.3: Magnetic susceptibility $\chi \left(\frac{\mu h}{k_B T} \right)$ at $\frac{J}{k_B T} = 0.2$ (solid), $\frac{J}{k_B T} = 0.5$ (dashed), $\frac{J}{k_B T} = 0.8$ (dotted). It diverges as $T \rightarrow 0$, signalling a $T = 0$ phase transition, i.e. no phase transition.

The magnetic susceptibility is

$$\chi(T, h) = \frac{\partial m}{\partial h} = \frac{\mu^2}{V J k_B T} \frac{\cosh \left(\frac{\mu h}{k_B T} \right)}{\sqrt{\sinh^2 \left(\frac{\mu h}{k_B T} \right) + e^{-4 \frac{J}{k_B T}}}}. \quad (5.9)$$

In the absence of an external field one gets

$$\chi_0(T) \equiv \chi(T, h = 0) = \frac{\mu^2}{V J} \frac{J e^{2 \frac{J}{k_B T}}}{k_B T}. \quad (5.10)$$

Observe that $\chi \rightarrow \infty$ as $T \rightarrow 0$, indicating $T_c = 0$, or in other words, no phase transition.

Let us now focus on the $h = 0$ case. Defining $K = \beta J$, the transfer matrix becomes

$$T_0 := T(h = 0) = \begin{pmatrix} e^K & e^{-K} \\ e^{-K} & e^K \end{pmatrix}. \quad (5.11)$$

We define the transformed spin $\sigma := \frac{S+1}{2} \in \{1, 0\}$ to calculate the matrix element

$$\begin{aligned} T_0(S, S') &:= \langle S|T_0|S' \rangle = (\sigma \quad 1 - \sigma) \begin{pmatrix} e^K & e^{-K} \\ e^{-K} & e^K \end{pmatrix} \begin{pmatrix} \sigma' \\ 1 - \sigma' \end{pmatrix} \\ &= 4\sigma\sigma' \sinh K - 2 \sinh K(\sigma + \sigma') + e^K \\ &= SS' \sinh K + \cosh K \\ &= \cosh K(1 + SS' \tanh K). \end{aligned} \quad (5.12)$$

Furthermore, for the purposes of the upcoming part, we diagonalise T_0 explicitly

$$T_0 = \frac{1}{\sqrt{2}} \begin{pmatrix} 1 & -1 \\ 1 & 1 \end{pmatrix} \begin{pmatrix} 2 \cosh K & 0 \\ 0 & 2 \sinh K \end{pmatrix} \frac{1}{\sqrt{2}} \begin{pmatrix} 1 & 1 \\ -1 & 1 \end{pmatrix}. \quad (5.13)$$

Hence

$$\begin{aligned} T_0^n &= \frac{1}{\sqrt{2}} \begin{pmatrix} 1 & -1 \\ 1 & 1 \end{pmatrix} \begin{pmatrix} 2^n \cosh^n K & 0 \\ 0 & 2^n \sinh^n K \end{pmatrix} \begin{pmatrix} 1 & 1 \\ -1 & 1 \end{pmatrix} \\ T_0^n(S, S') &= \frac{1}{2} (\sigma \quad 1 - \sigma) T_0^n \begin{pmatrix} \sigma' \\ 1 - \sigma' \end{pmatrix} \\ &= \frac{1}{2} (1 \quad -S) \begin{pmatrix} 2^n \cosh^n K & 0 \\ 0 & 2^n \sinh^n K \end{pmatrix} \begin{pmatrix} 1 \\ -S' \end{pmatrix} \\ &= 2^{n-1} \cosh^n K (1 + SS' \tanh^n K), \end{aligned} \quad (5.15)$$

where we used that

$$\frac{1}{\sqrt{2}} \begin{pmatrix} 1 & 1 \\ -1 & 1 \end{pmatrix} \begin{pmatrix} \sigma \\ 1 - \sigma \end{pmatrix} = \frac{1}{\sqrt{2}} \begin{pmatrix} 1 \\ 1 - 2\sigma \end{pmatrix} = \frac{1}{\sqrt{2}} \begin{pmatrix} 1 \\ -S \end{pmatrix}.$$

Please keep in mind that $T_0^a(S, S')T_0^b(S, S') \neq T_0^{a+b}(S, S')$. Also, as it can be seen from 5.6, for $N \gg 1$, the partition function is $Z_N \simeq (2 \cosh K)^N$.

Using these results, we can calculate the spin-spin correlator, or the Green's function $\langle S_i S_j \rangle \equiv G(i - j)$ for this simpler special case. Given that $i - j = n$, we can take advantage of the translational symmetry

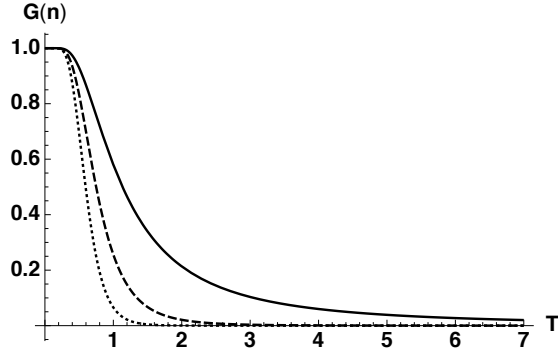


Figure 5.4: The dependence of the spin-spin correlator, or the Green's function $G(n)$ for the 1-d Ising model on the temperature T for different distances n . The solid curve is for $n = 2$, dashed curve is for $n = 5$ and dotted curve is for $n = 10$.

$$\begin{aligned}
\langle S_i S_j \rangle &= \langle S_1 S_{n+1} \rangle \equiv G(n) \\
&= \frac{1}{Z_N} \sum_{S_k} \prod_k S_1 S_{n+1} \langle S_k | T_0 | S_{k+1} \rangle \\
&= \frac{1}{Z_N} \sum_{S_1, S_{n+1}} S_1 T_0^n(S_1, S_{n+1}) S_{n+1} T_0^{N-n}(S_{n+1}, S_1) \\
&= \frac{1}{Z_N} \sum 2^{N-2} S_1 S_{n+1} \cosh^N K (1 + S S' \tanh^n K) (1 + S S' \tanh^{N-n} K) \\
&= \frac{1}{Z_N} (2 \cosh K)^N [\tanh^n K + \tanh^{N-n} K] \\
&\simeq \tanh^n K,
\end{aligned} \tag{5.16}$$

where in the last step we have assumed $N \gg 1$ and taken advantage of the fact that $\tanh K < 1 \implies \tanh^N K \rightarrow 0$. Thus we have found that the correlator (Green's function) decays more rapidly with increasing T as the distance n is increased (see Figure 5.4).

By definition $G(n)$ depends on the correlation length ξ in the following way

$$\begin{aligned}
G(n) &\equiv e^{-n/\xi} = \tanh^n K \\
\implies \xi &= -\frac{1}{\ln(\tanh K)}.
\end{aligned} \tag{5.17}$$

Recall that had found that $T_c = 0$ for the 1-d Ising model. Thus, we can find the behaviour of the correlation length near criticality as $K \rightarrow \infty$

$$\begin{aligned}
\xi^{-1}(T \rightarrow 0) &\stackrel{K \rightarrow \infty}{\equiv} -\ln(\tanh K) \\
&= [\ln e^K + \ln(1 + e^{-2K}) - \ln e^K - \ln(1 - e^{-2K})] \\
&\simeq e^{-2K} - (-e^{-2K}) = 2e^{-2K} \\
\implies \xi(T \rightarrow \infty) &\approx \frac{1}{2} e^{2K},
\end{aligned} \tag{5.18}$$

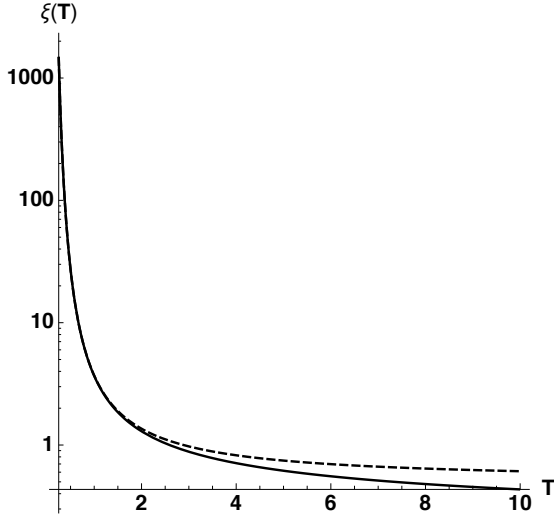


Figure 5.5: The correlation length $\xi(T)$ diverges as one approaches $T = 0$. This log-plot shows the criticality of the system at $T = 0$. We also note that the divergence of ξ with increasing T is very well approximated by the exponential $\frac{1}{2}e^{2K}$ (dashed curve).

which diverges at $T = T_c = 0$ as it should (see Figure 5.5).

We can also relate χ and G via the linear response argument (Kubo)

$$\begin{aligned} k_B T \chi(q=0) &= G(q=0) \stackrel{\mathcal{F}(G)}{=} \sum_{n=-\infty}^{\infty} G(n) = 2 \sum_{n=0}^{\infty} \tanh^n K - 1 \\ &= \frac{1 + \tanh K}{1 - \tanh K} \stackrel{\mathcal{F}(G)}{\rightarrow} e^{2K} \propto \xi, \end{aligned} \quad (5.19)$$

where \mathcal{F} stands for the Fourier transform.

We can also analyse the behaviour of g near $T \rightarrow T_c = 0$. From 5.7, we have

$$\begin{aligned} g(T, h=0) &= -J - k_B T \ln(1 + e^{-2K}) \\ &\stackrel{T \rightarrow 0}{\cong} -J - k_B T e^{-2K} = -J - \frac{1}{2} k_B T \xi^{-1}. \end{aligned} \quad (5.20)$$

In fact for $h \neq 0$, one has a nice scaling relation that nicely follows the Widom scaling ansatz $g(\tau, h) = \xi^{-(2-\alpha)/\nu} g_0(h\xi^{\Delta/\nu})$

$$\frac{g(T, h) + J}{k_B T} \stackrel{T \rightarrow 0}{\cong} -\xi^{-1} \left[\frac{1}{2} + \left(\frac{\mu h \xi}{k_B T} \right)^2 \right] \equiv \xi^{-1} g_0(h\xi), \quad (5.21)$$

with $\frac{2-\alpha}{\nu} = 1$ and $\Delta/\nu = 1$. This reflects the suitability of 1- d Ising model to consecutive coarse graining and rescaling.

Transfer matrix and discrete time Euclidean path integrals

The path integral formulation of a quantum mechanical partition function can be given in terms of the matrix element of the Euclidean (imaginary) propagator

for closed spacetime loops

$$Z = \text{tr} e^{-\beta \hat{\mathcal{H}}} = \langle S|U(N\Delta\tau)|S\rangle. \quad (5.22)$$

On the other hand, in the previous subsection, we have found that $Z_N = \langle S|T^N|S\rangle$. Thus we see that the transfer matrix formulation implies that the classical 1- d Ising problem can be restated in terms of operators in a 2- d Hilbert space for the spin-1/2 degree of freedom. In particular, the transfer matrix T plays the role of the Euclidean time-evolution operator

$$T \iff U(\Delta\tau), \quad (5.23)$$

for imaginary time duration $\Delta\tau$, which was 1 in our units. This gives the suspicion that the classical Ising problem in 1- d may have a mapping to an artificial quantum mechanical system.

Domain wall argument for 1- d Ising model short range order

We will now demonstrate that the 1- d Ising model indeed cannot sustain a long-range ordered phase due to topological defects, using a simpler argument. The topological defects to consider in this case are domain walls separating groups of parallel-aligned spins. Let us consider the free energy corresponding to a single

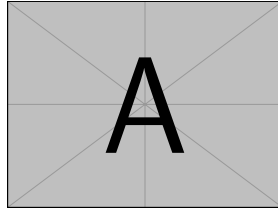


Figure 5.6: The topological defects, which are domain walls in 1- d Ising model, destroy the long-range ordered phase at any finite temperature.

such defect. Energy cost of a single domain wall is $U_{\text{dw}} = 2J$. There are $N - 1$ possible locations such a domain wall can occur in a grid of N spins. Therefore the entropy is $S_{\text{dw}} = k_{\text{B}} \log(N - 1)$. It can be seen that the free energy

$$F_{\text{dw}}(T) = U_{\text{dw}} - TS_{\text{dw}} = 2J - k_{\text{B}}T \log(N - 1) < 0 \quad \forall T, \quad (5.24)$$

for large N , i.e. in the thermodynamic limit. In particular, since the energy cost of the domain wall is independent of the size of the domains, the growth of random domains is not energetically opposed. Therefore, domain walls always reduce the free energy and thus flood the system, resulting in the prevention of the LRO phase at a finite temperature in the thermodynamic limits.

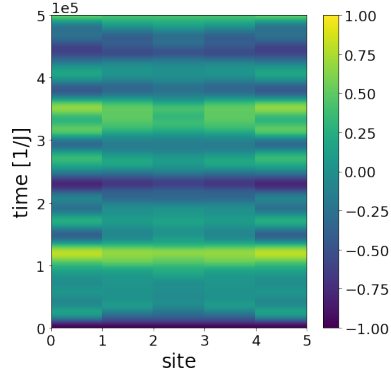


Figure 5.7: The oscillation of magnetisation in time for the uniform initial state $|\uparrow, \uparrow, \dots\rangle$. This demonstrates the quantum dynamics due to the transverse field.

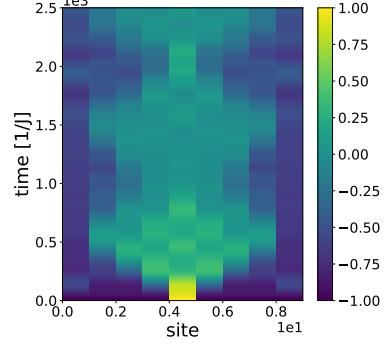


Figure 5.8: The breathing diffusion of magnetisation in time for the initial state $|\uparrow, \uparrow, \dots, \downarrow, \dots, \uparrow, \uparrow\rangle$. The finite size causes a collapse and revival of magnetisation.

5.2 Transverse field Ising model and quantum dynamics

The Hamiltonian for the antiferromagnetic transverse field Ising model is given by

$$\hat{\mathcal{H}} = J \sum_{i=1}^{N-1} \hat{\sigma}_i^z \hat{\sigma}_{i+1}^z - \Gamma \sum_{i=1}^N \hat{\sigma}_i^x.$$

This model was originally devised for describing protons in a periodic potential where each site is a double well potential. The spin-up/down corresponds to proton sitting in one of the wells of the double-well. The exchange term corresponds to interaction between protons in neighbouring sites. Transverse field corresponds to the tunneling possibility between one of the wells for each site. Because of the transverse field, the Hamiltonian is no longer diagonal in the $\hat{\sigma}^z$ basis, and this induces some mixing between the basis states $|\uparrow, \uparrow, \dots\rangle$, $|\downarrow, \uparrow, \dots\rangle$, etc. and hence results in quantum dynamics. This is best reflected if we consider the time evolution of a uniform initial state, e.g. $|\uparrow, \dots, \uparrow\rangle$. In Figure 5.7, we see that the overall magnetisation per site oscillates in time.

As a second example, we consider the case with $|\uparrow, \uparrow, \dots, \downarrow, \dots, \uparrow, \uparrow\rangle$ configuration, i.e. a uniform configuration except for the one spin in the middle. As shown in Figure 5.8, the opposite spin in the middle *diffuses* in time to the whole chain. Due to the finite system size, the diffusion has a breathing mode with a lower frequency compared to the uniform case oscillations. This is analogous to the collapse and revival of Bloch vectors in quantum optics.

0-d transverse field Ising model

Here we provide the exact calculation of for the 0- d (single spin) transverse field Ising model in order to demonstrate an intriguing phenomenon of Nature: mapping of a d -dimensional quantum system to a $(d + 1)$ -dimensional classical system.

The Hamiltonian is simply given by

$$\hat{\mathcal{H}} = -h\hat{\sigma}^z - \Gamma\sigma^x. \quad (5.25)$$

The Euclidean propogator is given by the Taylor expansion

$$e^{-\Delta\tau\hat{\mathcal{H}}} = \hat{U} + \mathcal{O}(\Delta\tau), \quad (5.26)$$

where we introduced

$$\hat{U} = \hat{\mathbb{1}} - \Delta\tau\hat{\mathcal{H}}. \quad (5.27)$$

In the matrix form this gives

$$\begin{pmatrix} 1 + \frac{\Delta\tau h}{2} & \frac{\Delta\tau\Gamma}{2} \\ \frac{\Delta\tau\Gamma}{2} & 1 - \frac{\Delta\tau h}{2} \end{pmatrix}. \quad (5.28)$$

If we discretise the temperature into M steps, the partition function at inverse temperature β can be expressed as

$$\begin{aligned} Z_M &= \text{tr} e^{-\beta\hat{\mathcal{H}}} = \text{tr} \left[\hat{U} + \mathcal{O}(\Delta\tau^2) \right]^M \\ &= \sum_{\{n_j\}} \prod_{j=1}^M \langle n_j | \hat{U} | n_{j+1} \rangle, \end{aligned} \quad (5.29)$$

where are $|n_j\rangle$ elements of the 2-dimensional Hilbert space for the spin-1/2 degree of freedom. Therefore, comparing with 5.3, we can formulate the 0- d TFIM problem in the same way as the 1- d classical Ising problem for $U = T + \mathcal{O}(\Delta\tau^2) = T$ in the continuous limit $\Delta\tau \rightarrow 0$. That is

$$\begin{pmatrix} e^H & e^{-2K} \\ e^{-2K} & e^H \end{pmatrix} = \begin{pmatrix} 1 + \frac{\Delta\tau h}{2} & \frac{\Delta\tau\Gamma}{2} \\ \frac{\Delta\tau\Gamma}{2} & 1 - \frac{\Delta\tau h}{2} \end{pmatrix}, \quad (5.30)$$

with $K = \beta J_{cl}$ and $H = \beta\mu h_{cl}$, or

$$K = -\frac{1}{2} \ln(\Delta\tau\Gamma/2), \quad (5.31)$$

$$H = \ln(1 + \Delta\tau h/2). \quad (5.32)$$

This establishes that the quantum mechanical 0- d TFIM can be exactly mapped to the classical Ising model with periodic boundary conditions. In fact, any d -dimensional quantum Ising model with Hamiltonian

$$\hat{\mathcal{H}} = -J \sum_{\langle i,j \rangle} S_i^z S_j^z - h \sum_i S_i^z - \Gamma \sum_i S_i^x \quad (5.33)$$

can be mapped to an *anisotropic* $(d + 1)$ -dimensional classical Ising model

We could thus use the same results from the 1- d Ising model to readily obtain the thermodynamic properties of the transverse field Ising model, or vice versa. An example is that there exists a long range ordered phase in $1 \geq d$ -dimensional TFIM, which we will show via the classical 2- d Ising model.

Continuum limit. Investigate the continuum limit, mention that the exchange coupling freezes. This leads to finite number of domain walls, which is the main point of the calculation. Mention Fradkin-Susskind work.

5.2.1 2-d Ising model

Peierls' argument for 2-d Ising model long range order

One can use Peierls' argument [20], which also involves topological defects, in order to show the possibility of a finite T_c LRO phase in the 2- d Ising model. In this case, instead of domain walls we have domain loops enclosing spin clusters. The essence of Peierls' argument is that the energy cost of the loops depend on the cluster size, thus there is a competition between energy minimisation and entropy, unlike the 1- d case. Energy cost of a loop of circumference ℓ is

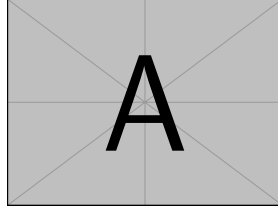


Figure 5.9: The topological defects, which come in the form of domain loops in 2- d Ising model cannot destroy the long-range ordered phase at sufficiently low temperatures.

$U_\ell = 2J\ell$, which clearly depends on the cluster size.

We can also give a rough estimate on the number of such loops as follows. The maximum size of a cluster with circumference ℓ is $(\ell/4)^2$, and a loop can start anywhere within the cluster. At the first step, it can grow towards 4 possible directions, and continue towards the remaining 3 directions in the next $\ell - 1$ steps in order to avoid crossing. However, this double-counts the 2 parities (clockwise or counter-clockwise) and ℓ starting points on the circumference; therefore we approximate the number of loops as

$$\Omega \sim \left(\frac{\ell}{4}\right)^2 \cdot 4 \cdot 3^{\ell-1} \frac{1}{2 \cdot \ell}. \quad (5.34)$$

Therefore we find the entropy as $S_\ell \sim k_B \ln \left[\left(\frac{\ell}{4}\right)^2 4 \cdot 3^{\ell-1} \frac{1}{2\ell} \right] = k_B \ln \left(\frac{\ell \cdot 3^\ell}{24} \right) \sim$

$\ell k_B \ln 3$, yielding the free energy

$$F_\ell(T) \sim 2J\ell - T\ell k_B \ln 3 = \ell(2J - Tk_B \ln 3). \quad (5.35)$$

We see that the free energy is positive for temperatures $0 < T_c < \frac{2J}{k_B \ln 3}$, in which regime, the domain loops are energetically opposed, and hence the uniform LRO phase is favoured below a finite T_c .

Onsager solution

Check the Onsager paper [19] and also [5] for the analytical results—plot them, and read the abstract to extract the main ideas that go into the proof. Onsager analytically showed in Ref. [19] that for the 2- d Ising model there exists an order-disorder phase transition, and the critical temperature in a square lattice is $k_B T_c = 2J / \ln(1 + \sqrt{2}) \approx 2.27J$

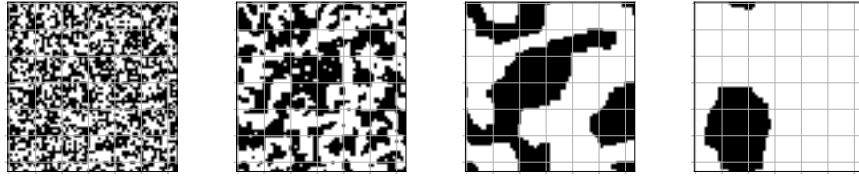


Figure 5.10: Order-disorder phase transition occurs at $k_B T_c = 2J / \ln(1 + \sqrt{2}) \approx 2.27J$ in 2- d Ising model.

Monte Carlo simulations

5.2.2 4-d Ising model and the mean-field result

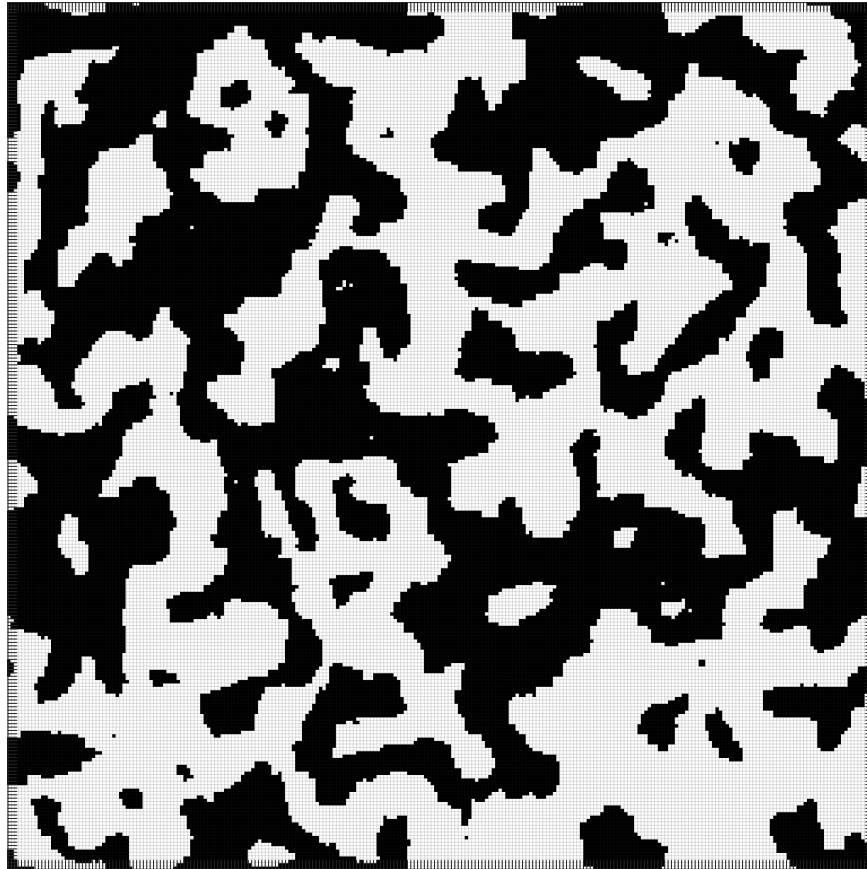
Get the results for the 4- d Ising model from Metropolis simulations and compare with the mean-field results—should agree!

5.3 XY model in d -dimensions

Assume that there is no external field. $\vec{S}_i = (\cos \Theta_i, \sin \Theta_i)$,

$$\mathcal{H} = -J \sum_{\langle i,j \rangle} \cos(\Theta_i - \Theta_j). \quad (5.36)$$

¹Astonishingly, Peirels' argument even gives an estimate for the value of the critical temperature.



[h]

Figure 5.11: Formation of spin clusters at T_c in a Monte Carlo simulation of the 2-d Ising model. There are domains of all sizes distributed according to a power law. This demonstrates the scale invariance of the system due to diverging correlation lengths at criticality.

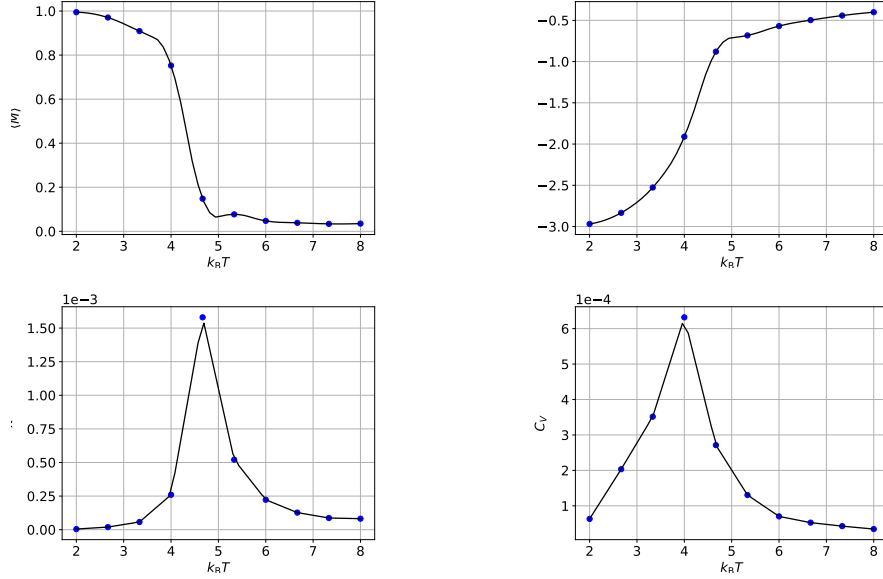


Figure 5.12: Monte Carlo simulation average thermodynamic quantities $\langle M \rangle$, $\langle E \rangle$, χ and c_V as a function of T for the $12 \times 12 \times 12$ cubic-lattice 3- d Ising model.

We assume that in the absence of fluctuations, in $T = 0$, the system is in a *uniform*² ground state with energy E_0 where all spins are aligned along a specific angle Θ_0 . Coarse graining, $\Theta_i \rightarrow \Theta(\vec{r})$, as the small deviations from this angle, i.e. $\cos(\Theta_i - \Theta_j) \approx 1 - (\Theta_i - \Theta_j)^2/2$, would produce an elastic energy. Observing that the quadratic fluctuation is the discrete gradient operator, the coarse grained (continuum) hamiltonian is

$$\mathcal{H} = E_0 + \frac{Ja^2}{2} \int \frac{d^d r}{a^d} [\nabla \Theta(\vec{r})]^2. \quad (5.37)$$

J thus describes the stiffness of the ordered state since it is the scale of the energy cost of elastic deformations, and a is the lattice spacing.

After coarse graining, the thermodynamics of the system is obtained from partition function given by a functional integral

$$\mathcal{Z} = e^{-\beta E_0} \int \mathcal{D}[\Theta(\vec{r})] \exp \left[-\beta \frac{Ja^2}{2} \int \frac{d^d r}{a^d} [\nabla \Theta(\vec{r})]^2 \right]. \quad (5.38)$$

²More specifically, here we are assuming that any possible spin configuration can be obtained by *continuously deforming* the uniform ground state or conversely, any spin configuration can continuously be deformed into the uniform ground state by the gaussian fluctuations. Are we justified to do so?

The order parameter is

$$\langle S_x \rangle = \Re \langle e^{i\Theta} \rangle = \frac{\int \mathcal{D}[\Theta(\vec{r})] e^{-\beta\mathcal{H}[\Theta(\vec{r})]} e^{i\Theta(\vec{r})}}{\int \mathcal{D}[\Theta(\vec{r})] e^{-\beta\mathcal{H}[\Theta(\vec{r})]}}. \quad (5.39)$$

However notice that the partition function is the same integral as given in 2.11 with the kernel G such that

$$G^{-1}(\vec{r}, \vec{r}') = \frac{\beta J a^2}{2} \frac{1}{a^d} \delta^d(\vec{r} - \vec{r}') \nabla^2, \quad (5.40)$$

which can be verified using integrating by parts, and noticing that the boundary term is vanishing. Hence by using 2.12 and identifying $a(\vec{r}) = i\delta^d(\vec{r} - \vec{r}')$, we simply obtain that

$$\begin{aligned} \langle S_x \rangle &= \Re \langle e^{i\Theta(\vec{r})} \rangle = \left\langle \exp \left[\int d^d r' i\delta^d(\vec{r} - \vec{r}') \Theta(\vec{r}') \right] \right\rangle \\ &= \exp \left[i\langle \Theta(\vec{r}) \rangle - \frac{1}{2} \langle \Theta^2(\vec{r}) \rangle + \frac{1}{2} \langle \Theta(\vec{r}) \rangle^2 \right]. \end{aligned} \quad (5.41)$$

However since $\Theta(\vec{r})$ generates an odd integrand, the $\langle \Theta(\vec{r}) \rangle$ terms vanish and we are left with

$$\langle S_x \rangle = \exp \left(-\frac{1}{2} \langle \Theta^2(\vec{r}) \rangle \right). \quad (5.42)$$

To calculate $\exp(-\frac{1}{2} \langle \Theta^2(\vec{r}) \rangle)$ we go into the Fourier (\vec{k} -)space.

\vec{k} -space: In the d -dimensional reciprocal space, we consider a quantised volume $V = L^d$. The volume per site is given by $V/N = v = a^d$, where a is the lattice constant. Then the Fourier transforms are given by

$$\Phi_{\vec{k}} = \int \frac{d^d r}{v} e^{-i\vec{k} \cdot \vec{r}} \Phi(\vec{r}), \quad \Phi(\vec{r}) = \frac{1}{N} \sum_{\vec{k}} e^{i\vec{k} \cdot \vec{r}} \Phi_{\vec{k}}. \quad (5.43)$$

Such sums result in delta functions in particular cases

$$\begin{aligned} \int \frac{d^d r}{V} e^{i(\vec{k} - \vec{k}') \cdot \vec{r}} &= \delta_{\vec{k}, \vec{k}'} \\ \frac{1}{V} \sum_{\vec{k}} e^{i\vec{k} \cdot (\vec{r} - \vec{r}')} &= \delta(\vec{r} - \vec{r}'). \end{aligned} \quad (5.44)$$

And the continuum limit $V \rightarrow \infty$ is given by

$$\sum_{\vec{k}} \rightarrow V \int \frac{d^d k}{(2\pi)^d}. \quad (5.45)$$

After this small mathematical interlude, we can calculate the elastic hamiltonian in \vec{k} -space

$$\begin{aligned}
\mathcal{H}_{\text{el}} &= \frac{Ja^2}{2} \int \frac{d^d r}{a^d} [\nabla \Theta(\vec{r})]^2 \\
&= \frac{ja^2}{2} \int \frac{d^d r}{a^d} \left(\nabla \sum_{\vec{k}} \frac{\Theta_{\vec{k}}}{N} e^{i\vec{k} \cdot \vec{r}} \right) \cdot \left(\nabla \sum_{\vec{k}'} \frac{\Theta_{\vec{k}'}}{N} e^{i\vec{k}' \cdot \vec{r}} \right) \\
&= -\frac{ja^2}{2N^2} \int \frac{d^d r}{a^d} \sum_{\vec{k}, \vec{k}'} \vec{k} \cdot \vec{k}' \Theta_{\vec{k}} \Theta_{\vec{k}'} e^{i(\vec{k} + \vec{k}') \cdot \vec{r}} \\
&= -\frac{ja^2}{2N^2} \sum_{\vec{k}, \vec{k}'} \frac{a^d N}{a^d} \delta_{\vec{k}, \vec{k}'} \vec{k} \cdot \vec{k}' \Theta_{\vec{k}} \Theta_{\vec{k}'} \\
&= \frac{ja^2}{2N} \sum_{\vec{k}} k^2 \Theta_{\vec{k}} \Theta_{-\vec{k}}. \tag{5.46}
\end{aligned}$$

We have

$$\langle \Theta^2(\vec{r}) \rangle = \sum_{\vec{k}, \vec{k}'} \frac{1}{N^2} \langle \Theta_{\vec{k}} \Theta_{\vec{k}'} \rangle e^{i\vec{r} \cdot (\vec{k} + \vec{k}')}. \tag{5.47}$$

The summand of 5.47 is finite only for the case $\vec{k} = -\vec{k}'$ ³

$$\langle \Theta_{\vec{k}} \Theta_{-\vec{k}} \rangle = \frac{\int \prod_{\vec{q}, \vec{p}} d\Theta_{\vec{p}} \Theta_{\vec{k}} \Theta_{-\vec{k}} \exp\left(-\beta \frac{Ja^2}{2N} q^2 \Theta_{\vec{q}} \Theta_{-\vec{q}}\right)}{\int \prod_{\vec{q}, \vec{p}} d\Theta_{\vec{p}} \exp\left(-\beta \frac{Ja^2}{2N} q^2 \Theta_{\vec{q}} \Theta_{-\vec{q}}\right)}.$$

Here notice that if not both \vec{q} and \vec{p} are equal to \vec{k} , then the denominator cancels the nominator. Hence we are left with

$$\langle \Theta_{\vec{k}} \Theta_{-\vec{k}} \rangle = \frac{\int d\Theta_{\vec{k}} \Theta_{\vec{k}} \Theta_{-\vec{k}} \exp\left(-\beta \frac{Ja^2}{2N} k^2 \Theta_{\vec{k}} \Theta_{-\vec{k}}\right)}{\int d\Theta_{\vec{k}} \exp\left(-\beta \frac{Ja^2}{2N} k^2 \Theta_{\vec{k}} \Theta_{-\vec{k}}\right)}. \tag{5.48}$$

Noting that $\Theta_{\vec{k}} \Theta_{-\vec{k}} = |\Theta_{\vec{k}}|^2$, we can perform the integration in the polar representation of the complex plane.

$$\begin{aligned}
\langle \Theta_{\vec{k}} \Theta_{-\vec{k}} \rangle &= \frac{\int_0^{2\pi} d\theta_{\vec{k}} \int_0^\infty d|\Theta_{\vec{k}}| |\Theta_{\vec{k}}| |\Theta_{\vec{k}}|^2 \exp\left(-\beta \frac{Ja^2}{2N} k^2 |\Theta_{\vec{k}}|^2\right)}{\int_0^{2\pi} d\theta_{\vec{k}} \int_0^\infty d|\Theta_{\vec{k}}| |\Theta_{\vec{k}}| \exp\left(-\beta \frac{Ja^2}{2N} k^2 |\Theta_{\vec{k}}|^2\right)} \\
&= \frac{\int_0^\infty dx x^3 \exp(-\alpha x^2)}{\int_0^\infty dx x \exp(-\alpha x^2)} \equiv \frac{I_3(\alpha)}{I_1(\alpha)}, \tag{5.49}
\end{aligned}$$

³Note that this is not due to the Fourier sum, but insted due to the ensemble average! See the calculation of spin-spin correlator.

where $\alpha = \frac{\beta J a^2}{2N} k^2$. Notice that $I_3(\alpha) = -\frac{\partial I_1(\alpha)}{\partial \alpha}$. Since $I_1(\alpha) = \frac{1}{2\alpha}$, we have

$$\langle \Theta_{\vec{k}} \Theta_{-\vec{k}} \rangle = \frac{1}{\alpha} = \frac{N k_B T}{J a^2 k^2}. \quad (5.50)$$

Note that this is the *equipartition theorem* $\langle \Theta_{\vec{k}} \Theta_{-\vec{k}} \rangle \frac{J a^2}{2} k^2 = \frac{k_B T}{2}$, i.e. because of the quadratic appearance in the hamiltonian, each Fourier mode consists of energy $k_B T/2$. Hence substituting this in 5.47, we get

$$\langle \Theta^2(\vec{r}) \rangle = \frac{1}{N^2} \frac{N k_B T}{J a^2} \sum_{\vec{k}} \frac{1}{k^2} \quad (5.51)$$

$$= \frac{1}{N} \frac{k_B T}{J a^2} \left(\frac{a}{2\pi} \right)^d \int d\Omega_d \int_0^{\frac{\pi}{a}} dk \frac{k^{d-1}}{k^2} \\ = \frac{1}{N} \frac{S^d a^{d-2}}{(2\pi)^d} \frac{k_B T}{J} \int_0^{\infty} dk k^{d-3} \quad (5.52)$$

$$= \begin{cases} \frac{1}{N} \frac{S^d}{(2\pi)^d} \frac{k_B T}{J(d-2)}, & d > 2 \\ \infty, & d \leq 2 \end{cases}, \quad (5.53)$$

or

$$\langle S_x \rangle = \exp \left(-\frac{1}{2} \langle \Theta^2(\vec{r}) \rangle \right) = \begin{cases} \text{constant}, & d > 2 \\ 0, & d \leq 2 \end{cases} \quad (5.54)$$

Therefore, we see that fluctuations diverge at $d \leq 2$ and the consideration of elastic gaussian distortions refine the incorrect mean-field predictions as they destroy the magnetic order in dimensions 2 and below.

Similarly one can also calculate the spin-spin correlator

$$C(\vec{r}, \vec{r}') = \langle \vec{S}(\vec{r}) \cdot \vec{S}(\vec{r}') \rangle = \exp \left\langle -[\Theta(\vec{r}) - \Theta(\vec{r}')]^2 / 2 \right\rangle \\ \left\langle -[\Theta(\vec{r}) - \Theta(\vec{r}')]^2 / 2 \right\rangle = \left\langle -[\Theta^2(\vec{r}) + \Theta^2(\vec{r}') - 2\Theta(\vec{r})\Theta(\vec{r}')] / 2 \right\rangle \quad (5.55) \\ \langle \Theta(\vec{r})\Theta(\vec{r}') \rangle = \sum_{\vec{k}, \vec{k}'} \frac{1}{N^2} \langle \Theta_{\vec{k}} \Theta_{\vec{k}'} \rangle e^{i(\vec{r} \cdot \vec{k} + \vec{r}' \cdot \vec{k}')} \\ = \left[\sum_{\vec{k} \neq \pm \vec{k}'} \frac{1}{N^2} \langle \Theta_{\vec{k}} \Theta_{\vec{k}'} \rangle + \sum_{\vec{k} = \vec{k}'} \frac{1}{N^2} \langle \Theta_{\vec{k}} \Theta_{\vec{k}'} \rangle + \sum_{\vec{k} = -\vec{k}'} \frac{1}{N^2} \langle \Theta_{\vec{k}} \Theta_{\vec{k}'} \rangle \right] e^{i(\vec{r} \cdot \vec{k} + \vec{r}' \cdot \vec{k}')} \\ = \left[\sum_{\vec{k} \neq \pm \vec{k}'} \frac{1}{N^2} \langle \Theta_{\vec{k}} \rangle \langle \Theta_{\vec{k}'} \rangle + \sum_{\vec{k}} \frac{1}{N^2} \langle \Theta_{\vec{k}}^2 \rangle + \sum_{\vec{k}} \frac{1}{N^2} \langle \Theta_{\vec{k}} \Theta_{-\vec{k}} \rangle \right] e^{i(\vec{r} \cdot \vec{k} + \vec{r}' \cdot \vec{k}')} \\ = \sum_{\vec{k}} \frac{1}{N^2} \langle \Theta_{\vec{k}} \Theta_{-\vec{k}} \rangle e^{i\vec{k} \cdot (\vec{r} - \vec{r}')} = \sum_{\vec{k}} \frac{1}{N^2} \frac{k_B T}{2J a^2 k^2} e^{i\vec{k} \cdot (\vec{r} - \vec{r}')}, \quad (5.56)$$

where in the last step the first term vanishes because of odd integrand and the second vanishes because of the angular integration of $d\Theta_{\vec{k}}$. By translation

invariance we can choose $\vec{r}' = 0$. Then

$$\langle [\Theta(\vec{r}) - \Theta(0)]^2 \rangle = \left(\frac{a}{2\pi}\right)^d \int d^d k \frac{k_B T}{J a^2 k^2} (1 - \cos \vec{k} \cdot \vec{r}). \quad (5.57)$$

Demonstrate the constancy ($< 3 - d$ below T_c), the exponential ($1 - d$) and algebraic decay ($2 - d$) of the correlation functions by approximating this integral (take oscillating part to be constant?).

$$\langle [\Theta(\vec{r}) - \Theta(0)]^2 \rangle = \begin{cases} \text{constant}, & d > 2 \\ \frac{1}{den}, & d \leq 2 \\ \text{exp}, & d = 1 \end{cases} \quad (5.58)$$

$$\text{content...} \quad (5.59)$$

To summarise, we have considered thermally excited, elastic low-energy gaussian distortions. We see that in dimensions 3 and above, there can be long range order below a critical temperature. In 1-dimension, there is only short range order, the domain walls destroy the order. In 2-dimensions, this model indicates the correlation between spins decay *algebraically at all temperatures*. Algebraic functions have no scale, hence the system has no typical length scale (self-similar). Such a behaviour is typical at critical point, i.e. for systems undergoing a phase transition. This means that there is a quasi-long range order that survives at all temperatures, without a phase transition. However such a prediction is empirically invalidated. One can argue that the reason of inaccuracy is that the Gaussian approximation for small fluctuations is only valid at low temperatures. Indeed, expanding a periodic function up to quadratic order, we neglect the fact that it is periodic, i.e. Θ is compact (angular). On the other hand, RG treatment suggests that including the higher order gradients in the expansion is irrelevant for this problem. The resolution to this problem required a breakthrough [1, 15, 14].

5.3.1 Kosterlitz-Thouless-Berezinskii transition in 2-d XY model

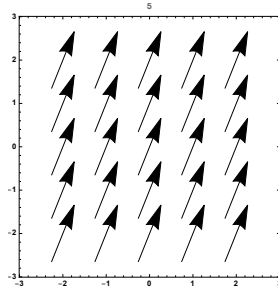


Figure 5.13: A uniformly ordered ground state for the 2 dimensional XY model. This corresponds to a topological charge of $n = 0$.

Whilst doing the gradient expansion for the Gaussian fluctuations, we have assumed that the local minima of the hamiltonian functional 5.37 occur only

when the spin field is uniformly aligned along a direction. Equivalently, we have implicitly argued that *any spin configuration* can continuously be deformed into a uniformly aligned spin configuration by gaussian fluctuations. However, if the spins are in a configuration that contains **topological defects**, this assumption is invalid.

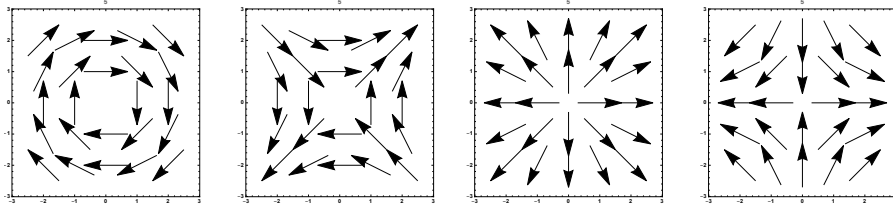


Figure 5.14: Spin configurations with topological defects. From left to right the topological charge n and the constant phase ϕ : $n = 1, \phi = \pi/2, n = -1, \phi = \pi/2, n = 1, \phi = 0, n = -1, \phi = 0$.

It is possible to find configurations where spins are aligned in a way such that upon the traversal of a closed path, the angle of the spins are rotated by $2\pi n$, where n , the charge of the topological defect, is an integer⁴. In 2 dimensions⁴, along with the uniform configuration ($n = 0$), these can be vortices ($n = 1$) and anti vortices ($n = -1$), see Figure 5.14. The discreteness of n makes it impossible to find any⁵ continuous deformation that transforms these configurations to a uniform $n = 0$ configuration as seen in Figure 5.15.

The crucial point is that such configurations with topological defects also provide local extrema for the hamiltonian 5.37. To see this, we take the functional derivative of the hamiltonian with respect to the spin angle field $\Theta(\vec{r})$. Let us consider the 2 dimensional case

$$0 = \frac{\delta \mathcal{H}[\Theta(\vec{r}), \nabla \Theta(\vec{r})]}{\delta \Theta(\vec{r})} = \frac{\delta}{\delta \Theta(\vec{r})} \left[E_0 + \frac{J}{2} \int d^2 r [\nabla \Theta(\vec{r})]^2 \right] \Big|_{\Theta=\Theta_0}. \quad (5.60)$$

This equation is of the Euler-Lagrange type given in 1.6. Therefore we simply get

$$0 = \left\{ \frac{\partial}{\partial \Theta(\vec{r})} - \nabla \cdot \frac{\partial}{\partial [\nabla \Theta(\vec{r})]} \right\} [\nabla \Theta(\vec{r})]^2 \Big|_{\Theta=\Theta_0} \\ \implies \nabla^2 \Theta(\vec{r}) \Big|_{\Theta=\Theta_0} = 0. \quad (5.61)$$

Noting that in polar coordinates $\nabla^2 = \frac{1}{r} \frac{\partial}{\partial r} \left(r \frac{\partial}{\partial r} \right) + \frac{1}{r^2} \frac{\partial^2}{\partial \theta^2}$, one can find that a specific solution to this Laplace equation for the angle variable is

$$\Theta_0(\vec{r}) = \Theta_0(\theta, \phi) = n\theta + \phi, \quad \phi = \text{constant}, \quad n \in \mathbb{Z}. \quad (5.62)$$

⁴In higher dimensions e.g. one may have helical structures with $|n| > 1$, also see *skyrmions* in $O(3)$ Heisenberg model (see Figure 5.17).

⁵Let alone gaussian.

The general solution is the linear superposition of such terms

$$\Theta_0^s = \sum_i \Theta_0^i = \sum_i (n_i \theta_i + \phi_i) \quad (5.63)$$

centered at different points $\vec{r}_0 = 0$, $\vec{r}_1 = 0$, etc.

For $n = 0$, equation 5.62 implies a uniformly ordered ground state as shown in Figure 5.13. On the other hand, for finite n one finds also extremal configurations with the vortices or anti-vortices ($n = \pm 1$) (see Figure 5.14), with a finite spin gradient field

$$\nabla \Theta_0 = n \frac{\hat{\theta}}{r}, \quad (5.64)$$

which has a singularity in the origin. In particular⁶ it can be seen that

$$\oint_{\partial \mathcal{R}} d\vec{l} \cdot \nabla \Theta_0 = \begin{cases} 2\pi r |\nabla \Theta_0| = 2\pi n, & r = 0 \in \mathcal{R} \\ 0, & r = 0 \notin \mathcal{R}. \end{cases} \quad (5.65)$$

In the former case the loop encloses a vortex and the RHS is called the *winding number*.

Therefore, since we have been able to recognise that the 2-dimensional XY spin system admits multiple types of spin field configurations which yield local minima, we can express the partition function as a sum over all these extremal configurations Θ_0 and quadratic fluctuations Θ_f upon them

$$\begin{aligned} \mathcal{Z} = e^{-\beta E_0} \sum_{\{\Theta_0\}} \int \mathcal{D}[\Theta_f(\vec{r})] \exp \{ -\beta \mathcal{H}[\Theta_0(\vec{r})] \} \\ \times \exp \left\{ -\frac{\beta}{2} \int d^2 r_1 \int d^2 r_2 \Theta_f(\vec{r}_1) \Theta_f(\vec{r}_2) \frac{\delta^2 \mathcal{H}}{\delta \Theta(\vec{r}_1) \delta \Theta(\vec{r}_2)} \right\}. \end{aligned} \quad (5.66)$$

Furthermore we can calculate the energy of an isolated (anti-)vortex

$$E_v = \frac{J}{2} \int d^2 r (\nabla \Theta)^2 = \frac{J n^2}{2} \int_0^{2\pi} d\theta \int_a^L r dr \frac{1}{r^2} = \pi n^2 J \ln \left(\frac{L}{a} \right), \quad (5.67)$$

where L is the finite system size and a is the lattice spacing. We see that in a macroscopically large system even a single vortex costs high energy.

Now consider a singly charged vortex-anti-vortex pair. Assuming that the former is located at \vec{r} and the latter at \vec{r}_0 , the gradient field of such a field is short ranged

$$|\nabla \Theta_0^v(\vec{r}) + \nabla \Theta_0^{\bar{v}}(\vec{r} - \vec{r}_0)| \sim \frac{1}{r^2}. \quad (5.68)$$

An anti-vortex sucks up the effect of the vortex (see Figure 5.16). The field is unnoticed far away from the location of the pair. Indeed, we can also calculate

⁶In a simply-connected region by making use of the Stokes' theorem one can find that this integral is 0 because $\nabla \times \nabla f = 0$, $\forall f$.

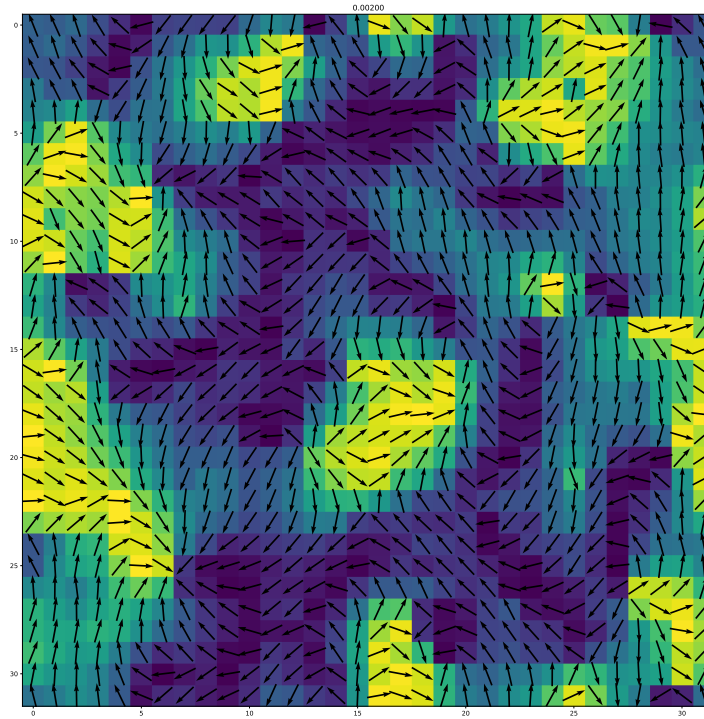


Figure 5.15: $2-d$ Heisenberg spins form clusters even at very low temperatures. The mechanism behind the formation of these clusters is due to the existence of vortices, which typically occur around the corners of them. The robustness of these clusters against the tendency towards the low energy long-range ordered phase is higher compared to the Ising model, because the vortices are topological defects that cannot be continuously deformed into a uniform configuration. This configuration is generated through the Monte Carlo simulation via the Metropolis algorithm

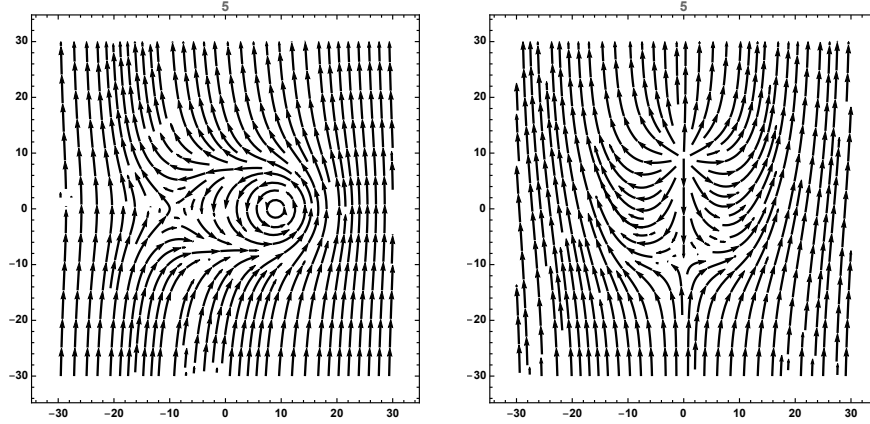


Figure 5.16: Vortex-anti-vortex pairs.

the circulation of an isolated vortex-anti-vortex pair by integrating along a large enough loop which is the union of two paths, encircling the vortex and the anti-vortex. The integral is the sum of the result from each loop, which are 2π and -2π , respectively, giving a circulation of 0.

The energy of a vortex pair of charges n_1 and n_2 separated by distance R is [How to prove this?](#)

$$E_{n_1, n_2}(R) = \pi J(n_1 + n_2)^2 \ln(L/a) - 2\pi J n_1 n_2 \ln(R/a). \quad (5.69)$$

We can define the vortex charge density in a spin system by

$$n_v(\vec{r}) = \sum_i n_i \delta(\vec{r} - \vec{r}_i). \quad (5.70)$$

Note that this expression also includes all the $n = 0$ charges, i.e. the uniformly ordered states. Then, the total hamiltonian of the system can simply be expressed as a sum of elastic deformations and the gas of vortices

$$\mathcal{H} = \frac{J}{2} \int \frac{d^2 r}{a^2} [\nabla \Theta]^2 - \pi J \int d^2 r \int d^2 r' n_v(\vec{r}) n_v(\vec{r}') \left[\ln \frac{|\vec{r} - \vec{r}'|}{a} - \ln \frac{L}{a} \right]. \quad (5.71)$$

This hamiltonian provides the process that can destroy the quasi-long-range order (QLRO) at high temperatures: in the low temperature phase, the vortices are pairwise bound, and thus they do not cause much distortion from the uniform ground state, the gaussian fluctuations are a good approximation, and the conclusion that QLRO phase is preserved is valid. With increasing temperature, more vortices occur and they *screen* the attractive interaction between the vortices, eventually leading to the dissociation of pairs. Hence the increasing number of free vortices destroy the QLRO phase.

One can approximate the critical temperature for the QLRO phase through the following argument: The configurational entropy is related to the number

of possibilities to place a vortex at one of $(L/a)^2$ lattice sites $S = k_B \ln(L/a)^2$. The free energy of a single vortex is thus

$$F = (\pi J - 2k_B T) \ln(L/a). \quad (5.72)$$

We argue that the temperature that this free energy becomes negative denotes the point where it becomes favourable to generate such vortices, which is given by

$$k_B T_{\text{KT}} = \frac{\pi}{2} J. \quad (5.73)$$

Finally note that the Kosterlitz-Thouless transition has no order parameter associated to it, thus it does not break any symmetry, and it is of infinite order.

5.3.2 Order parameter, energy, susceptibility and the specific heat

Include graphics obtained from Monte Carlo simulations for the order parameter, energy, susceptibility and the specific heat.

5.4 Heisenberg model in d -dimensions

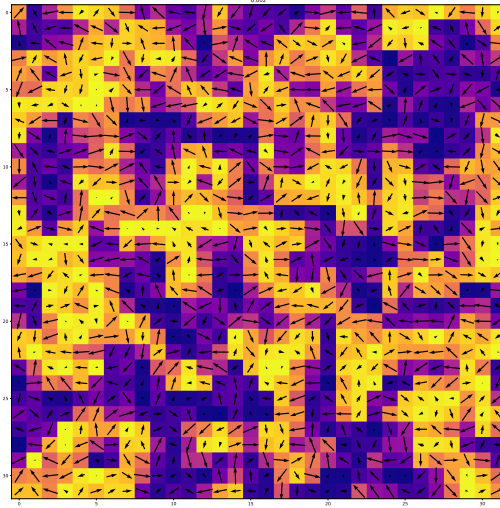


Figure 5.17: $2-d$ Heisenberg spins at low temperatures. The configuration is generated through the Monte Carlo simulation via the Metropolis algorithm

Include graphics obtained from Monte Carlo simulations for the order parameter, energy, susceptibility and the specific heat.

5.4.1 Quantum Heisenberg model

The Hamiltonian for the quantum Heisenberg model is given by

$$\hat{\mathcal{H}} = J \sum_{\langle i,j \rangle} \vec{\sigma}_i \cdot \vec{\sigma}_{i+1},$$

where $\vec{\sigma}_i = (\sigma_i^x, \sigma_i^y, \sigma_i^z)$ is the Pauli vector for spin site i .

Since the total magnetisation $M^z = \sum_i \sigma_i^z$ commutes with the hamiltonian, $[\mathcal{H}, M^z] = 0$, this is a symmetry of the system and M^z is conserved. Consequently, \mathcal{H} and M^z have a shared eigensystem and thus we can label the energy eigenstates via the angular momentum quantum numbers. As the dimension of

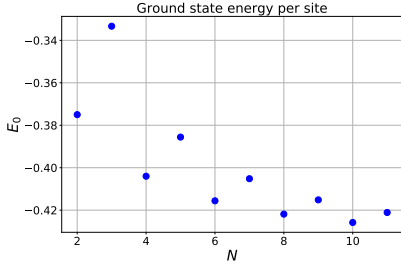


Figure 5.18: The ground state energy per spin in the 1- d quantum Heisenberg model oscillates as a function of the number of spin-sites N .

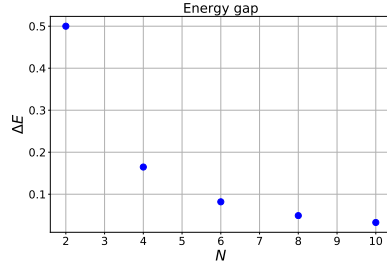


Figure 5.19: The gap between the ground state and the lowest excited state monotonically reduces with increasing the number of spin-sites N .

the Hilbert space grows exponentially with the system size, we can approach this problem via exact diagonalisation (ED) only for small systems of size $N \sim 10^1$.

In 1- d , the ground state energies $E_0(N)$ for \mathcal{H} , obtained via ED, are shown in Figure 5.18. It is clearly seen that the energy oscillates, due to antiferromagnetic frustration at odd number of sites. This phenomenon occurs both for open and periodic boundary conditions, but for different reasons. In periodic boundary conditions, it is clear that two parallel aligned neighbouring spins increase the energy for odd N compared to $N + 1$. On the other hand, in the case of open boundary conditions, the reason is that the system cannot a singlet state for the unpaired spin. In other words, the unpaired spin indicates that the lowest energy state is a finite magnetisation eigenstate. As an aside, in Figure 5.19, it can be seen that the lowest energy gap $\Delta E = E_1 - E_0$ reduces with increasing system size N .

5.5 Monte-Carlo methods for spin models

One can alternatively use Monte-Carlo simulations to sample configurations of a system randomly, to approximate the phase space of a physical system. If the

sample is sufficiently large, this approach can provide an accurate calculation of thermodynamic averages. In the context of spin models, Monte Carlo simulations come in handy, especially for the cases where the analytical derivation of these quantities is either very intricate (e.g. 2-*d* Ising model) or currently unattained (e.g. 3-*d* Ising model).

Markov chains

In terms of efficiency, it is necessary to employ an importance sampling method to explore the large pool of configurations in the phase space. An example to avoid frequently sampling regions that the system is unlikely to be found is the Markov chain algorithm.

Here one starts from a chosen non-equilibrium state and passes from one configuration to another via a stochastic process, whose steps are indexed by a virtual time τ . Probability of chain consisting of subsequent configurations X and Y is given by the probability $T(X \rightarrow Y)$ of proposing a transition from X to Y , and the probability $A(X \rightarrow Y)$ of accepting that move. T should satisfy following three properties:

1. Ergodicity: all configurations in the phase space are proposed within a *finite* number of steps.
2. Normalisation: $\sum_Y T(X \rightarrow Y) = 1$.
3. Reversibility: $T(X \rightarrow Y) = T(Y \rightarrow X)$. This is necessary in order to ensure that elementary processes are time reversal symmetric.

The probability of a Markov chain is simply given by

$$W(X \rightarrow Y) = T(X \rightarrow Y) \cdot A(X \rightarrow Y). \quad (5.74)$$

Let us denote the distribution of configurations $\{X\}$ at stochastic step τ as $p(X, \tau)$. The stochastic evolution of p is given by the master equation.

$$\frac{dp(X, \tau)}{d\tau} = \sum_Y p(Y)W(Y \rightarrow X) - \sum_X p(X)W(X \rightarrow Y). \quad (5.75)$$

An important property of Markov chains is that the steady state p_{st} , such that $\dot{p}_{st} = 0$ is always reached within a finite number of steps. For equilibrium systems, the steady state can be imposed to be the equilibrium state and thus $p_{st} \stackrel{!}{=} p_{eq}$. Observe that the master equation implies the condition

$$p_{eq}(Y)W(Y \rightarrow X) = p_{eq}(X)W(X \rightarrow Y) \quad (5.76)$$

for the equilibrium distribution and the Markov chain probabilities. This is known as the *condition of detailed balance*.

Furthermore, W should satisfy the following three properties:

1. Ergodicity: all configurations are reachable.

2. Normalisation: $\sum_Y W(X \rightarrow Y) = 1$.
3. Homogeneity: $\sum_Y p_{\text{st}}(Y)W(Y \rightarrow X) = p_{\text{st}}(X)$.

To sample the phase space in a given physical problem, one should devise an expression for W , or A that depends on the system, and satisfies the detailed balance condition.

5.5.1 Metropolis algorithm

A possible choice of A that satisfies the detailed balance condition is

$$A(X \rightarrow Y) = \min \left[1, \frac{p_{\text{eq}}(Y)}{p_{\text{eq}}(X)} \right]. \quad (5.77)$$

For the canonical ensemble, the equilibrium distribution at given β is $p_{\text{eq}}(X) = \exp(-\beta E(X))/Z_\beta$. Thus we get the acceptance probability

$$A(X \rightarrow Y) = \min [1, \exp(-\beta \Delta E(X \rightarrow Y))], \quad (5.78)$$

where the $\Delta(X \rightarrow Y) = E(Y) - E(X)$ is the energy cost of a transition to configuration Y from X . We see that the step is always accepted if the energy decreases, and otherwise it is accepted $\exp(-\beta \Delta E)$ of the time. Note that $\Delta E = 0$ moves are also always accepted.

Below, we give a detailed implementation of this algorithm, called the *single spin-flip* Metropolis algorithm [17], for the 2-*d* Ising model in Python.

```
#Indices of the nearest neighbours (periodic boundary conditions)
def nbrs(S,i,j):
    u=(j-1)%np.size(S,0); d=(j+1)%np.size(S,0)
    l=(i-1)%np.size(S,1); r=(i+1)%np.size(S,1)
    return u,d,l,r
```

```
#Calculates the total energy of a given configuration
def Energy(S,J):
    L=np.size(S,0) #sidelength of the lattice
    energy = 0 #initialise the energy
    for i in range(len(S)): #iterate over all lattice sites
        for j in range(len(S)):
            energy += energy_ij(S,S[j,i],J,i,j)/2. #total energy
    return energy
```

```
#Calculates the total energy of a given configuration
def Energy(S,J):
    L=np.size(config,0) #sidelength of the lattice
    energy = 0 #initialise the energy
    for i in range(len(config)): #iterate over all lattice sites
        for j in range(len(config)):
            S = config[j,i] #get the spin of lattice site (i,j)
            u,d,l,r=nbrs_2d(config,i,j) #nearest neighbours
            eng+=-J*S*(config[j,r]+config[j,l]+config[u,i]+config[d,i])/2
    return eng
```

```

#Metropolis algorithm for the XY model
def metropolis_XY(kT,S,J,L,ens):
    M_avg=0; E_avg=0; M2_avg=0; E2_avg=0 #initialise averages
    E=Energy(S,J) #initial energy
    for t in np.arange(ens):
        #Attempt flipping the random (ii,jj)th spin
        rand=np.random.randint(L, size=2); ii=rand[0]; jj=rand[1]
        sigma_o=S[jj,ii] #pick a random spin
        #Generate spin in random direction
        a=np.random.rand()*2-1; sgn=np.random.randint(2)*2-1
        sigma_n=np.array([a, sgn*np.sqrt(1-a**2)]) #flipped spin
        E_o=energy_ij(S,sigma_o,J,ii,jj) #orig. energy of chosen spin
        E_n=energy_ij(S,sigma_n,J,ii,jj) #new energy of the chosen spin
        delta_E=-E_o+E_n #energy cost of the spin flip
        if delta_E<0: #flip the spin if energy is reduced
            S[jj,ii]=sigma_n #flip the spin
            E+=delta_E #update the energy
        else: #if not, flip the spin with frequency Boltzmann factor
            p=np.exp(-delta_E/kT) #update Boltzmann factor
            x=np.random.uniform() #uniform random variable between 0,1
            if x<p:
                S[jj,ii]=sigma_n #flip the spin
                E+=delta_E #update the energy

```

5.5.2 Cluster algorithms

Discuss cluster algorithms. The idea originates from the mapping between the bond-percolation model and the Potts model on an arbitrary graph (Kasteleyn-Fortuin theorem.)

Wolff algorithm

Read [27].

5.6 Mermin-Wagner-Hohenberg theory

In systems with a continuous symmetry, every long range ordered phase is destroyed by fluctuations in dimensions 1 or 2. A transition into an ordered phase necessarily requires a spontaneous breaking of a continuous symmetry, but then the order parameter may undergo fluctuations in a continuum of directions. These long wavelength fluctuations can be modelled as spin waves which cost little energy. These are called Goldstone modes.

5.6.1 Equipartition theorem and susceptibility sum rule

A generic recipe for quadratic hamiltonians in the classical case is as follows. Suppose that we have a quadratic hamiltonian such as

$$\mathcal{H} = \alpha\Phi^2(\vec{r}) + |\nabla\Phi(\vec{r})|^2. \quad (5.79)$$

In general, one can take a quadratic hamiltonian into the following form via Fourier transformation

$$\mathcal{H} = \sum_{\vec{k}} \epsilon_{\vec{k}} |\Phi_{\vec{k}}|^2, \quad (5.80)$$

where $\epsilon_{\vec{k}}$ is a function of \vec{k} and $\Phi_{\vec{k}}$ is the Fourier transform of the order parameter field. Then by the *equipartition theorem*, we readily have the correlator

$$\langle |\Phi_{\vec{k}}|^2 \rangle \epsilon_{\vec{k}} = \frac{k_B T}{2}. \quad (5.81)$$

We can then use the susceptibility sum rule to get the real space representation of the non-local correlator

$$\langle \Phi^2(\vec{r}) \rangle = \frac{1}{N} \sum_{\vec{k}} \langle |\Phi_{\vec{k}}|^2 \rangle \quad \text{then,} \quad (5.82)$$

$$\langle \Phi^2(\vec{r}) \rangle = \frac{1}{N} \sum_{\vec{k}} \frac{k_B T}{2\epsilon_{\vec{k}}} \sim \int d^d k \frac{k_B T}{\epsilon_{\vec{k}}}. \quad (5.83)$$

This allows us to read off the non-local correlator right from the quadratic Hamiltonian.

Using this result, we can show that the phenomenon of Hohenberg-Mermin-Wagner is trivially universal in the classical case. Let the Hamiltonian have only the Gaussian elastic energy: $\mathcal{H} \sim (C/2)|\nabla\Phi|^2$. Then we can easily see that the fluctuations destroy the order in $d = 1, 2$ as we observe infrared divergence:

$$\langle \Phi^2 \rangle \sim \int d^d k \frac{k_B T}{Ck^2} \sim T \int_0 dk k^{d-3} \sim \frac{T}{d-2} k^{d-2} \Big|_0 \begin{cases} \rightarrow \infty, & d = 1, 2, \\ \text{finite}, & \text{otherwise.} \end{cases} \quad (5.84)$$

Chapter 6

Landau mean-field theory

Landau mean-field theory [16] involves a phenomenological (Taylor) expansion of the free energy around the proximity of a phase transition. This expansion is done in accordance with the symmetries of the system in order to be able to apply the notion of spontaneous symmetry breaking. Landau free energy functional F is the part of the free energy of the system that is related to the phase transition, such that $F_{\text{total}} = F + F_{\text{rest}}$.

The notions that are used in Landau theory are mostly adopted from the framework of magnetic phase transitions that we have discussed, but it applies to a general scenario. For instance, the phases can be described by an order parameter field $\Phi(\vec{r})$ which is 0 in the disordered phase and becomes finite in the ordered phase. Consequently F can be expressed by the following power series expansion around T_c in terms of the small $\Phi(\vec{r})$

$$F[T, \Phi] = \int d^d r f[T, \Phi(\vec{r})] = \int d^d r \left[\frac{r}{2} \Phi^2 + u \Phi^4 + u' \Phi^6 + \frac{c}{2} |\nabla \Phi|^2 \right]. \quad (6.1)$$

This is to be interpreted as the effective hamiltonian which is coarse grained over the microscopic degrees of freedom, forgetting about the distinction between different microscopic states $\Phi_\mu(\vec{r})$ that give the same macroscopic order parameter $\phi(\vec{r})$, and also neglecting the part of the phase space of the system away from the phase transition. Because of the coarse graining, the coefficients r, u, u', c in general depend on T . These are found by fitting the resulting expressions derived from the theory to the experimental results. There are some exceptional cases where the coefficients can be calculated from a microscopic theory, e.g. derivation of Ginzburg-Landau theory from Bardeen-Cooper-Schrieffer (BCS)-theory of superconductors.

The Legendre transform of F in $h(\vec{r})$, the conjugate variable of $\Phi(\vec{r})$, yields the analog of Gibbs free energy

$$G[T, \vec{h}(\vec{r})] = F[T, \Phi(\vec{r})] - \int d^d r \vec{h}(\vec{r}) \cdot \vec{\Phi}(\vec{r}). \quad (6.2)$$

As in magnetic phase transitions, the conjugate field \vec{h} breaks the symmetry

even above the critical point. We can obtain the order parameter from G by taking the functional derivative

$$\begin{aligned} \frac{\delta G}{\delta \vec{h}} &= \frac{\delta F}{\delta \vec{h}} - \frac{\delta}{\delta \vec{h}} \int d^d r \vec{h} \cdot \vec{\Phi} = -\frac{\partial \vec{h} \cdot \vec{\Phi}}{\partial \vec{h}} \\ \implies \frac{\delta G}{\delta \vec{h}(\vec{r})} &= -\vec{\Phi}(\vec{r}), \end{aligned} \quad (6.3)$$

because F does not depend on \vec{h} . Furthermore, we can regard $\vec{\Phi}$ as a constrained parameter for G , hence by minimising the Legendre transformation, we get that

$$\begin{aligned} 0 &= \frac{\delta G}{\delta \vec{\Phi}} = \frac{\delta F}{\delta \vec{\Phi}} - \frac{\delta}{\delta \vec{\Phi}} \int d^d r \vec{h} \cdot \vec{\Phi} = \frac{\delta F}{\delta \vec{\Phi}} - \vec{h} \\ \implies \frac{\delta F}{\delta \vec{\Phi}(\vec{r})} &= \vec{h}(\vec{r}), \end{aligned} \quad (6.4)$$

in analogy to the thermodynamical relations.

6.1 Saddle point approximation

The last term in 6.1 is the first term in the gradient expansion, and it corresponds to the elastic distortions (gaussian fluctuations) in the system. Note that higher orders in gradients are neglected, and it follows that F describes the high-energy/long-wavelength physics of the order parameter. The partition function is given by

$$\mathcal{Z}_L = \int \mathcal{D}[\Phi(\vec{r})] e^{-\beta F[T, \Phi(\vec{r})]}. \quad (6.5)$$

A good starting point is to neglect this elastic energy and approximate this functional integral by the maximal integrand. The latter is the *saddle point approximation*, which yields a mean-field theory partition function

$$\mathcal{Z}_{\text{mf}} = e^{-\beta F_{\text{mf}}(T)}. \quad (6.6)$$

The mean-field free energy corresponds to averaging out all space dependencies to reduce the problem into one depending on a single variable, which is the coarse grained order-parameter field Φ . The true free energy at a given temperature is obtained by minimising F_{mf} over all values of Φ . This suggests that the Landau theory shares the same philosophy as fluid-dynamics. It assumes that only the fluctuations on the atomic scale matter and the continuous, coarse-grained macroscopic order parameter Φ fluctuates only in response to the external conjugated drive-field H . In particular, it is important to note that both the van der Waals and Weiss mean-field theories are special cases of the Landau mean-field theory.

The Landau theory implicitly assumes that analyticity of the partition function is maintained during this spatial averaging process. However, as we will

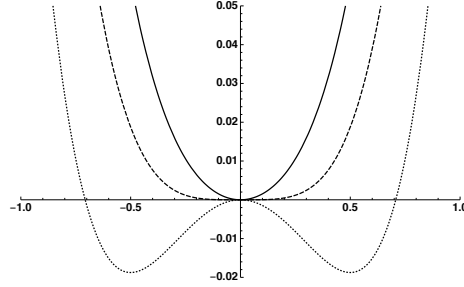


Figure 6.1: Landau free energy functional for the 2nd order phase transitions.

see shortly, the loss of analyticity, leading to a description of critical phenomena arises from averaging over the values of overall order-parameter field Φ . It is important to note, however, that the non-analyticity arising from this theory is only valid for the case of thermodynamic limit where the system size approaches to infinity $V \rightarrow \infty$. In finite systems, the minimisation rule is invalid, and the non-analiticities are alleviated to smooth analytic results.

6.1.1 Second order phase transitions

The magnetic systems that we have discussed exhibit second order phase transitions and have either parity or continuous rotation symmetry. Therefore the Landau free energy functional can be expanded in Φ^2 . Neglecting the elastic term, we have

$$f(T, \Phi) = \frac{r(T)}{2} \Phi^2 + u \Phi^4, \quad (6.7)$$

where we assumed a constant $u > 0$, ensuring the stability of the system and the existence of a finite minimum. Phenomenologically we know that at $T > T_c$, the free energy must be minimised by $\Phi = 0$, thus $r(T > T_c) > 0$, and at $T < T_c$, f should be minimal for non-zero Φ , corresponding to the ordered phase. The simplest ansatz that satisfies this is the linear function $r(T) = r_0(T - T_c)$, $r_0 > 0$.

Plot the results. Explicitly draw attention to the equivalence between these phenomenologically motivated results and the magnetic (Weiss mean-field, which on contrary, derives from a microscopical hamiltonian) (and liquid-gas?, also derived from microscopical considerations) cases.

We will now proceed by obtaining the (mean-field) critical exponents as given in the following table:

α	β	δ	γ	ν	η
$c_V \sim \tau ^{-\alpha}$	$\Phi \sim \tau ^\beta$	$\Phi \sim h ^{1/\delta}$	$\chi \sim \tau^\gamma$	$\xi \sim \tau ^{-\nu}$	$\chi(r) \sim \left(\frac{1}{r}\right)^{(d-2+\eta)}$

Table 6.1: Definition of critical exponents.

β for order parameter at $h = 0$: To find the order parameter in the absence of h is equivalent to finding the minima of f .

$$0 = \left. \frac{\partial f}{\partial \Phi} \right|_{\Phi_m} = r(T)\Phi_m + 4u\Phi_m^3$$

$$\Rightarrow \Phi_m = \begin{cases} 0, & \Phi > 0, \\ \pm \sqrt{-\frac{r(T)}{4u}}, & \Phi < 0. \end{cases} \quad (6.8)$$

Hence we see that $\beta = 1/2$.

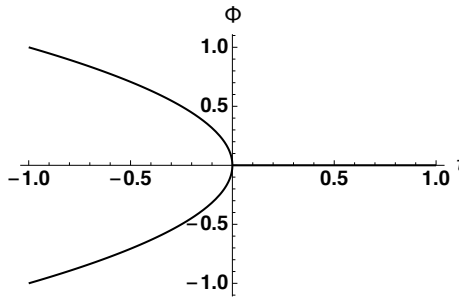


Figure 6.2: At the critical temperature the order parameter starts to assume one of the two finite values of the opposite sign due to spontaneous symmetry breaking.

δ for critical isotherm: h is given by

$$h(T) = \frac{\partial f}{\partial \Phi} = r(T)\Phi + 4u\Phi^3. \quad (6.9)$$

At the critical isotherm, the first term vanishes, and we get

$$\Phi(h, T = T_c) = \left(\frac{h}{4u} \right)^{1/3}, \quad (6.10)$$

hence we get that $\delta = 3$.

α for heat capacity: The free energy for $h = 0$ is found by substituting the value for Φ_m below and above the critical point:

$$f(T, h = 0) = \begin{cases} -\frac{r_0^2(T-T_c)^2}{16u}, & T < T_c, \\ 0, & T > T_x. \end{cases} \quad (6.11)$$

The heat capacity is given by

$$c_v = -T \frac{\partial^2 f}{\partial T^2} = \begin{cases} T \frac{r_0^2}{8u}, & T < T_x \\ 0, & T > T_c. \end{cases} \quad (6.12)$$

We see that there is a jump discontinuity which is denoted by $\alpha = 0$.

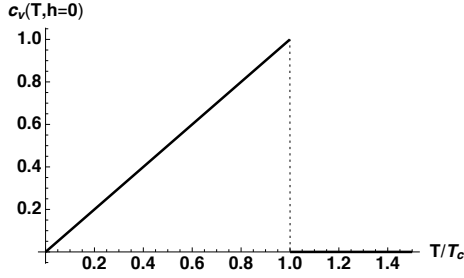


Figure 6.3: The specific heat shows a jump discontinuity at the critical temperature.

γ for Susceptibility: The susceptibility is given by $\chi = \frac{\partial \Phi}{\partial h} = \left(\frac{\partial^2 f}{\partial \Phi^2} \right)^{-1}$. Thus at $h = 0$, we have

$$\chi = (r(T) + 12u\Phi^2)^{-1} = \begin{cases} (r(T) - 3r(T))^{-1} = \frac{1}{2|r(T)|}, & T < T_c \\ \frac{1}{r(T)}, & T > T_c. \end{cases} \quad (6.13)$$

Hence we find that $\gamma = 1$.

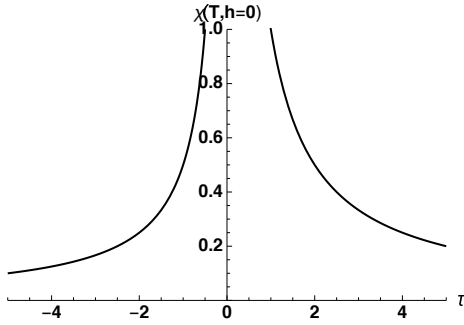


Figure 6.4: The divergence of the susceptibility at the critical temperature indicates a scaling behaviour.

Table 6.2 summarises our findings so far.

α	β	δ	γ	ν	η
0	1/2	3	1	-	-

Table 6.2: Mean-field critical exponents.

ν for correlation length and η for non-local susceptibility (correlation function): To obtain ν and η one has to include the elastic term, which can also be treated within the Gauss model.

We find the correlation function by taking two functional derivatives of the free energy and taking the Fourier transform. (Take the functional derivatives) What we get is

$$\chi^{-1}(q) = r(T) + 12u\Phi^2 - cq^2. \quad (6.14)$$

We then recast it into the following form to get the correlation length (explain relation to critical opalacence and scattering experiments and where did this expression firs arise!)

$$\chi(q) = \frac{1}{c} \frac{\xi^2}{1 + q^2 \xi^2}, \quad (6.15)$$

with

$$\xi = \left(\frac{c}{r(T) + 12u\Phi^2} \right)^{1/2} = \begin{cases} \left(\frac{c}{2|r(T)|} \right)^{1/2}, & T < T_c \\ \left(\frac{c}{r(T)} \right)^{1/2}, & T > T_c \end{cases} \quad (6.16)$$

from which we get $\nu = 1/2$.

One gets the non-local susceptibility $\chi(r)$ by taking the Fourier transform of $\chi(q)$. The result is

$$\chi(r) = \frac{1}{cr^{d-2}} \begin{cases} \frac{1}{4\pi} \exp\left(-\frac{r}{\xi}\right), & d = 3 \\ \frac{1}{2\pi} \frac{\exp\left(-\frac{r}{\xi}\right)}{\sqrt{\frac{r}{\xi}}}, & d = 2. \end{cases} \quad (6.17)$$

What we see is that at $T \neq T_c$, the correlation function decreases exponentially with distance. However at $T = T_c$, $\xi(T = T_c) \rightarrow \infty$ cancelling the exponential factor, and thus the leading to the algebraic decay of the correlation function with the inverse distance distance raised to the power $d - 2 + \eta = d - 2$, i.e. $\eta = 0$ for the mean-field theory.

We recall this behaviour of $\chi(r)$ from the Berezinskii phase in the 2- d XY model, where the system had an algebraically decaying correlation function below the critical temperature. Since the algebraic decay characterises a system at criticality, we say that the Berezinskii phase is critical at all temperatures $T < T_c$.

6.1.2 First order phase transitions

The first order transition can be made possible by the introduction of both the 3rd power term or the 6th power term! Illustrate that there are now 3 important temperatures T_c and the spinodals where the metastable states become unstable. This behaviour is because of the fact that the free energy can now have *local minima* at finite or 0 order parameter ϕ along with the global minimum. Note that magnetic systems do exhibit 1st order transitions, as well, but the 3rd power term is forbidden in that context due to the parity or rotation symmetry of the spins in $O(n)$ model. *Derive the $\phi - h$ (analogous to $v - p$ diagram in liquid-gas transition) diagram and $g - h$ diagram to demonstrate hysteresis!!* Also mention hysteresis in context of (non-diverging at T_c) susceptibility in comparison with 2nd order transitions. Scaling of spinodal curves.

The free energy density is given by

$$f = \frac{r}{2} \Phi^2 - w\Phi^3 + u\Phi^4. \quad (6.18)$$

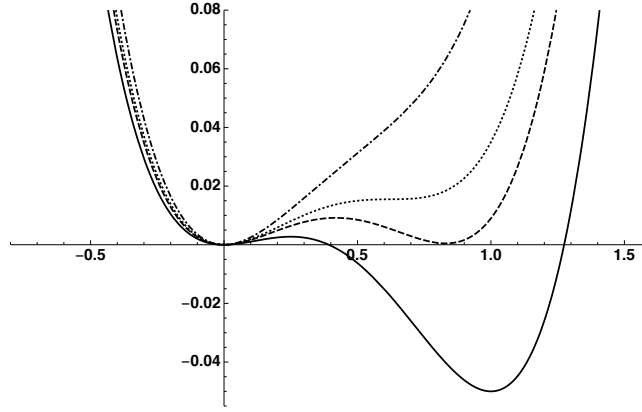


Figure 6.5: Landau free energy functional for the 1st order phase transition.

Here $r := r_0(T - T^*)$, where T^* is the *spinodal* temperature where the free energy changes sign and is no longer a local minimum at $\Phi = 0$. Because of the odd powered term, we now have the possibility to have asymmetric minima, one at $\Phi_m = 0$ and the other at $\Phi_m > 0$, one of which would correspond to the metastable phase.

The critical point T_c is the point where the metastable phase at $\Phi = 0$ becomes a stable phase, i.e. $f(\phi_m > 0) = 0$. Thus the condition for the critical point is given by

$$0 = \frac{\partial f}{\partial \Phi} \implies 0 = r - 3w\Phi + 4u\Phi^2 \quad (6.19)$$

$$0 = f \implies 0 = r/2 - w\phi + u\Phi^2, \quad (6.20)$$

which yields that

$$r_c = \frac{w^2}{2u}, \text{ or } T_c = \frac{w^2}{2r_0u} + T^*, \quad (6.21)$$

and the $\Phi > 0$ minimum is at

$$\Phi_m = \frac{w}{2u}. \quad (6.22)$$

At the other spinodal temperature T^{**} , f has no longer got a local minimum $\Phi > 0$. This means that

$$0 = \frac{\partial^2 f}{\partial \Phi^2} \text{ and} \quad (6.23)$$

$$0 = \frac{\partial f}{\partial \Phi}, \quad (6.24)$$

which implies that $\Phi^{**} = \frac{3w}{8u}$, and hence

$$r^{**} = \frac{9w^2}{16u}. \quad (6.25)$$

Note that the separations of the spinodals is different: $r^{**} - r_c = \frac{w^2}{16u}$, $r_c - r^* = \frac{8w^2}{16u}$, i.e. the spinodal above the critical temperature is closer to the critical temperature by a factor of 8.

Using this knowledge, we construct another phenomenological free energy to study the caloric properties of the system

$$f = \begin{cases} 0, & T > T_c \\ (r(T) - r_c) \frac{\Phi_m^2}{2}, & T < T_c. \end{cases} \quad (6.26)$$

From this we readily obtain the *jump* in entropy and thus the latent heat

$$\Delta S = S_m - S_0 = -\frac{\partial f(T_c^+)}{\partial T} + \frac{\partial f(T_c^-)}{\partial T} = -r_0 \Phi_m^2 = -\frac{r_0 w^2}{8u^2}. \quad (6.27)$$

$$\ell = |T_c \Delta S| = \frac{r_0 w^2 T_c}{8u^2}. \quad (6.28)$$

Finally note that on contrary to 2nd order phase transitions, the correlator $\chi = \left(\frac{\partial^2 f}{\partial T^2}\right)^{-1}$ does not diverge at the critical point as the curves corresponding to the stable phase are cut off at $T = T_c$. Only divergence occurs at the spinodals. As a consequence, we do not have any scaling laws since we cannot define any critical exponents. For first order phase transitions there exists no critical behaviour.

6.1.3 Multicritical points

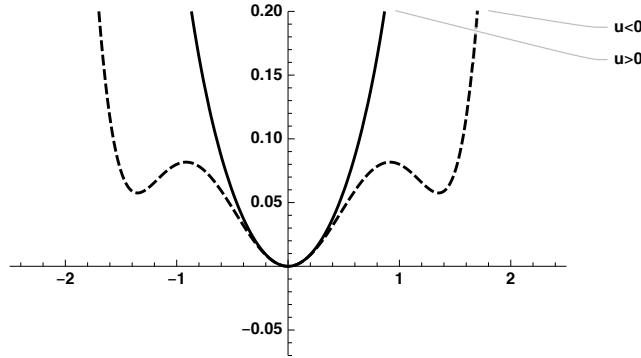


Figure 6.6: Tricritical behaviour.

E.g. tricritical point: three lines of critical points meet at the critical point. Note what Gibbs phase rule implies (wikipedia) about the number of components of the system!! Subtle point: system has two drives; Δ ($\sim p$ pressure) and h (conjugate to Φ), this is what allows to have a second order transition line, or a critical line. The proof that the critical and multicritical lines meet smoothly. **Multicritical exponents.** Physical example He mixture.

α	β	δ	γ	ν	η
1/2	1/4	5	1	1/2	0

Table 6.3: Tricritical exponents.

6.2 Beyond Landau theory

It is subtle whether Gaussian model is one step beyond the Landau mean field theory, which takes the saddle point approximation to the functional integral. The addition of the first term in the gradient expansion corresponds to long wavelength elastic distortions upon the mean field. Yet, in order to be able to do exact calculations, we drop the Φ^4 term, and the theory becomes unstable below the critical temperature. To calculate the effect of these fluctuations, we now have to calculate the integrals, but as it can be understood from the name, they are luckily Gaussian integrals, which can be evaluated exactly, as we have already encountered several times now.

Lattice field free energy

We consider a d -dimensional lattice with lattice constant a and the real valued field $\Phi_\nu := \Phi(\vec{r}_\nu)$ defined at each N lattice site labeled by ν . The corresponding free energy functional including the Gaussian fluctuation term is given by

$$F[\Phi_\nu] = \sum_\nu \left(\frac{r}{2} \Phi_\nu^2 + u \Phi_\nu^4 \right) + \sum_{\nu, \nu'} \frac{c_{\nu, \nu'}}{2} (\Phi_\nu - \Phi_{\nu'})^2. \quad (6.29)$$

We treat this functional as the effective hamiltonian of the system, hence we will refer to F as \mathcal{H} . Notice that, for $u = 0$, this is the same as the hamiltonian used for the approximation of XY model. Note that we treat the free energy as the effective Hamiltonian of the system, thus the partition function derives from \mathcal{H} . The simplest case is when both the Φ^4 and the elastic terms are 0, where the partition function can be evaluated by a generic gaussian integral

$$\begin{aligned} \mathcal{Z} &= \int \prod_\nu d\Phi_\nu \exp \left[-\beta \frac{r}{2} \sum_\mu \Phi_\mu^2 \right] \\ &= \int \prod_\nu \prod_\mu d\Phi_\nu \exp \left[-\beta \frac{r}{2} \Phi_\mu^2 \right] = \int \prod_\nu d\Phi_\nu \exp \left[-\beta \frac{r}{2} \Phi_\nu^2 \right] \\ &= \sqrt{\frac{2\pi k_B T}{r}}^N. \end{aligned} \quad (6.30)$$

We can go into the continuum limit using $\sum_\nu = N$, $\int d^d r = V \implies \sum_\nu = \int \frac{d^d r}{v}$, where $v = \frac{V}{N}$. Defining the elastic constant $c = \sum_\nu c_{\nu, 0} R_\nu^2$ we have the familiar Gaussian free energy

$$\mathcal{H}[\Phi(\vec{r})] = \int \frac{d^d r}{v} \left\{ \frac{r}{2} \Phi^2(\vec{r}) + u \Phi^4(\vec{r}) + \frac{c}{2} [\nabla^2 \Phi(\vec{r})] \right\}. \quad (6.31)$$

We can represent this free energy in the Fourier space.

$$\begin{aligned}
\mathcal{H}[\Phi_{\vec{k}}] &= \int \frac{d^d r}{v} \left\{ \frac{r}{2} \frac{1}{N^2} \sum_{\vec{k}_0, \vec{k}_1} \Phi_{\vec{k}_0} \Phi_{\vec{k}_1} e^{i\vec{r} \cdot (\vec{k}_0 + \vec{k}_1)} \right. \\
&\quad + \frac{c}{2} \frac{1}{N^2} \sum_{\vec{k}_0, \vec{k}_1} \Phi_{\vec{k}_0} \Phi_{\vec{k}_1} \nabla e^{i\vec{k}_0 \cdot \vec{r}} \cdot \nabla e^{i\vec{k}_1 \cdot \vec{r}} \\
&\quad \left. + u \frac{1}{N^4} \sum_{\vec{k}_0, \vec{k}_1, \vec{k}_2, \vec{k}_3} \Phi_{\vec{k}_0} \Phi_{\vec{k}_1} \Phi_{\vec{k}_2} \Phi_{\vec{k}_3} e^{i\vec{r} \cdot (\vec{k}_0 + \vec{k}_1 + \vec{k}_2 + \vec{k}_3)} \right\} \\
&= \frac{1}{2N} \sum_{\vec{k}_0, \vec{k}_1} (r + ck^2) \Phi_{\vec{k}_0} \Phi_{\vec{k}_1} \delta_{\vec{k}_0, \vec{k}_1} \\
&\quad + \frac{u}{N^3} \sum_{\vec{k}_0, \vec{k}_1, \vec{k}_2, \vec{k}_3} \Phi_{\vec{k}_0} \Phi_{\vec{k}_1} \Phi_{\vec{k}_2} \Phi_{\vec{k}_3} \delta_{\vec{k}_0, \vec{k}_1 + \vec{k}_2 + \vec{k}_3} \\
&= \sum_{\vec{k}} \frac{(r + ck^2)}{2N} |\Phi_{\vec{k}}|^2 + \frac{u}{N^3} \sum_{\vec{k}_1, \vec{k}_2, \vec{k}_3} \Phi_{\vec{k}_1} \Phi_{\vec{k}_2} \Phi_{\vec{k}_3} \Phi_{-\vec{k}_1 - \vec{k}_2 - \vec{k}_3}. \quad (6.32)
\end{aligned}$$

6.3 Gauss model

Landau theory also accords with slowly varying space dependent magnetisation. This is achieved by a generalisation of the free energy, which is known as the Landau-Ginzburg model [11]. Let us, for the moment, take $u = 0$. This is the Gauss model¹. This free energy allows us to compute the correlator χ and the correlation length ξ , and reads

$$\begin{aligned}
\mathcal{H}[\Phi_{\vec{k}}] &= \sum_{\vec{k}} \frac{(r + ck^2)}{2N} |\Phi_{\vec{k}}|^2 \\
&:= \frac{k_B T}{N} \sum_{\vec{k}} \Phi_{\vec{k}}^* G_0^{-1}(\vec{k}) \Phi_{\vec{k}}, \quad (6.33)
\end{aligned}$$

where the kernel

$$NG_0(\vec{k}) = \langle \Phi_{\vec{k}} \Phi_{-\vec{k}} \rangle = \frac{Nk_B T}{r + ck^2} \quad (6.34)$$

is the Green's function of a free theory. This is the equipartition theorem, i.e. every \vec{k} -mode with energy $E_{\vec{k}} = (r + ck^2)|\Phi_{\vec{k}}|^2/N$ involves a thermal energy $2k_B T/2$. Note that this model cannot explain the behaviour below T_c because $r < 0$ has no minima, and the system is unstable. Hence we cannot extract the exponents β and δ using this model. However, we can still obtain the scaling and divergence of fluctuations and heat capacity as $T \rightarrow T_c^+$.

¹since the added spatial fluctuations are of Gaussian form.

The partition function is given by

$$\begin{aligned} \mathcal{Z} &= \lim_{a \rightarrow \infty} \int \mathcal{D}[\Phi_{\vec{k}}] \left| \frac{\partial(\{\Phi_{\nu}\})}{\partial(\{\Phi_{\vec{k}}\})} \right| \exp \{-\beta \mathcal{H}[\Phi_{\vec{k}}]\} \\ &= \int \prod'_{k < \Lambda} N^{-1} d\phi_{\vec{k}} d|\Phi_{\vec{k}}| \left| \frac{\partial(\Phi_{\vec{k}}, \Phi_{\vec{k}}^*)}{\partial(\phi_{\vec{k}}, |\Phi_{\vec{k}}|)} \right| \exp \left\{ -\beta \sum'_{\vec{k}} \frac{(r + ck^2)}{N} |\Phi_{\vec{k}}|^2 \right\}, \end{aligned} \quad (6.35)$$

where \sum' and \prod' respectively denote sum and product over half of the \vec{k} values, since $\Phi_{\vec{k}}^* = \Phi_{-\vec{k}}$ and otherwise we overcount the degrees of freedom². We calculate the Jacobian³

$$\left| \frac{\partial(\Phi_{\vec{k}}, \Phi_{\vec{k}}^*)}{\partial(\phi_{\vec{k}}, |\Phi_{\vec{k}}|)} \right| = \left| \frac{\partial|\Phi_{\vec{k}}|e^{i\phi_{\vec{k}}}}{\partial\phi_{\vec{k}}} \frac{\partial|\Phi_{\vec{k}}|e^{i\phi_{\vec{k}}}}{\partial|\Phi_{\vec{k}}|} - \frac{\partial|\Phi_{\vec{k}}|e^{i\phi_{\vec{k}}}}{\partial|\Phi_{\vec{k}}|} \frac{\partial|\Phi_{\vec{k}}|e^{-i\phi_{\vec{k}}}}{\partial\phi_{\vec{k}}} \right| = 2|\Phi_{\vec{k}}|.$$

Therefore

$$\begin{aligned} \mathcal{Z} &= \int \prod'_{k < \Lambda} \frac{2}{N} d\phi_{\vec{k}} d|\Phi_{\vec{k}}| |\Phi_{\vec{k}}| \exp \left\{ -\beta \sum'_{\vec{k}} \frac{(r + ck^2)}{N} |\Phi_{\vec{k}}|^2 \right\} \\ &= \prod'_{k < \Lambda} \frac{2}{N} \frac{2\pi}{2} \frac{k_{\text{B}}T}{(r + ck^2)} \\ &= \prod'_{k < \Lambda} \sqrt{\frac{2\pi k_{\text{B}}T}{r + ck^2}}, \end{aligned} \quad (6.36)$$

which reduces to 6.30 when $c = 0$.

Free energy, specific heat, susceptibilities and correlators

The free energy of the system near a phase transition is given by $F = F_{\text{mf}} + F_{\text{Gauss}}$. [Plot the diverging specific heat. Plot the diverging susceptibility, find the critical exponent. Find the corresponding correlation length.](#)

The Gauss free energy is

$$F_{\text{Gauss}} = -k_{\text{B}}T \log \mathcal{Z} = -\frac{k_{\text{B}}T}{2} \sum_k^{\Lambda} \log \frac{2\pi k_{\text{B}}T}{r + ck^2}. \quad (6.37)$$

We go into the continuum, where the integral has lower and upper cutoffs. Λ , is the upper UV cutoff for the finite lattice spacing that we have introduced before,

²The system has N degrees of freedom, whereas there are $2N$ real Fourier components due to the imaginary and real parts.

³We can also parametrise in terms of the real and imaginary parts of the Fourier components

$$\Re\Phi_{\vec{k}} = \frac{1}{2}(\Phi_{\vec{k}} + \Phi_{\vec{k}}^*), \quad \Im\Phi_{\vec{k}} = \frac{i}{2}(\Phi_{\vec{k}}^* - \Phi_{\vec{k}}),$$

which also corresponds to a Jacobian with a factor of 2.

and the lower infrared cutoff is the inverse correlation length ξ^{-1} , i.e. since we are interested in the critical behaviour, we are calculating the free energy within the correlation distance, which diverges near criticality. Hence

$$\begin{aligned}
\frac{F_{\text{Gauss}}}{V} &= -\frac{k_{\text{B}}T}{2} \int \frac{d^d k}{(2\pi)^d} \log \frac{2\pi k_{\text{B}}T}{r + ck^2} \\
&= -\frac{k_{\text{B}}TS_{d-1}V}{2(2\pi)^d} \int_{\xi^{-1}}^{\Lambda} dk k^{d-1} \log \frac{2\pi k_{\text{B}}T}{r + ck^2} \\
&\approx \frac{k_{\text{B}}TS_{d-1}V}{(2\pi)^d} \int_{\xi^{-1}}^{\Lambda} dk k^{d-1} \log k \\
&\approx \frac{k_{\text{B}}TS_{d-1}V}{d(2\pi)^d} k^d \log k \Big|_{\xi^{-1}}^{\Lambda} = \frac{k_{\text{B}}TS_{d-1}V}{d(2\pi)^d} (\Lambda^d \log \Lambda + \xi^{-d} \log \xi). \quad (6.39)
\end{aligned}$$

where the approximations are done in order to focus on the singular behaviour, and in the last step of integration we have done integration by parts and taken the boundary term, whilst neglecting the other term since it is finite. Thus we recognise that the second term is singular, and focus on it

$$\frac{F_{\text{sing}}}{V} := \frac{S_{d-1}}{d(2\pi)^d \xi^d} \log \xi. \quad (6.40)$$

From this singular part, we can obtain the power law for the scaling behaviour of c_V . We recall that $\xi \sim |\tau|^{-\nu}$ and thus

$$\begin{aligned}
c_V &\sim -T \frac{\partial^2 (F_{\text{sing}}/V)}{\partial \tau^2} \sim \partial_{\tau}^2 (\nu |\tau|^{\nu d} \log |\tau|) \\
&= \partial_{\tau} [(-\nu^2 d \log |\tau| + \nu) |\tau|^{\nu d - 1}] \\
&= [-\nu^2 d + (\nu d - 1)(-\nu^2 d \log |\tau| + \nu)] |\tau|^{\nu d - 2} \\
&\sim |\tau|^{\nu d - 2}. \quad (6.41)
\end{aligned}$$

Hence we realise that $\alpha = 2 - \nu d$. Furthermore, by taking $u = 0$, we realise that the exponents for γ and ν are the same as in the mean field theory of second order phase transitions. Also, one can obtain $\chi(r)$ through the susceptibility sum rule, which yields the same integral as in 2nd order Landau theory, thus $\eta = 0$. Hence, taking $\nu = 1/2$, we get that $\alpha = d/2 - 2$. On contrary to the mean field result, we do not get a jump in the specific heat, but instead, we get a divergence for dimensions below 4 as we approach T_c from above.

It is crucial to note that the origin of this divergence in c_V is the infrared cutoff ξ^{-1} . Due to the long wavelength fluctuations (Goldstone modes) introduced by the Gauss hamiltonian causes the jump to become a divergence, and the long range order is destroyed.

One can also get c_V from the integral form of the free energy as follows

$$c_V = -T \frac{\partial^2 (F_{\text{Gauss}}/V)}{\partial T^2} \sim T \frac{k_{\text{B}}T}{2} \int \frac{d^d k}{(2\pi)^d} \left(\frac{\partial_T r}{r + ck^2} \right)^2 + \text{less singular terms.} \quad (6.42)$$

The correlation length is given by $\xi = \sqrt{c/r(T)}$ (same as the Landau mean field expression for 2nd order phase transitions with $u = 0$). We can express c_V in terms of this as follows

$$\begin{aligned} c_V &\sim k_B \int \frac{d^d k}{(2\pi)^d} \left(\frac{T \partial_T r}{r + ck^2} \right)^2 = k_B \int \frac{d^d k}{(2\pi)^d} \frac{\xi^4}{c^2} \left(\frac{T \partial_T r}{1 + \xi^2 k^2} \right)^2 \\ &= \xi^{4-d} k_B \int \frac{d^d x}{(2\pi)^d} \frac{1}{c^2} \left(\frac{T \partial_T r}{1 + x^2} \right)^2 \\ &\sim \xi^{4-d} k_B \int_0^{\Lambda \xi} dx \frac{x^{d-1}}{(1 + x^2)^2}. \end{aligned} \quad (6.43)$$

The integral is finite for $1 < d$. Hence we get the same scaling for c_V , $\alpha = d/2 - 2$ as before.

α	β	δ	γ	ν	η
$d/2 - 2$	-	-	1	1/2	0

Table 6.4: Critical exponents in Gauss model.

6.4 Gaussian approximation to free energy functionals

A systematic method to approximate any free energy functional by a gaussian form. Expand the free energy around the mean value (not the minimum! because the minimum and the mean does not overlap in case of an asymmetry?).

6.4.1 Φ^4 theory and the Hartree approximation

The ϕ^4 term makes the fluctuations interact/ couples the interactions. Explain how the approximate inclusion of the ϕ^4 term induces a reduction in critical temperature. Note that the proper way of treating the Φ^4 term and thus the interaction between the fluctuations and the order parameter field.

α	β	δ	γ	ν	η
1/2	1/4	5	1	1/2	0

Table 6.5: Critical exponents in self consistent Hartree.

6.5 Ginzburg criterion

When fluctuations become comparable to the mean field, the theory breaks down. The Ginzburg criterion [10] identifies this critical region characterised by

the Ginzburg temperature T_G . There are two methods to find T_G . First is due to Ginzburg: one enters the critical region when the mean field jump is matched by the diverging Gauss model c_v function. Draw the jumping mean field c_v and the diverging Gauss c_v on the same figure. The second method is to identify the point where the fluctuations within one coherence volume (determined by the correlation length) reach the magnitude matching the actual mean field. Show that this amounts for counting number of the degrees of freedom that is contained in the microscopic coherence volume ξ_0^d .

In terms of the correlation length ξ , the Ginzburg criterion is given by

$$\left[\frac{\xi(T)}{\xi_0} \right]^{d-4} \Big|_{T=T_G} = \frac{A_d k_B}{\Delta c_v \xi_0^d}, \quad (6.44)$$

or equivalently the Ginzburg temperature T_G is

$$1 - \frac{T_G}{T_c} = \frac{1}{2} \left(\frac{A_d k_B}{\Delta c_v \xi_0^d} \right)^{2/(4-d)}. \quad (6.45)$$

Observe that there is an *upper critical dimension* d_U , above which the fluctuations never get relevant. For the Φ^4 theory $d_U = 4$.

We can interpret the quantity $\Omega = \xi_0^d \Delta c_v / k_B$ as the number of degrees of freedom in the coherence volume. Hence we can write

$$1 - \frac{T_G}{T_c} \sim \left(\frac{1}{\Omega} \right)^{2/(4-d)}. \quad (6.46)$$

For $d < d_U$, we see that if $\Omega \lesssim 1$, then $T_G \sim 0$, i.e. the extent of the critical region is large. On contrary, if $\Omega \gg 1$, then $T_G \sim T_c$, i.e. the critical region is small, in other words, the mean-field theory holds. But this is sensible, because the mean field result should become more and more realistic as the number of degrees of freedom that supports the mean-field increases. [For example, in fractal geometries such as hierarchical lattices the mean-field gets more accurate?](#)

Put emphasis on the meaning of the microscopic correlation length (coherence length) $\xi_0 = \sqrt{\frac{c}{r_0 T_c}}$.

Chapter 7

Critical properties of Bose-Einstein condensation

7.1 Introduction to Bose-Einstein condensation
(BEC)

7.2 Gross-Pitaevskii equation (GPE)

7.3 Bogoliubov approximation

7.3.1 Superfluidity

Landau critical velocity

7.4 Reduced one-body density matrix

7.4.1 Order parameter of the condensate

Chapter 8

Scaling hypothesis

The developments of a full set of scaling hypotheses [4, 21, 12, 3] established that only 2 of the 6 critical exponents are independent. The four scaling laws (Widom, Josephson, Fisher, Rushbrooke) are as follows

$$\begin{aligned}\gamma &= \nu(2 - \eta) && \text{(Fisher)} \\ \alpha + 2\beta + \gamma &= 2 && \text{(Rushbrooke)} \\ \gamma &= \beta(\delta - 1) && \text{(Widom)} \\ \nu d &= 2 - \alpha. && \text{(Josephson)}\end{aligned}$$

8.1 Geometric (length) scaling

We start from the Landau Φ^4 theory $\mathcal{H} = \int d^d r \left[\frac{r}{2} \Phi^2 + \frac{c}{2} (\nabla \Phi)^2 + u \Phi^4 \right]$ and assume that there is only one relevant length scale, $\mathcal{L} \sim \xi \sim |T - T_c|^{-\nu}$ near criticality. We will see that under this assumption, dimensional arguments give rise to mean-field scaling. The mistake is due to the fact that the system actually has two important length scales; in addition to the macroscopic scale ξ (the IR cutoff), there is also the UV cutoff Λ^{-1} due to the finite lattice constant, which should also be considered. This microscopic length scale influences the fluctuations in the critical region. Nevertheless, the geometric scaling arguments yield the correct scaling laws.

The first step in constructing our dimensional arguments is to obtain a unitless Hamiltonian.

$$\beta \mathcal{H} := \tilde{\mathcal{H}} = \int d^d r \left[\frac{\tilde{r}}{2} \tilde{\Phi}^2 + \frac{1}{2} (\nabla \tilde{\Phi})^2 + \tilde{u} \tilde{\Phi}^4 \right], \quad (8.1)$$

where we absorbed c in Φ via $\tilde{\Phi} = \sqrt{\beta c} \Phi$ and introduced

$$\tilde{r} := r/c, \quad \tilde{u} := u/(\beta c^2). \quad (8.2)$$

We directly conclude that since $[\beta\mathcal{H}] = 1$,

$$\frac{[\tilde{\Phi}]^2}{\mathcal{L}^2} \cdot \mathcal{L}^d \stackrel{!}{=} 1 \implies [\tilde{\Phi}] = \mathcal{L}^{1-d/2}. \quad (8.3)$$

Furthermore it also follows that

$$[\tilde{r}]\mathcal{L}^d\mathcal{L}^{2-d} \stackrel{!}{=} 1 \implies [\tilde{R}] = \mathcal{L}^{-2}, \quad (8.4)$$

and

$$[\tilde{u}]\mathcal{L}^d\mathcal{L}^{4-2d} \stackrel{!}{=} 1 \implies [\tilde{u}] = \mathcal{L}^{d-4}. \quad (8.5)$$

We now consider the correlator $(\beta c)G(r) = \langle \tilde{\Phi}(r)\tilde{\Phi}(0) \rangle$ and we see that

$$[G] = [\tilde{\Phi}]^2 = \mathcal{L}^{2-d}. \quad (8.6)$$

If we rescale the length scale $\mathcal{L} \rightarrow \mathcal{L}' = \epsilon\mathcal{L}$ we then get

$$\begin{aligned} \mathcal{L}^{2-d}G(r) &= (\mathcal{L}')^{2-d}G'(r') \\ G(r) &= \epsilon^{2-d}G'(r'), \end{aligned}$$

or we express the rescale quantity in terms of the original quantity as

$$\epsilon^{d-2}G(r) = G'(r'). \quad (8.7)$$

On the other hand, we know that, near $T = T_c$, we expect that

$$\begin{aligned} G(r, T_c) &\sim \left(\frac{1}{r}\right)^{d-2+\eta} \quad \text{and} \\ G'(r', T_c) &\sim \left(\frac{1}{r'}\right)^{d-2+\eta} = \epsilon^{d-2+\eta} \left(\frac{1}{r}\right)^{d-2+\eta} = \epsilon^{d-2+\eta}G(r, T_c). \end{aligned} \quad (8.8)$$

Comparing 8.7 and 8.8, we deduce that our geometrical argument leads to the trivial anomalous exponent for the correlator $\eta = 0$, as in the mean-field theory.

Anomalous exponent for $G(r)$. On a less formal level, we can propose the ansatz

$$G(r, T_c) \sim \left(\frac{1}{r}\right)^{d-2+\eta} \cdot a^\eta, \quad (8.9)$$

where a is a microscopic length scale, say the lattice constant, in order to get both the consistent scaling for $G(r)$ and a finite value for the anomalous exponent η . To see this, let us rescale $G(r)$:

$$\begin{aligned} G'(r', T_c) &\sim (r')^{-d+2-\eta}(a')^\eta = \epsilon^{d-2+\eta}\epsilon^{-\eta}r^{-d+2-\eta}a^\eta \\ &\stackrel{!}{\sim} \epsilon^{d-2}G(r, T_c). \end{aligned} \quad (8.10)$$

This makes it clearer, that the anomalous exponents arise due to a microscopic length scale a .

Anomalous exponent for Φ . Since $G(r) = \langle \Phi(r)\tilde{\Phi}(0) \rangle$, we can alternatively argue that the field itself carries an anomalous exponent, i.e.

$$[\tilde{\Phi}] = \mathcal{L}^{1-d/2+\eta/2}, \quad (8.11)$$

which directly leads to the correct general behaviour $G \sim \mathcal{L}^{2-d+\eta}$ near $T = T_c$.

Anomalous exponent for ξ . We can also put forward an ansatz for the macroscopic length scale ξ to incorporate the effects of the microscopic length scale a on it:

$$\xi = \frac{1}{\sqrt{\tilde{r}}} f(\tilde{r}a^2). \quad (8.12)$$

Observe that at the critical point, the unitless argument $x = \tilde{r}a^2 = 0$. If $f(x \rightarrow 0) \rightarrow \text{finite}$, then

$$\xi(T \rightarrow T_c) \sim |T - T_c|^{-1/2}, \quad (8.13)$$

i.e. $\nu = 1/2$, which is the mean-field exponent. If however, there is a divergence, i.e. $f(x \rightarrow 0) \sim x^\theta$, then

$$\xi \sim \tilde{r}^{-1/2}(\tilde{r}a^2)^\theta \sim |T - T_c|^{\theta-1/2} \stackrel{!}{=} |T - T_c|^{-\nu}. \quad (8.14)$$

Therefore we conclude that $\nu = 1/2 - \theta$. That means that we get an anomalous dimension θ for the macroscopic length scale ξ on top of the canonical¹ exponent $1/2$.

We conclude that the introduction of a microscopic length scale can cause deviations of critical exponents from the mean-field values.

Now, incorporating the changes concerning the anomalous exponents, we have

$$[\beta f] = \mathcal{L}^{-d} \quad (8.15)$$

$$[G] = \mathcal{L}^{2-d+\eta} \quad (8.16)$$

$$[\Phi] = \mathcal{L}^{1-d/2-\eta/2} \quad (8.17)$$

$$[\beta^{-1}\chi] = \left[\int d^d r G(r) \right] = \mathcal{L}^{2-\eta} \quad (8.18)$$

$$[h] = [\beta H] = \mathcal{L}^{-1-d/2+\eta/2}, \text{ such that } \left[\beta \int d^d r H \Phi \right] = 1. \quad (8.19)$$

Thus we get

$$c_V = T \partial_T^2 f \stackrel{8.15}{\sim} \tau^{\nu d-2} \stackrel{!}{=} \tau^{-\alpha} \implies \alpha = 2 - \nu d, \quad (8.20)$$

$$\chi \stackrel{8.18}{\sim} \tau^{\nu\eta-2\nu} \stackrel{!}{=} \tau^{-\gamma} \implies \gamma = \nu(2 - \eta), \quad (8.21)$$

$$h \stackrel{8.19}{\sim} \tau^{\nu(1+d/2-\eta/2)} \stackrel{!}{=} \tau^{\beta\delta} \implies \beta\delta = \nu(1 + d/2 - \eta/2), \quad (8.22)$$

$$\Phi \stackrel{8.17}{\sim} \tau^{-\nu(1-d/2-\eta/2)} \stackrel{!}{=} \tau^\beta \implies \beta\nu(1 - d/2 - \eta/2). \quad (8.23)$$

¹Mean-field.

The relation 8.20 is the Josephson hyperscaling law. The relation 8.21 is the Fisher scaling law. (8.20) + (8.21) + 2(8.23) leads to the Rushbrooke scaling law. Finally, (8.22) – (8.23) = (8.21) leads to the Widom scaling law. Therefore, we recovered all four scaling laws from dimensional arguments.

8.2 Widom scaling

A more physical argument leading to the same scaling laws.

Widom's scaling ansatz [25] combines the two distinct scaling behaviours of the order parameter in temperature and the external drive into one scaling ansatz

$$m(\tau, h) \sim |\tau|^\beta \mathcal{M}_\pm \left(\frac{h}{|\tau|^\Delta} \right), \quad (8.24)$$

where, \mathcal{M}_\pm , $+$: $\tau > 0$, $-$: $\tau < 0$ are two scaling functions and the exponents β and Δ (the gap exponent) are thereby taken to be universal. The usefulness of this ansatz comes from the fact that it implies that if we collect the data for m and h at different temperatures and for different *systems*, due to universality, one obtains a data collapse. In other words, if one plots $m|\tau|^\beta$ versus $h|\tau|^\Delta$ for different systems, all the data collapses onto a single curve determined by the function \mathcal{M}_\pm for the correct critical exponents β and Δ as $T \rightarrow T_c$. This provides a robust experimental and also a numerical method for determining the exponents.

8.3 Homogeneous function scaling

Will be useful in the RG scaling arguments.

8.4 Untypical examples

8.4.1 Scaling form near multicritical point

Consider a tricritical system, whose free energy functional is given by

$$\beta\mathcal{H} = \int d^d r f = \int d^d r \left[\frac{r(T, \Delta)}{2} \Phi^2 + \frac{1}{2} (\nabla \Phi)^2 + u(T, \Delta) \Phi^4 + w \Phi^6 - h \Phi \right], \quad (8.25)$$

where $w > 0$, $u \geq 0$ (for stability), Δ is another "order destroying variable", e.g. hydrodynamic pressure, h is the external magnetic field and $r = r_0(1 - T/T_c) = r_0\tau$, as always.

The Widom scaling ansatz which we will investigate is [13]

$$f(\tau, u, h) \propto |\tau|^{2-\alpha} f_0 \left(\frac{u}{|\tau|^{\Delta_u}}, \frac{h}{|\tau|^{\Delta_h}} \right). \quad (8.26)$$

8.4.2 Vortex-glass scaling in a superconductor near T_c

See the analysis of vortex lattice in type-II superconductors in presence of disorder [6]

8.5 Scaling in finite sized systems

Read [7, 8] for specific heat anomaly for the Ising system on a finite lattice, and other finite-size and boundary effects.

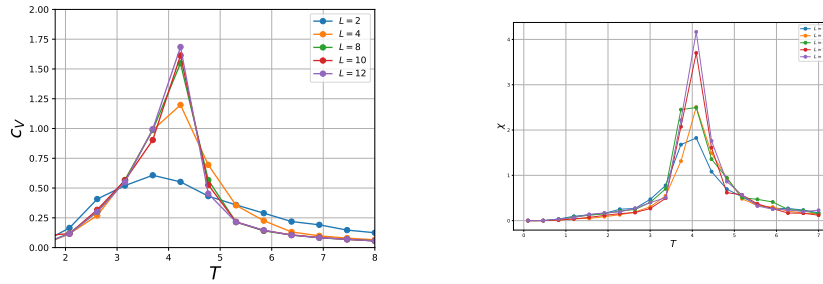


Figure 8.1: Finite size scaling of the susceptibility χ (right) and the specific heat c_V (left) in the 3-dimensional simple cubic lattice Ising model for different system sizes L^3 . We observe higher peaks and narrower critical regions for larger system sizes as the system converges to the thermodynamic limit.

Let us denote by ξ the correlation length corresponding to the system in the thermodynamic limit. For finite systems at $T = T_c$, the correlation length ξ does not diverge, but it instead converges to the system size L . This also hinders the divergences in the specific heat and susceptibility per particle. That is, $\chi \sim \xi^{\gamma/\nu} \rightarrow L^{\gamma/\nu}$ and $c_V \sim \xi^{\alpha/\nu} \rightarrow L^{\alpha/\nu}$ near $T = T_c$. This indicates that the peaks get higher as the system size grows as shown in Figure 8.5. Furthermore, we expect that as long as $\xi \ll L$, χ and c_V should behave similar to the thermodynamic limit. Thus we put forward the following ansatz

$$\chi \sim \xi^{\gamma/\nu} \chi_0(L/\xi), \quad (8.27)$$

where χ_0 is a unitless scaling function such that

$$\chi_0(x) = \begin{cases} \text{constant} & x \gg 1 : \text{away from criticality,} \\ x^{\gamma/\nu} & x \rightarrow 0 : \text{critical.} \end{cases} \quad (8.28)$$

We define

$$\mathcal{F}(x) = x^{-\gamma} \chi_0(x^\nu),$$

or $\chi_0(L/\xi) = \mathcal{F}((L/\xi)^{1/\nu})(L/\xi)^{\gamma/\nu} = \mathcal{F}(L^{1/\nu}|\tau|)(L/\xi)^{\gamma/\nu}$, with $\tau = T - T_c$. This leads to the following *finite-size scaling function*

$$\chi_L(T) = L^{\gamma/\nu} \mathcal{F}(L^{1/\nu}|\tau|). \quad (8.29)$$

We can therefore obtain the critical exponents by computing the susceptibility

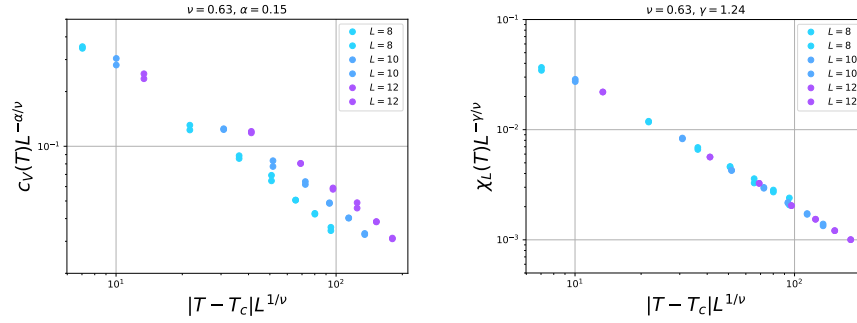


Figure 8.2: Data collapse occurs for good estimates of the critical exponents. Such an analysis yields $\nu \simeq 0.63$, $\alpha \simeq 0.15$ and $\gamma \simeq 1.24$ for the 3- d Ising model.

or the specific heat for small systems of different sizes, and determining the values that lead to a data collapse for the latter scaling function as in Figure 8.5.

8.5.1 Binder cumulant

The Binder cumulant [2] is defined as

$$U_L := 1 - \frac{\langle M^4 \rangle}{3 \langle M^2 \rangle_L^2} \stackrel{\text{Ising}}{=} \begin{cases} \frac{2}{3}, & T \ll T_c, \\ \text{constant}, & T = T_c, \\ 0, & T \gg T_c, \end{cases} \quad (8.30)$$

with the indicated values for the Ising model. We see that U_L is independent of the system size at $T = T_c$. Therefore, by simulating the system for different sizes L , we can locate the critical temperature where Binder cumulants for all cases are equal to the same constant.

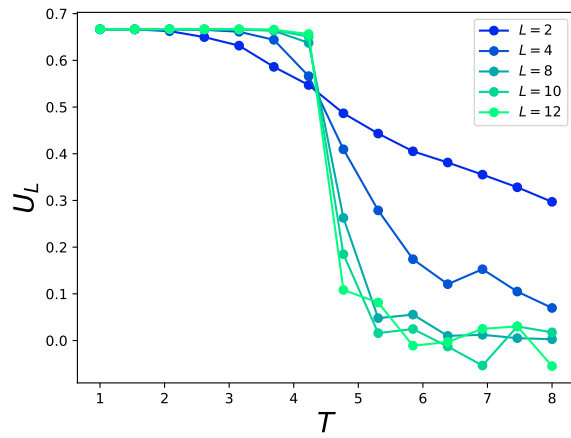


Figure 8.3: Binder cumulants for finite L 3- d Ising systems. Computing the Binder cumulant U_L for small systems of different sizes allows to determine T_c , at the location where all U_L are equal. In this case this indicates $T_c \simeq 4.51$.

Chapter 9

Renormalisation-group theory

The renormalisation-group approach is a framework of strategies for studying physical phenomena that involve crucial ingredients in many different size scales. In case of critical phenomena, the strategy is to tackle the problem in steps, by carrying out statistical averages over thermal fluctuations at sequentially growing length scales at each step. Eventually, the fluctuations at all scales are averaged out. For a historical account of the concept, the interested reader is directed to Ref. [26].

In order to consistently apply the renormalisation procedure, one has to consider a Hamiltonian depending on a complete set of coupling constants $\{K\}$

$$\mathcal{H} = \sum_{\alpha=1}^{M \rightarrow \infty} \tilde{K}_{\alpha} \tilde{O}_{\alpha}, \quad \text{with } \tilde{O}_{\alpha} = \sum_i \prod_{k \in C_{\alpha}} \tilde{\sigma}_{i+k}, \quad (9.1)$$

where C_{α} denotes the range of couplings (nearest neighbour, next nearest neighbour, etc.). The reason is that, the renormalisation procedure generates new couplings at each step.

On a formal level, the renormalisation group approach can be outlined as follows

1. Using the dimensionless Hamiltonian $\mathcal{K} = -\beta\mathcal{H}$,

$$\mathcal{Z}_N[K] = \text{Tr}_{\{\sigma_i\}} \exp(\mathcal{K}[K, \{\sigma_i\}]) \quad (9.2)$$

defines the free energy per particle via $f[K] = N^{-1} \ln \mathcal{Z}_N[K]$.

2. RG transformation

$$R_b : K \rightarrow K' \quad (9.3)$$

combines b^d degrees of freedom into one, in a new set of block variables $\{\sigma'_I\}$, with potentially new couplings emerged.

3. The corresponding hamiltonian $\mathcal{K}[K', \{\sigma'_I\}]$ describing the couplings of new block variables $\{\sigma'_I\}$ is obtained by tracing out all configurations $\{\sigma_i\}$ that produce this $\{\sigma'_I\}$

$$\exp(\mathcal{K}[K', \{\sigma'_I\}]) = \text{Tr}_{\{\sigma_i\}} P_\Lambda(\{\sigma_i\}, \{\sigma'_I\}) \exp(\mathcal{K}[K, \{\sigma_i\}]), \quad (9.4)$$

where Λ denotes the set of parameters that completely specify the transformation rule. Note that the projector P_Λ can be viewed as a conditional probability ($P_\Lambda(\{\sigma_i\}, \{\sigma'_I\}) = P_\Lambda(\{\sigma'_I\}|\{\sigma_i\})$) and it satisfies

$$1 = \sum_{\{\sigma'_I\}} P_\Lambda(\{\sigma_i\}, \{\sigma'_I\}), \quad (9.5)$$

i.e. $\{\sigma'_I\}$ is spanned by the image of R_b .

Note that it follows that, defining $N' = N/b^d$,

$$\begin{aligned} \mathcal{Z}_{N'}[K'] &= \text{Tr}_{\{\sigma'_I\}} \exp(\mathcal{K}[K', \{\sigma'_I\}]) \\ &= \text{Tr}_{\{\sigma'_I\}} \text{Tr}_{\{\sigma_i\}} P_\Lambda(\{\sigma_i\}, \{\sigma'_I\}) \exp(\mathcal{K}[K, \{\sigma_i\}]) \\ &= \text{Tr}_{\{\sigma_i\}} \exp(\mathcal{K}[K, \{\sigma_i\}]) = \mathcal{Z}_N[K]. \end{aligned} \quad (9.6)$$

This means that the RG transformations preserve the form of the partition function and thus the free energy per degree of freedom.

9.1 Renormalisation-group (RG) equations

One uses the renormalisation-group (RG) equations to find out the fixed points of the coefficient vectors. These fixed points correspond to critical points or stable or unstable (bulk) phases of the system.

9.1.1 Fixed points K^*

A fixed point of a RG transformation is defined by

$$K^* := R_b[K^*]. \quad (9.7)$$

It is clear that R_b shrinks lengths by a factor of b , therefore

$$R_b : \xi[K] \rightarrow \xi[R_b[K]] = \xi[K]/b. \quad (9.8)$$

But at a fixed point K^* , $\xi[K^*]/b = \xi[R_b[K^*]] = \xi[K^*]$, i.e.

$$\xi[K^*]/b = \xi[K^*] \implies \xi[K^*] = \begin{cases} 0, & \text{bulk phase,} \\ \infty, & \text{critical point.} \end{cases} \quad (9.9)$$

Thus we conclude that the fixed points K^* of an RG transformation locate the bulk phases and the critical phase transitions in a system with arbitrary set of coupling constants $\{K\}$.

Basin of attraction $\mathcal{B}[K^*]$ of a fixed point K^* .

A point K in the parameter space is said to be in the basin of attraction of K^* if

$$\lim_{n \rightarrow \infty} R_b^n[K] = K^*. \quad (9.10)$$

Then it follows that $\xi[K] = b^n \xi[R_b^n[K]] \xrightarrow{n \rightarrow \infty} b^n \xi[K^*] \rightarrow \begin{cases} \infty, & \text{critical,} \\ 0, & \text{bulk phase.} \end{cases}$

Therefore, we conclude that all points $K \in \mathcal{B}[K_c^*]$ of a critical fixed point K_c^* are critical. We thus say that $\mathcal{B}[K_c^*]$ defines the critical manifold. *This is the basis of universality:* all¹ Hamiltonians whose coupling constants $K \in \mathcal{B}[K_c^*]$ have the same critical behaviour, with the same critical exponents.

9.1.2 Linearised RG equations

One can linearise the RG equations near the fixed points. The modified problem is now an eigenvalue problem and the eigenvalues are the scaling exponents λ_τ of the coefficients for e.g. τ . If the scaling exponent (or the gap exponent) is negative, then we say that those parameters are *irrelevant*, since they vanish under rescaling.

Finding critical exponents.**9.1.3 Kadanoff's block spin transformation**

Systematic coarse graining of the spins by rescaling the lattice constant, hence producing new coefficients J (and hence T_c) and etc. Why is this method naive? Assuming that the problem has a translation invariance, the RG procedure can be performed in the form of blocks, i.e. the projector is factorised into independent contributions from equivalent real-space blocks $V \subset \{\sigma_i\}$ such that

$$P(\{\sigma'_I\}, \{\sigma_i\}) = \prod_{j=1}^n P_\Lambda(V_j, H_j), \quad (9.11)$$

where $\{V_j\}_{j=1}^n \subset \{\sigma_i\}$ and $\{H_j\}_{j=1}^n \subset \{\sigma'_I\}$. P_Λ now defines the coarse-graining transformation of a single block and thus Λ is substantially smaller.

9.2 Position space RG in lattice systems

Explain the flow of fixed points and critical lines in the parameter phase space.

¹potentially, with vast differences

9.2.1 Decimation RG and the transfer matrix method

1-d Ising model

1-d Potts model

Potts model is the generalisation of Ising model with $q \geq 2$ state spins. The Hamiltonian is given by

$$\mathcal{H} = -J \sum_{\langle i,j \rangle} \delta_{\sigma_i \sigma_j} - h \sum_i \sigma_i, \quad (9.12)$$

where $\sigma_i \in \{1, \dots, q\}$ and $\delta_{\sigma_i \sigma_j}$ is the Kronecker delta. Note that there exists a connection between the Potts model and the bond percolation model. By considering the Potts model on an arbitrary graph of nodes connected with bonds, one can show that the partition functions of the two systems are related, which is known as the Kasteleyn-Fortuin theorem [9].

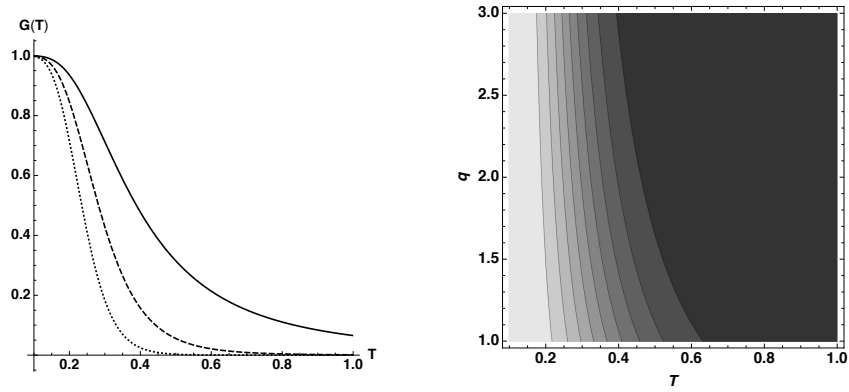


Figure 9.1: Spin-spin correlator for Potts model for ferromagnetic coupling ($K > 0$). On the left figure The solid curve is for $n = 2$, dashed curve is for $n = 5$ and dotted curve is for $n = 10$. On the right, the contour plot is plotted for $n = 10$.

1-d Spin-1 model

Clock model

XY model

One dimensional gas

9.2.2 The Niemeijer-van Leeuwen cumulant approximation

See [18].

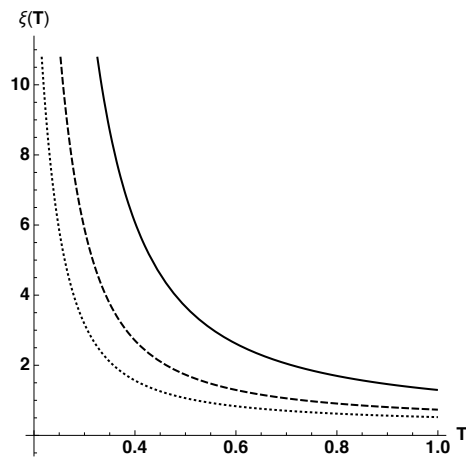


Figure 9.2: Potts model correlation length for ferromagnetic coupling ($K > 0$). The solid curve is for $q = 2$, dashed curve is for $q = 5$ and dotted curve is for $q = 10$.

2-d Ising model

9.2.3 The Migdal-Kadanoff bond moving approximation

9.2.4 Monte Carlo simulations

9.2.5 BKT-transition

Read [15, 14].

9.3 k -space RG

9.4 Renormalisation-group Monte Carlo (MCRG)

[22] [23]

Chapter 10

Real space RG using neural networks

10.1 Machine learning

10.2 Neural networks

10.2.1 Restricted Boltzmann machines

Chapter 11

RG in catastrophe optics and caustics

Chapter 12

Critical exponents

- $-\alpha$ is the critical exponent for the specific heat at $h = 0$.
- β is the critical exponent of the order parameter as a function of $|\tau| = 1 - T/T_c$ at $h = 0$.
- $1/\delta$ is the critical exponent of the order parameter as a function of h on the critical exponent, i.e. $T = T_c$.
- $-\gamma$ is the critical exponent for the magnetic susceptibility at $h = 0$.
- $-\nu$ is the critical exponent for correlation length
- η is the anomalous dimension for the non-local susceptibility: $\chi(r) \sim \left(\frac{1}{r}\right)^{2-d+\eta}$.

Weiss mean-field	α	β	$1/\gamma$	$-\delta$	η	phase transtition
Ising	0	1/2	1/3	-1	0	✓LRO
XY	0	1/2	1/3	-1	0	✓LRO
Heisenberg	0	1/2	1/3	-1	0	✓LRO

1D	α	β	$1/\delta$	$-\gamma$	η	phase transtition
Ising						✗
XY						✗
Heisenberg						✗

2D	α	β	$1/\delta$	$-\gamma$	η	phase transtition
Ising						✓LRO
XY						✓QLRO
Heisenberg						✗

3D	α	β	$1/\delta$	$-\gamma$	η	phase transtition
Ising						✓LRO
XY						✓LRO
Heisenberg						✓LRO

Part III

Non-equilibrium statistical mechanics

The volume in phase space is *locally* conserved. In other words, the phase space density $\rho(\vec{p}, \vec{q})$ corresponding to a physical system consisting of N particles follows the continuity equation

$$\frac{\partial \rho}{\partial t} + \nabla \cdot (\rho v) = 0, \quad (12.1)$$

where v is the phase space velocity, describing current ρv . Using Hamilton's equations of motion and Poisson brackets, one can express this equation describing the time evolution of ρ in a more sophisticated way

$$\frac{\partial \rho}{\partial t} = \{\mathcal{H}, \rho\}, \quad (12.2)$$

which is also known as Liouville's theorem.

In *thermal equilibrium*, the system reaches an equilibrium steady state, where the phase space density no longer evolves in time. In terms of the Poisson brackets, $\{\mathcal{H}, \rho\} = 0$ implies that ρ only depends on quantities that are invariant on the kinetics of the system. Among these, the preferred quantities are usually chosen to be studied are the thermodynamic ones such as T , E , p , V , etc.

The convenience, and the beauty of equilibrium statistical mechanics is that the system is fully characterised by a (time independent) Hamiltonian \mathcal{H} , and as a result, the kinetics, in the sense that the temporal order for occurrences of possible configurations is redundant in obtaining the macroscopic thermodynamical quantities of the system. However, in nature, the equilibrium systems are more the exception than the rule. It is rarely the case that the phase space density does not have an explicit dependence on time. Indeed, the very process of equilibration requires non-equilibrium processes. Such processes can have very distinct time-scales. These scales can be used to classify different non-equilibrium systems, such as near- and far-from-equilibrium systems, among with non-equilibrium steady states.

Near-equilibrium: linear response, fluctuation-dissipation theorem.

We have seen in many cases of equilibrium systems that the physical properties of a system show a power law dependence on temperature near the critical point T_c , defining 6 critical exponents, 4 of which are related through scaling laws. On the other hand, in non-equilibrium phase transitions, further quantities shows such a behaviour. An example is the diverging correlation time at T_c , which causes a phenomenon called the *critical slowing down*.

Explain what percolation is. Isotropic percolation is an equilibrium process, whereas anisotropic (directed) percolation is a non-equilibrium process. Yet, both have an associated order parameter $P(p) \sim (p - p_c)^\beta$ describing a critical phase transition between two phases. The critical properties of directed and isotropic percolation belong to different classes of universality. This illustrates that although it is not possible to define a free energy in non-equilibrium statistical mechanics, one can still distinguish between first- and second-order phase transitions by considering the behaviour of the order parameter.

12.0.1 Temporal correlations

Let us consider a quantity A that depends on the configuration X_i of the system: $A = A(X_i)$. The complete set of configurations $\{X_i\}$ are assumed to be generated via a stochastic (Markov chain) process, whose steps we denote by τ . This means that the image of the function $X(\tau)$ is $\{X_i\}$. The stochastic evolution of the configuration is governed by the Markov chain probability $W(X(\tau) \rightarrow X(\tau + 1)) = T(X(\tau) \rightarrow X(\tau + 1))A(X(\tau) \rightarrow X(\tau + 1))$, which is chosen to fulfill the detailed balance condition, i.e. $W(X(\tau) \rightarrow X(\tau + 1)) = \frac{p(X, \tau + 1)}{p(X, \tau)} W(X(\tau + 1) \rightarrow X(\tau))$. This means that the evolution of $X(\tau)$ is implicitly determined by the distribution of configurations $p(X, \tau)$ which evolve according to the master equation. Therefore it is appropriate to define the ensemble average of A in a given stochastic step τ as

$$\langle A(\tau) \rangle = \sum_i p(X_i, \tau) A(X_i). \quad (12.3)$$

In particular, since the configuration takes a distinct value $X(\tau)$ at τ , we can say that $A(X(\tau)) = A(\tau)$. Then we can alternatively average over all Markov chains that start with configuration $X(\tau_0)$ and become $X(\tau)$ at step τ . However, due to the master equation given the initial configuration $X(\tau_0)$, Markov chain is defined completely. It follows that

$$\langle A(\tau) \rangle = \sum_X p(X(\tau_0), \tau_0) A(\tau) = \sum_X p(X(\tau_0), \tau_0) A(X(\tau)), \quad (12.4)$$

where the sum is done over all initial configurations $X(\tau_0)$.

Let us now introduce the *non-linear* temporal correlation function

$$\Phi_A^{\text{nl}} = \frac{\langle A(\tau) \rangle - \langle A(\infty) \rangle}{\langle A(\tau_0) \rangle - \langle A(\infty) \rangle}, \quad (12.5)$$

where $\tau > \tau_0$. Typically Φ_A^{nl} is a monotonically decaying function between unity and zero, limits occurring at $\tau = \tau_0$ and $\tau \rightarrow \infty$, respectively. We may define the *non-linear* correlation time

$$\tau_A^{\text{nl}} = \int_0^\infty \Phi_A^{\text{nl}}(\tau) d\tau. \quad (12.6)$$

which describes the relaxation time into equilibrium in a Markov chain. Numerical studies established that near the critical point of a second-order phase transition there occurs a phenomenon of *critical slowing down*, i.e. τ_A^{nl} shows a power law divergence

$$\tau_A^{\text{nl}} \sim |T - T_c|^{-z_A^{\text{nl}}}, \quad (12.7)$$

meaning that the equilibrium cannot be reached in a finite number of stochastic steps near $T = T_c$ ¹.

¹Does this indicate that the system is intrinsically non-equilibrium during the phase transition?

We may also define the *linear* temporal correlation function of quantities A and B as

$$\Phi_{AB}(\tau) = \frac{\langle A(\tau_0)B(\tau) \rangle - \langle A(\tau_0) \rangle \langle B(\tau_0) \rangle}{\langle A(\tau_0)B(\tau_0) \rangle - \langle A(\tau_0) \rangle \langle B(\tau_0) \rangle}, \quad (12.8)$$

where $\langle A(\tau_0)B(\tau) \rangle = \sum_X p(X(\tau_0), \tau_0) A(X(\tau_0)) B(X(\tau))$. Similarly, to the non-linear correlation function, $\Phi_{AB}(\tau)$ decays from unity to zero as τ goes from τ_0 to ∞ . For $A = B$, we have the autocorrelation function

$$\Phi_A = \frac{\langle A(\tau_0)A(\tau) \rangle - \langle A(\tau_0) \rangle^2}{\langle A^2(\tau_0) \rangle - \langle A(\tau_0) \rangle^2}. \quad (12.9)$$

The *linear* correlation time τ_{AB} describes relaxation towards equilibrium

$$\tau_{AB} = \int_0^\infty \Phi_{AB}(\tau) d\tau, \quad (12.10)$$

which also reflects the critical slowing down phenomenon through a power-law divergence

$$\tau_{AB} \sim |T - T_c|^{-z_A}. \quad (12.11)$$

There exist numerically supported conjectures relating the critical exponents z_ϕ for order parameter correlations and z_E for energy correlations to β and α

$$z_\phi - z_\phi^{\text{nl}} = \beta, \quad (12.12)$$

$$z_E - z_E^{\text{nl}} = 1 - \alpha. \quad (12.13)$$

We have seen that the correlation length $\xi \sim |T - T_c|^{-\nu}$ approaches a value on the order of the system size \mathcal{L} at $T = T_c$, forming the basis of the scaling hypothesis. It follows that

$$\tau_A \sim \mathcal{L}^{z_A/\nu}. \quad (12.14)$$

This implies that the number of stochastic steps required to reach equilibrium increases as a power law with the system size.

12.1 Time dependent Ginzburg-Landau (TDGL) model

The TDGL equation of motion for the order parameter ϕ is given as

$$\frac{\partial \phi}{\partial t} = -\Gamma \frac{\delta \mathcal{F}}{\delta \phi} + \theta(\vec{r}, t), \quad (12.15)$$

where \mathcal{F} is the free energy functional of the Landau ϕ^4 mean-field functional with Gaussian fluctuations

$$\mathcal{F}(\phi) = \int \mathcal{D}[\phi] \left[\frac{r}{2} \phi^2 + u \phi^4 + \frac{C}{2} |\nabla \phi|^2 \right]. \quad (12.16)$$

The relevant chapter in Kardar [13].

12.2 Non-equilibrium phase transitions

12.2.1 Directed percolation

12.2.2 Dicke model phase transition

12.2.3 Exciton-polariton condensation

12.2.4 Mott transition

Bibliography

- [1] V. Berezinskii. Violation of long range order in one-dimensional and two-dimensional systems with a continuous symmetry group. *Zh. Eksp. Teor. Fiz.*, 59(907):907–920, 1970.
- [2] K. Binder. Critical properties from monte carlo coarse graining and renormalization. *Phys. Rev. Lett.*, 47:693–696, Aug 1981.
- [3] C. Domb and D. L. Hunter. On the critical behaviour of ferromagnets. *Proceedings of the Physical Society*, 86(5):1147–1151, nov 1965.
- [4] J. W. Essam and M. E. Fisher. Padé approximant studies of the lattice gas and ising ferromagnet below the critical point. *The Journal of Chemical Physics*, 38(4):802–812, 1963.
A. E. Ferdinand and M. E. Fisher. Bounded and inhomogeneous ising models. i. specific-heat anomaly of a finite lattice. *Phys. Rev.*, 185:832–846, Sep 1969.
- [5] R. P. Feynman. *Statistical mechanics : a set of lectures*. Advanced book classics series. Westview Press, Boulder, 1998.
- [6] D. S. Fisher, M. P. A. Fisher, and D. A. Huse. Thermal fluctuations, quenched disorder, phase transitions, and transport in type-ii superconductors. *Phys. Rev. B*, 43:130–159, Jan 1991.
M. E. Fisher. Correlation functions and the critical region of simple fluids. *Journal of Mathematical Physics*, 5(7):944–962, 1964.
- [7] M. E. Fisher and M. N. Barber. Scaling theory for finite-size effects in the critical region. *Phys. Rev. Lett.*, 28:1516–1519, Jun 1972.
- [8] M. E. Fisher and A. E. Ferdinand. Interfacial, boundary, and size effects at critical points. *Phys. Rev. Lett.*, 19:169–172, Jul 1967.
- [9] C. M. Fortuin, P. W. Kasteleyn, and J. Ginibre. Correlation inequalities on some partially ordered sets. *Communications in Mathematical Physics*, 22:89–103, June 1971.
- [10] V. Ginzburg. *Fiz. Tverd. Tela*, 2:2031, 1960.

- [11] V. L. Ginzburg and L. D. Landau. On the Theory of superconductivity. *Zh. Eksp. Teor. Fiz.*, 20:1064–1082, 1950.
- [12] L. P. Kadanoff. Scaling laws for ising models near T_c . *Physique Physique Fizika*, 2:263–272, Jun 1966.
- [13] M. Kardar. *Statistical Physics of Fields*. Cambridge University Press, Cambridge, 2007.
- [14] J. Kosterlitz and D. Thouless. Chapter 5 two-dimensional physics. volume 7 of *Progress in Low Temperature Physics*, pages 371 – 433. Elsevier, 1978.
J. M. Kosterlitz. The critical properties of the two-dimensional xy model. *Journal of Physics C: Solid State Physics*, 7(6):1046–1060, mar 1974.
- [15] J. M. Kosterlitz and D. J. Thouless. Ordering, metastability and phase transitions in two-dimensional systems. *Journal of Physics C: Solid State Physics*, 6(7):1181–1203, apr 1973.
- [16] L. D. Landau. On the theory of phase transitions. I. *Phys. Z. Sowjet.*, 11:26, 1937.
L. D. Landau. On the theory of phase transitions. II. *Phys. Z. Sowjet.*, 11:545, 1937.
- [17] N. Metropolis, A. W. Rosenbluth, M. N. Rosenbluth, A. H. Teller, and E. Teller. Equation of state calculations by fast computing machines. *The Journal of Chemical Physics*, 21(6):1087–1092, 1953.
N. Metropolis and S. Ulam. The monte carlo method. *Journal of the American Statistical Association*, 44(247):335–341, 1949.
- [18] T. Niemeijer and J. M. J. van Leeuwen. Wilson theory for spin systems on a triangular lattice. *Phys. Rev. Lett.*, 31:1411–1414, Dec 1973.
- [19] L. Onsager. Crystal statistics. i. a two-dimensional model with an order-disorder transition. *Phys. Rev.*, 65:117–149, Feb 1944.
- [20] R. Peierls. On ising’s model of ferromagnetism. *Mathematical Proceedings of the Cambridge Philosophical Society*, 32(3):477–481, 1936.
- [21] G. S. Rushbrooke. On the thermodynamics of the critical region for the ising problem. *The Journal of Chemical Physics*, 39(3):842–843, 1963.
- [22] R. H. Swendsen. Monte carlo renormalization group. *Phys. Rev. Lett.*, 42:859–861, Apr 1979.
R. H. Swendsen. Monte carlo renormalization-group studies of the $d = 2$ ising model. *Phys. Rev. B*, 20:2080–2087, Sep 1979.

- [23] R. H. Swendsen. Monte carlo calculation of renormalized coupling parameters. *Phys. Rev. Lett.*, 52:1165–1168, Apr 1984.
- R. H. Swendsen. Monte carlo calculation of renormalized coupling parameters. i. $d = 2$ ising model. *Phys. Rev. B*, 30:3866–3874, Oct 1984.
- R. H. Swendsen. Monte carlo calculation of renormalized coupling parameters. ii. $d = 3$ ising model. *Phys. Rev. B*, 30:3875–3881, Oct 1984.
- [24] P. Weiss. L’hypothèse du champ moléculaire et la propriété ferromagnétique. *J. Phys. Theor. Appl.*, 6(1):661–690, 1907.
- [25] B. Widom. Surface tension and molecular correlations near the critical point. *The Journal of Chemical Physics*, 43(11):3892–3897, 1965.
- [26] K. G. Wilson. The renormalization group and critical phenomena. *Rev. Mod. Phys.*, 55:583–600, Jul 1983.
- [27] U. Wolff. Collective monte carlo updating for spin systems. *Phys. Rev. Lett.*, 62:361–364, Jan 1989.